Universidade de Aveiro Departamento de Química
Ano 2014

Miguel Ângelo Mouta Martins Aroso

Caracterização da ZG16p, uma lectina singular dos grânulos de zimogénio pancreáticos em mamíferos

Characterisation of ZG16p, a unique mammalian lectin from pancreatic zymogen granules

Universidade de Aveiro Departamento de Química
Ano 2014

Miguel Ângelo Mouta Martins Aroso

Caracterização da ZG16p, uma lectina singular dos grânulos de zimogénio pancreáticos em mamíferos

Characterisation of ZG16p, a unique mammalian lectin from pancreatic zymogen granules

Tese apresentada à Universidade de Aveiro para cumprimento dos requisitos necessários à obtenção do grau de Doutor em Bioquímica, realizada sob a orientação científica do Doutor Michael Schrader, Professor Auxiliar Convidado da Universidade de Aveiro e do Doutor Francisco Manuel Lemos Amado, Professor Associado da Universidade de Aveiro

Apoio financeiro da FCT, do POCTI e do FSE no âmbito do III Quadro Comunitário de Apoio através da bolsa (SFRH/BD/48722/2008)

POPH QUALIFICAR É CRESCER. QREN QUADRO DE REFERÊNCIA ESTRATÉGICO NACIONAL PORTUGAL 2007.2013 GOVERNO DA REPÚBLICA PORTUGUESA UNIÃO EUROPEIA Fundo Social Europeu

To my parents and brothers

o júri

presidente

Doutora Anabela Botelho Veloso
Professora Catedrática da Universidade de Aveiro

Doutor Carlos Jorge Alves Miranda Bandeira Duarte
Professor Associado com Agregação da Faculdade de Ciências e Tecnologia da Universidade de Coimbra

Doutor Francisco Manuel Pereira Peixoto
Professor Associado com Agregação do Centro de Investigação e de Tecnologias Agroambientais e Biológicas da Universidade de Trás-os-Montes e Alto Douro

Doutor Francisco Manuel Lemos Amado
Professor Associado da Universidade de Aveiro

Doutora Maria do Rosário Gonçalves dos Reis Marques Domingues
Professora Auxiliar com Agregação da Universidade de Aveiro

Doutora Ana Luísa Monteiro Carvalho
Professora Auxiliar da Faculdade de Ciências e Tecnologia da Universidade de Coimbra

agradecimentos

"No man is an island, entire of itself; every man is a piece of the continent, a part of the main." (John Donne, 1624)

I would like to express my special appreciation and gratitude to my supervisors for giving me the opportunity to accomplish this dissertation: to Professor Michael Schrader for the continuous support, enthusiasm and deepest knowledge, your advice has been invaluable; and to Professor Francisco Amado for encouraging my research, for allowing me to grow as a research scientist and for all insightful discussions.

I'm deeply thankful to all friends and colleagues from "my" lab: Ana Gouveia, Ana Rita, Cris, Daniela, Débora, Fátima, Hannah, Isabel, Judith, Luís, Maria João, Markus, Mónica, Nina, Sílvia, Sofia. Thank you all for your support and friendship. And to our "adopted" lab members, Sónia and Bruno, for being an example of joy and kindness.

I'm very grateful to all colleagues from the Centre for Cell Biology (CBC), in particular to the Neurosciences lab and specially to the Signal Transduction Lab: Professor Margarida for all the kindness and generosity over this years and to her staff (Catarina, Emanuel, Joana, João, Juliana, Korrodi, Maria João, Mega and Sara) the best neighbours.

An enormous thanks to all colleagues and friends from Chemistry Department for the support and always making me feel at home: Alexandre Ferreira, Ana Isabel Padrão, André Silva, Catarina Ramos, Claúdia Simões, Conceição Fonseca, Cristina Barros, Elizabete Maciel, Renato Alves, Sofia Guedes, Susana Aveiro and Zita Cotrim. A special thanks to Rui Vitorino and Rita Ferreira for all the technical support, advices and friendship over the past years.

To Pedro, Vânia, Armando, Franklin and Joana, friends of a life time, I just hope to give back at least a little bit from what you give to me. Thank you all for the companionship and support during this years.

To my family, my mother, father and brothers for their continuous support during my life, and to my nephews for bringing extra joy and happiness to our life.

At last, to my dearest love Maria, I am forever grateful to you.

palavras-chave

Matriz submembranar, proteínas associadas à membrana, biogénese de organelos, pancreas exócrino, pancreatite

resumo

Os mecanismos de biogénese dos grânulos secretores e a secreção regulada das enzimas digestivas, nas células acinares do pâncreas, ainda não são totalmente compreendidos. Para esclarecer estes processos, que são de importância biológica e clínica (ex., pancreatite), é necessário um melhor conhecimento molecular dos componentes da membrana dos grânulos, as suas funções e interações. A aplicação da proteómica contribuiu largamente para a identificação de novas proteínas dos grânulos de zimogénio (ZG) mas ainda não foi acompanhada por uma melhor caracterização das suas funções. Este estudo teve como objectivos a) o isolamento e identificação de novas proteínas associadas à membrana dos ZG; b) a caracterização das propriedades bioquímicas e da função da lectina ZG16p, uma proteína associada a membrana dos ZG; c) explorar o potencial da ZG16p como uma nova ferramenta para marcar o compartimento endolisossomal. Inicialmente, efetuamos uma abordagem proteómica ao estudo das frações dos ZG, a qual nos levou à identificação de novas proteínas periféricas da ZGM com capacidade de se ligarem a proteoglicanos (Chymase e PpiB). Depois, começamos a desvendar as propriedades moleculares e (múltiplas) funções da lectina ZG16p. A ZG16p é uma proteína única nos mamíferos com capacidade de se ligar a glicanos e a proteoglicanos. Pela primeira vez, foi revelado que a ZG16p é extremamente resistente a proteases através do desenvolvimento de um ensaio de digestão com enterokinase. Adicionalmente, demonstrei que a ZG16p se liga a um complexo de elevado peso molecular (também resistente a proteases) e forma homodímeros muito estáveis. À luz destas descobertas, nós sugerimos que a ZG16p poderá actuar como um elo de ligação aos proteoglicanos, ajudando na formação e estabilização de uma rede/estrutura (matriz submembranar) ligada ao lúmen da ZGM, que desempenhará uma função importante durante a segregação e empacotamento dos zimogénios. A ZG16p poderá atuar como um elo de ligação entre a matriz e os zimogénios agregados devido à sua capacidade para formar dímeros. Adicionalmente, a resistência da ZG16p a protéases poderá ser de maior importância após a secreção, uma vez que é sabido que a ZG16p se liga a fungos patogénicos nos intestinos. Investiguei ainda, o papel dos domínios de ligação da ZG16p na sua segregação para os ZG em células AR42J, um modelo pancreático. A mutação pontual dos motivos de ligação a glicanos e a proteoglicanos não alterou a segregação da ZG16p para os ZG. Também demonstrei que quando a ZG16p se encontra no citoplasma liga-se ao compartimento endolisossomal. Como é sabido, a desregulação da autofagia devido ao funcionamento defeituoso dos lisossomas está associado à pancreatite, por isso iremos discutir o papel potencial da ZG16p nesta doença.

keywords

Submembranous matrix, membrane-associated proteins, organelle biogenesis, exocrine pancreas, pancreatitis

abstract

The mechanisms of secretory granule biogenesis and regulated secretion of digestive enzymes in pancreatic acinar cells are still not well understood. To shed light on these processes, which are of biological and clinical importance (e.g., pancreatitis), a better molecular understanding of the components of the granule membrane, their functions and interactions is required. The application of proteomics has largely contributed to the identification of novel zymogen granule (ZG) proteins but was not yet accompanied by a better characterization of their functions. In this study we aimed at a) isolation and identification of novel membrane-associated ZG proteins; b) characterization of the biochemical properties and function of the secretory lectin ZG16p, a membrane-associated protein; c) exploring the potential of ZG16p as a new tool to label the endo-lysosomal compartment. First, we have performed a suborganellar proteomics approach by combining protein analysis by 2D-PAGE and identification by mass spectrometry, which has led to the identification of novel peripheral ZGM proteins with proteoglycan-binding properties (e.g., chymase, PpiB). Then, we have unveiled new molecular properties and (multiple) functions of the secretory lectin ZG16p. ZG16p is a unique mammalian lectin with glycan and proteoglycan binding properties. Here, I revealed for the first time that ZG16p is highly protease resistant by developing an enterokinase-digestion assay. In addition I revealed that ZG16p binds to a high molecular weight complex at the ZGM (which is also protease resistant) and forms highly stable dimers. In light of these findings I suggest that ZG16p is a key component of a predicted submembranous granule matrix attached to the luminal side of the ZGM that fulfils important functions during sorting and packaging of zymogens. ZG16p, may act as a linker between the matrix and aggregated zymogens due to dimer formation. Furthermore, ZG16p protease resistance might be of higher importance after secretion since it is known that ZG16p binds to pathogenic fungi in the gut. I have further investigated the role of ZG16p binding motifs in its targeting to ZG in AR42J cells, a pancreatic model system. Point mutations of the glycan and the proteoglycan binding motifs did not inhibit the targeting of ZG16p to ZG in AR42J cells. I have also demonstrated that when ZG16p is present in the cytoplasm it interacts with and modulates the endo-lysosomal compartment. Since it is known that impaired autophagy due to lysosomal malfunction is involved in the course of pancreatitis, a potential role of ZG16p in pancreatitis is discussed.

Table of contents

List of Figures

List of Tables

Abbreviations

1D	Monodimensioal
2D	Bidimensional
α-CHCA	α-cyano-4-hydroxycinnamic Acid
aa	amino acid
ACN	Acetonitrile
ANIT	α-napthylisothiocyanate
APS	Ammonium Persulfate
ATCC	American Type Culture Collection
ATP	Adenosine Triphosphate
BanLec	Banan Lectin
BiP	Immunoglobulin Binding Protein
BM	Binding Motif
bp	base pairs
BSA	Bovine Serum Albumin
CBP	Carboxypeptidase
CCK	Cholecystokinin
cDNA	Complementary DNA
CEL	Bile Salt-Activated Lipase
CHAPS	3-[(3-Cholamidopropyl) dimethylammonio]-1-propanesulfonate
CNS	Central Nervous System
Co-IP	Co-Immunoprecipitation
CRD	Carbohydrate Recognition Domain
CTL	C-type Lectin
CTRC	Chymotrypsin C
CV	Condensing Vacuole
Dexa	dexamethasone
DMEM	Dulbecco's Modified Eagle Medium
DMSO	Dimethyl Sulfoxide
DNA	Deoxyribonucleic Acid
dNTP	Deoxynucleotide Triphosphate
DSP	Dithiobis(succinimidylpropionate)
DTT	Dithiothreitol
ECL	Enhanced Chemiluminescence
EDTA	Ethylenediamintetraacetic Acid
EEA1	Early Endosome Antigen 1
ELA	Elastase
EM	Electron Microscopy
ER	Endoplasmatic Reticulum
ESI	Electrospray Ionization
FA	Formic Acid

FASP	Filter-Aided Sample Preparation
FBS	Fetal Bovine Serum
FOY 305	Gabexate Mesilate
fw	forward
GAG	Glycosamynoglycan
GFP	Green Fluorescent Protein
GIT	Gastrointestinal Tract
gJRL	Galactose-binding Jacalin-Related Lectin
GP2	Glycoprotein 2
GPI	Glycosylphosphatidylinisotol
HBS	HEPES Buffered Saline
HEPES	4-(2-hydroxyethyl)piperazine-1-ethanesulfonic Acid
His	Polyhistidine
HMW	High Molecular Weight
H_2O_2	Hydrogen Peroxide
HPLC	High-Performance Liquid Chromatography
HPRT	Heparitinase
HRP	Horse Radish Peroxidase
IMF	Immunofluorescence
IPG	Immobilized pH Gradient
IPTG	Isopropyl β-D-1-thiogalactopyranoside
ISG	Immature Secretory Granule
JRL	Jacalin-Related Lectin
kDa	Kilodalton
KOD	DNA Polymerase from *Thermococcus kodakaraensis*
LAMP	Lysosome-Associated Membrane Protein
LB	Lysogeny Broth
MALDI	Matrix-Assisted Laser Desorption/Ionization
mc	Monoclonal
MES	2-(N-Morpholino)ethanesulfonic Acid
Micros.	Microsomes
MOPS	3-(N-morpholino)propanesulfonic Acid
mJRL	Mannose-binding Jacalin-Related Lectin
mRNA	Messenger RNA
MS	Mass Spectrometry
Muc2	Mucin-2
Muc5AC	Mucin-5AC
OD	Optical Density
PA	Polyacrylamide
PAGE	Polyacrylamide Gel Electrophoreses
PBS	Phosphate Buffered Saline
pc	Polyclonal
PCR	Polymerase Chain Reaction

PDAC	Pancratic Ductal Adenocarcinome
PDI	Protein Dissulfide Isomerase
PEI	Polyethyleneimine
PFA	Paraformaldehyde
PGM	Proteoglycan binding Motif
pI	Isoelectric Point
PI-PLC	Phosphatidylinositol-Specific Phospholipase C
PJ	Pancreatic Juice
PMSF	Phenylmethanesulfonyl Fluoride
PpiB	Peptidyl-prolyl Cis-trans Isomerase B
PTM	Posttranslational modification
RE	Restriction Enzyme
Reg	Regenerating Protein Family
RMCP1	Rat Mast Cell Chymase 1, Chymase
RNA	Ribonucleic Acid
RNase A	Ribonuclease A
RT	Room Temperature
rv	Reverse
SDS	Sodium Dodecyl Sulfate
Sh	Sheep
TAE	Tris-Acetate-EDTA
TCA	Trichloroacetic Acid
TEMED	Tetramethylethylenediamine
TexasRed-tf	TexasRed-Transferrin
TFA	Trifluoroacetic Acid
TfnR	Transferrin
TGN	Trans-Golgi Network
TGN38	Trans-Golgi Network Integral Membrane Protein
TRITC	Tetramethylrhodamine Isothiocyanate
Tris	Tris(hydroxymethyl)aminomethane
TOF	Time-of-Flight
U	Unit
UV	Ultraviolet
V	Volt
WB	Western Blot
ZG16p	Zymogen Granule Membrane Protein 16
ZG	Zymogen Granule
ZGC	Zymogen Granule Content
ZGM	Zymogen Granule Membrane

INTRODUCTION

1. Introduction

1.1. The exocrine pancreas

The pancreas is a unique exocrine and endocrine organ located in the retroperitoneal region of the upper abdominal cavity. The cells of the pancreas are arranged into distinct lobules composed primarily by acinar cells (digestive enzyme-producing cells) of the exocrine pancreas, by the ductal structures that conduct the digestive enzymes to the duodenum and by distinct clusters of endocrine cells, the islets of Langerhans, that secrete hormones directly into the blood (e.g. insulin) (Figure 1). The majority of the pancreatic tissue mass, circa 90-95%, is present within the exocrine compartment of the organ (Lewis, 2008). The acinar cell was the model system in which the fundamental details of the secretory pathway were first elucidated by Palade (Palade, 1975). This cell is highly polarised, with two distinct plasma membrane domains - a small apical domain, which accounts for less than 10% of the total surface area, and a much larger basolateral domain (Figure 1). Along with hepatocytes, the pancreatic acinar cells exhibit the highest rate of protein synthesis among cells in higher organisms. More than 90% of the newly synthesized proteins are targeted to the secretory pathway (Scheele et al., 1978) and are packaged into large secretory granules, also designated as zymogen granules (ZG) (Schrader, 2004), and further stored at the apical domain of the cell.

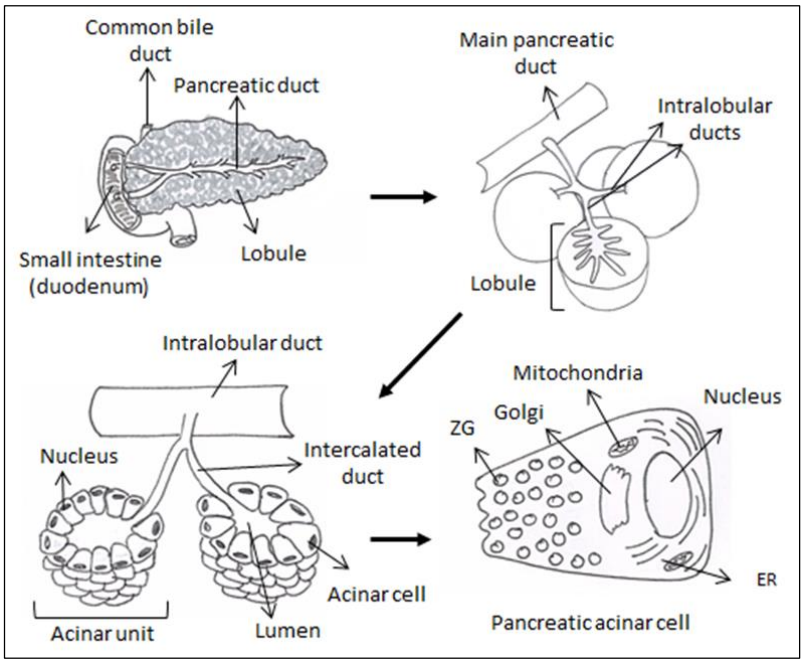

Figure 1. Structure of the exocrine pancreas. The exocrine pancreas is organised in lobules that are constituted by acinar units, which consist of acinar cells surrounding a lumen. The polarity of the acinar cells is shown with the nucleus surrounded by ER in the basal domain and with the ZG in the apical domain. The contents of the ZG are secreted into the intercalated ducts that join to form the intralobular ducts, which merge into the main pancreatic duct. The bile duct comes into close contact with the termination of the main pancreatic duct and they empty into the duodenum together.

The ZG store digestive enzymes (endo- and exoproteases, lipases, glycosidases, and RNAse) that are mostly synthesized as inactive precursors (zymogens) which are only activated through limited proteolysis within the intestinal lumen. Stimulation of receptors in the basolateral membrane by secretagogues such as acetylcholine and cholecystokinin, generates a second messenger response that is dominated by the release of Ca^{2+} from intracellular stores (Kasai et al., 1993; Thorn et al., 1993), which in turn triggers granule fusion leading to the secretion of digestive enzymes into the lumen of the duct (Wasle and Edwardson, 2002). One of the main roles of pancreatic ducts is to provide a structural framework for acinar and islet cells and to convey digestive enzymes from acinar cells to the duodenum (Hegyi et al., 2011). Furthermore, the duct cells secrete fluid that helps in the transport of digestive enzymes, and secrete bicarbonate (HCO^{3-}) that neutralizes gastric acid and provides an optimum pH environment for digestive enzymes in the duodenum. HCO^{3-} is also a chaotropic ion that helps in the solubilisation of macromolecules preventing the aggregation of digestive enzymes and mucins (Lee et al., 2012). The human pancreas secretes 1-2 liters of pancreatic juice per day, a clear, alkaline, isotonic fluid rich in digestive enzymes secreted by the acinar cells (Lee and Muallem, 2008). The pancreatic duct system delivers the pancreatic juice into the duodenum, where conversion of trypsinogen to trypsin is mediated by proteolytic cleavage via enterokinase, a heterodimeric type II membrane protein of the brush border of duodenal enterocytes. Activated trypsin then proteolytically cleaves and activates the other zymogens (Zheng et al., 1999).

1.2. Zymogen granule biogenesis and exocytosis in the exocrine pancreas

The multiple enzymes characteristic of the pancreas are synthesized by ribosomes, associated with the membranes, and inserted into the lumen of the rough endoplasmic reticulum (ER). In the supranuclear region, the Golgi complex receives the products of the ER and processes them further (Bockman, 2008). Then, the selection/sorting of proteins to be packaged in ZG takes place at the trans-Golgi network (TGN) and might involve selective protein aggregation and protein-membrane interactions. Some of the ZG enzymes form protein complexes already within the lumen of the ER (Kleene et al., 1999a; Tooze et al., 1989). The protein complexes progressively aggregate at the mildly acidic pH and high Ca^{2+} levels within the TGN and form dense core aggregates that are supposed to interact with the

TGN membrane (Figure 2) (Colomer et al., 1996; Dartsch et al., 1998; Freedman and Scheele, 1993; Gómez-Lázaro et al., 2010; Leblond et al., 1993). While the selective aggregation of ZG proteins has been well documented, their interaction with the TGN/ZG membrane is poorly understood at the molecular level, and neither a common sorting signal nor a sorting receptor has been identified so far.

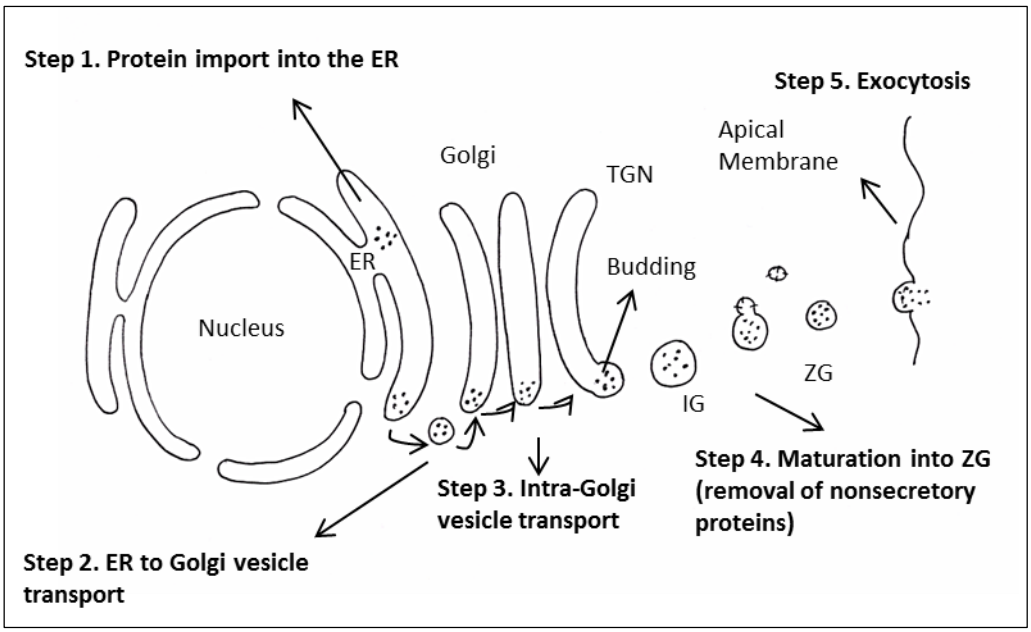

Figure 2. Zymogen granule biogenesis and exocytosis in the exocrine pancreas. ER – endoplasmic reticulum; TGN – Trans-Golgi Network; IG – Immature Granule; ZG – Zymogen Granules.

Two models have been proposed to account for the sorting of regulated secreted proteins in exocrine and endocrine cells (Arvan and Castle, 1992, 1998). One is viewed as an active model for sorting (‘sorting by entry’), where membrane binding of secretory proteins is assumed to depend on a ‘sorting receptor’ within the TGN (e.g., a transmembrane protein), and entry into forming granules is restricted to receptor-mediated trafficking. The other model is a passive model (‘sorting by retention’), where aggregation of regulated secretory proteins is the primary sorting event. In this model, a receptor is not required and entry into the forming granule is not solely restricted to regulated secretory proteins. The non-secretory proteins fail to aggregate and are removed from the maturing granules in a clathrin-dependent process. In this case, the immature secretory granule can also be a site for sorting. However, the retention of the granule-specific membrane components is likely to involve their interaction with regulated secretory proteins (Gómez-Lázaro et al., 2010).

Sorting during ZG biogenesis is also supposed to take place after the TGN, at the level of the ZG itself. Ultrastructural studies indicate that parts of the Golgi cisternae become

dilated and filled with electron-opaque material. These condensing vacuoles (CVs), the initial stage of ZG, then pinch off as immature granules, which mature into ZG by the selective removal of nonsecretory proteins (via a clathrin-mediated process called 'constitutive-like secretion') and further condensation of the aggregated zymogens occurs, as well as a reduction in granule size (Arvan and Castle, 1992; Dahan et al., 2005; Gómez-Lázaro et al., 2010; Klumperman et al., 1998).

ZG are transported in a cytoskeleton-assisted fashion to the apical plasma membrane where they dock to the plasma membrane (Masedunskas et al., 2012). It is now accepted that docking and fusion requires specific heterotrimeric interactions between membrane-associated SNARE proteins (soluble N-ethylmaleimide-sensitive factor attachment protein receptors): syntaxin, SNAP25 (25 kDa synaptosome-associated protein) and VAMP (vesicle associated membrane protein). However, each step of the process (tethering, docking, priming and fusion) is assisted by specific accessory proteins (e.g., Rab27b, synaptotagmin-like proteins). Ca^{2+}-stimulated acinar secretion triggers an early rapid phase of exocytosis that is mediated by VAMP2-specific SNARE interactions and is likely controlled by the Ca^{2+}-sensing protein syt1 and accessory protein complexin 2 (Messenger et al., 2014). Following a secretory stimulus, up to 30% of the cellular vesicle content is secreted over extended time periods of up to an hour (Valentijn et al., 1999; Williams, 2006). The apical plasma membrane takes a massive addition of membrane material from the ZG, however the overall size of this domain is maintained constant by a dynamic process of compensatory membrane endocytosis (Geron et al., 2013; Gómez-Lázaro et al., 2010; Massarwa et al., 2009). Upon exocytosis of the ZG, the digestive enzymes are exposed to the alkaline pH of the acinar/ductal lumen, and the proteins are solubilized for their transit to the duodenum (Freedman et al., 1994). Once in the intestinal tract, granule proteins, in addition to digestion, are also supposed to fulfil regulatory and protective functions, for example, in host defence (Bach et al., 2006; Gómez-Lázaro et al., 2010; Szmola and Sahin-Tóth, 2007; Tateno et al., 2012).

1.3. Proteomics of pancreatic zymogen granules

Proteomics workflows have been developed to reliably identify the protein complement of whole organelles, as well as for protein assignment to subcellular location (Drissi et al., 2013). Proteomics has been used to study the exocrine pancreas and its diseases

in various manners including understanding its physiology, identification of biomarkers of disease, and understanding the mechanism of disease (Williams, 2013). The exocrine pancreas served as the model that first established the role of intracellular compartments in the secretory pathway (Palade, 1975), and ZG have been used as a model system to study secretory-granule biogenesis and regulated secretion in general. The molecular mechanisms required for ZG formation at the TGN and for the packaging and sorting of cargo proteins, as well as for granule fusion and exocytosis, are still poorly defined. According to recent models, part of the molecular machinery required for digestive enzyme sorting, granule trafficking and exocytosis is supposed to be associated with the ZG membrane (ZGM). In addition to basic research interests, ZG also play important roles in pancreatic injury and disease (Gaisano and Gorelick, 2009; Thrower et al., 2010). Therefore, there is currently great interest in the identification and molecular characterization of ZG and ZGM components (Gómez-Lázaro et al., 2010).

1.3.1. Isolation and subfractionation of zymogen granules

Zymogen granules represent highly abundant organelles of the exocrine pancreas that can be easily isolated due to their large size and quantity. Isolated ZG can be lysed and further separated into a ZG content (ZGC) and membrane (ZGM) fraction. Isolation procedures for ZG from dog (Hokin, 1955), bovine and guinea pig pancreas (Greene et al., 1963; Tartakoff et al., 1974), as well as for porcine (Rutten et al., 1975) and rat pancreas (Borta et al., 2010; Chen and Andrews, 2008; de Lisle et al., 1984; Pâquet et al., 1982; Rindler, 2006), have been described (Gómez-Lázaro et al., 2010). Subcellular fractionation is the most widely used method, which after tissue homogenization and differential centrifugation results in a relatively pure ZG fraction (≥90%). To achieve a higher degree of purity, sucrose or percoll gradient fractionation is often applied (Borta et al., 2010; Gómez-Lázaro et al., 2010; de Lisle et al., 1984; Pâquet et al., 1982; Rindler, 2006).

The efficiency of the isolation and the enrichment of ZG proteins as well as the presence of potential contaminations is often monitored by SDS-PAGE, immunobloting and enzyme activity measurements for marker proteins (e.g., amylase, GP2). In addition, the organelle integrity and the presence of contaminating subcellular structures in the ZG fractions, which include mitochondria, ER and large lysosomes are verified by electron microscopy (Gómez-Lázaro et al., 2010). Intact ZG can be gently lysed at pH 8, which

corresponds to the physiological conditions at which the ZGC proteins become soluble in the pancreatic duct, after exocytosis. Then, the ZGC and membrane subfractions can be obtained by centrifugation. The isolated membranes have been treated with potassium bromide and/or carbonate at pH 11 to liberate membrane-associated proteins from transmembrane and membrane-anchored proteins (Figure 3) (Chen and Andrews, 2008; Chen et al., 2006; Hoops and Rindler, 1991; Schmidt et al., 2000). However, some ZGC proteins are still found in the ZGM fraction and *vice versa*. This may be due to the observation that some ZGC proteins exist in a soluble and membrane-associated pool (Borta et al., 2010; Chen et al., 2006, 2008; Rindler, 1992; Schmidt et al., 2000). Furthermore, some ZGM proteins are enzymatically cleaved and released in a soluble form (e.g., GP-2, a major glycosylphosphatidylinositol [GPI]-anchored ZGM glycoprotein) (Gómez-Lázaro et al., 2010; Rindler and Hoops, 1990).

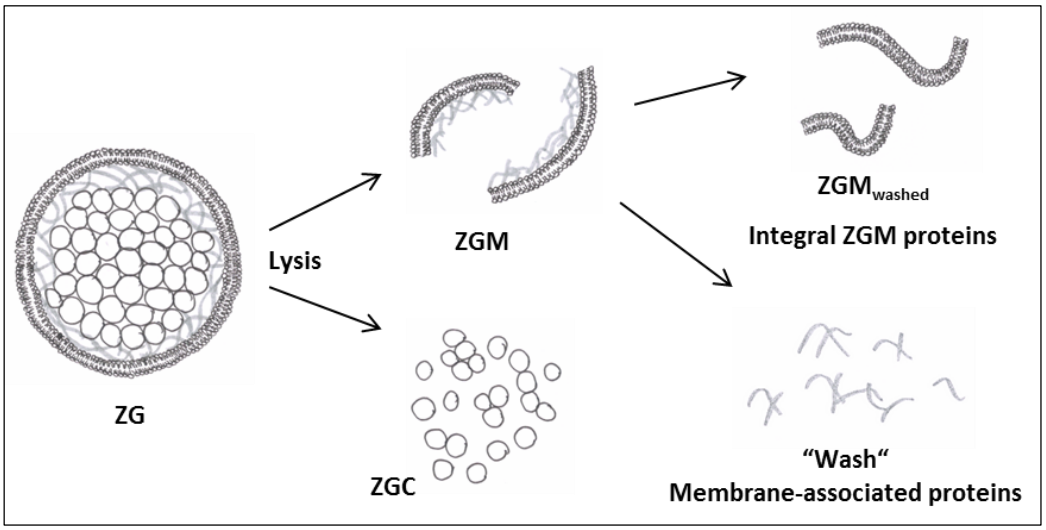

Figure 3. Subfractionation of zymogen granules (ZG). Isolated ZG can be lysed at pH 8 by freezing and thawing. The content (ZGC) and membrane (ZGM) subfractions are obtained by centrifugation. After treating the isolated membranes with carbonate at pH 11.5, a subfraction with integral membrane proteins (ZGMwashed) and a subfraction with membrane-associated proteins (Wash) is obtained by ultracentrifugation.

1.3.2. Separation of zymogens

Introduced by George Scheele, bidimensional (2D) separation of proteins in slab gels using isoelectric focusing (IEF) in the first dimension and SDS-PAGE in the second dimension (Scheele, 1975) was used for the analysis of the complex mixture of soluble proteins secreted by the exocrine pancreas. For the first time it was possible to analyse simultaneously the major exportable proteins in subcellular fractions, obtained after

homogenization, and in extracellular fluids (e.g., pancreatic juice [PJ] or incubation medium) contributing to the determination of the intracellular transport of pulse-labeled proteins along the secretory pathway (Scheele et al., 1978). In combination with the development of pancreatic lobules as an *in vitro* model of biological response (Scheele, 1975; Scheele and Palade, 1975) and, thus, the efficient study of protein synthesis, 2D-SDS-PAGE has furthermore provided valuable insights into the differential regulation of gene expression in the rat pancreas in response to hormones (Adler et al., 1983; Schick et al., 1984a) and different nutrients (Kern et al., 1987; Schick et al., 1984b). In addition, 2D-SDS-PAGE has been used to identify many of the abundant ZG proteins (Bieger and Scheele, 1980; Borta et al., 2010; Kleene et al., 1999a; Scheele et al., 1981). In the 1980s, guinea pig and human exocrine pancreatic proteins were the most thoroughly described systems analysed by 2D-SDS-PAGE. Owing to limited resolution and sensitivity, however, a relatively simple protein composition for the ZGM was proposed. The recent improvements in organellar proteomics revealed a more-complex picture of the components of the ZGM (Chen et al., 2006, 2008; Rindler et al., 2007). Alternative procedures besides the traditional 2D-SDS-PAGE, such as double SDS-PAGE, have demonstrated their capacity to resolve membrane proteins (Faust et al., 2008), but the main developments were due to the application of nongel-based techniques, such as high-performance liquid chromatography (HPLC) with improved capacity to resolve membrane and membrane-associated proteins, mostly applied after in-solution digestion (Chen et al., 2006, 2008; Rindler et al., 2007; Sun and Jiang, 2013).

1.3.3. Identification of ZG proteins by mass spectrometry

Mass spectrometry (MS) is an analytical technique aiming at the study in the gas phase of ionised molecules, in order to determine their molecular weight (m/z ratio), characterize their structure and determine their abundance (Silva et al., 2013). The technical innovations in MS, protein-identification methods and database annotation over the last 20 years have allowed scientists to rapidly and systematically detect thousands of proteins in complex biological samples (Aebersold and Mann, 2003; Han et al., 2008; Kim et al., 2014; Wilhelm et al., 2014). In this respect, MS has become the method of choice for the analysis of complex protein samples (Aebersold and Mann, 2003; Lane, 2005), where the development of ‘soft’ ionization methods is the main responsible for its success in the

proteomics field. Presently, two ionization techniques, namely electrospray ionization (ESI) (Fenn et al., 1989) and MALDI (Karas and Hillenkamp, 1988; Tanaka et al., 1988), are playing a significant role in MS-based peptide analysis (Fröhlich and Arnold, 2006; Han et al., 2008).

Until recently, the major ZG proteins have been identified by the purification of proteins, N-terminal peptide sequencing techniques and the specific immunolocalization of granule components. The introduction of mass spectrometry in the proteomic study of ZG resulted in a better characterization of the ZG proteome, and contributed mainly to the discovery of additional ZGM proteins (Berkane et al., 2007; Chen et al., 2006; Rindler et al., 2007; Sun and Jiang, 2013) and ZGM associated proteins (Borta et al., 2010). The combination of 2D-SDS-PAGE and 2D-LC allowed, for the first time, the separation and subsequent identification by mass spectrometry of a total of 101 proteins from purified ZGM (Chen et al., 2006). The separation of rat ZG proteins by combining 1D-SDS-PAGE with LC resulted in the identification of a total of 371 proteins by MS (Rindler et al., 2007). More recently, the combination of FASP (filter-aided sample preparation), that combines the advantages of complete sample solubilisation with in-solution digestion, and 2D-LC-MS/MS allowed the identification of 800 proteins in mouse ZG by MS (Sun and Jiang, 2013).

1.4. Proteoglycans and zymogen granules

Sulfated proteoglycans have previously been identified as constituents of pancreatic zymogen granules and in the fluid of pancreatic ductal system (Berg and Young, 1971; Reggio and Palade, 1978; Tartakoff et al., 1975). Furthermore, Scheele et al. (1994) reported that in acinar cells of the rat pancreas more than 90% of sulfated-labeled proteoglycans were associated with the ZGM, and could be released by treatment of ZGM with sodium carbonate at pH 11.2 (Scheele et al., 1994). In addition, a reticular network on the inner surface of ZGM had been observed by freeze-fracture and deep-etching studies several years ago (Cabana et al., 1981). GP-2 was described to be associated with fibrillar material in lysates of ZG, in the acinar lumen and in pancreatic juice (Beaudoin et al., 1991; Grondin et al., 1992). Based on these findings, Scheele and co-workers postulated the existence of a submembranous granule matrix at the luminal surface of ZGM and presented further evidence that during granule exocytosis the release of the putative matrix is mediated by the

alkaline pH present in the acinar lumen and the activation of phosphatidylinositol-specific phospholipase C (PI-PLC) (Freedman et al., 1998a). The release of the hypothetical matrix is supposed to be a prerequisite for the efficient recycling of granule membranes via endocytosis (Freedman et al., 1998a, 1998b; Schrader, 2004). The submembranous matrix model predicts the presence of high molecular weight components (e.g., a proteoglycan scaffold and associated (glyco)proteins) attached to the luminal side of the granule membrane. This scaffold is supposed to fulfil important functions during the sorting and packaging of secretory proteins (Scheele et al., 1994; Schrader, 2004). The glycoconjugate scaffold underneath the ZGM is suggested to serve as the backbone of a complex membrane matrix, and a bridge between the ZGM and the zymogens.

Moreover, sulfated proteoglycans were found to be associated with lipid microdomains in the ZGM (Kalus et al., 2002; Schmidt et al., 2001). These lipid microdomains and associated proteins (e.g., GP2) were involved in the attachment of the matrix proteoglycans to the granule membrane (Schmidt et al., 2001). Recently, Kumazawa-Inoue and colleagues isolated heparin sulfate proteoglycans from rat pancreatic zymogen granules and characterized the glycosaminoglycan (GAG) chains but the identification of the core protein was unsuccessful (Kumazawa-Inoue et al., 2012). Sulfated proteoglycans are present in multiple intracellular compartments, such as endosomes, lysosomes, nucleus and especially in storage organelles of immunosecretory, neurosecretory cells (Gallagher, 1989; Gallagher et al., 1986; Kolset and Gallagher, 1990; Prydz and Dalen, 2000). The negatively charged proteoglycans in secretory granules of haemopoietic cells and mast cells are involved in the binding of small positively charged molecules, such as histamine (Rönnberg et al., 2012).

Since specific membrane receptors or sorting signals have not yet been identified in exocrine cells, the concept of the submembranous matrix offers an interesting alternative to understand the packaging and sorting of a complex mixture of proteins in an exocrine system. Furthermore, the submembranous matrix might have protective and mechanical properties, e.g., to maintain membrane curvature, granule shape and stability (Schrader, 2004).

1.5. Lectins in the Pancreas

1.5.1. Lectins

Lectins are carbohydrate-binding proteins, excluding sugar-specific antibodies, receptors of free mono- or disaccharides for transport or chemotaxis and enzymes modifying the bound carbohydrate (Gabius et al., 2002). Some of the well-characterized roles of lectins are in cell-cell communication, host-pathogen interactions, tissue development, metastasis and embryogenesis (Raval et al., 2004).

Lectins were first found and described in plants, but in subsequent years multiple lectins were isolated from microorganisms and animals (Sharon and Lis, 2004) and now they can be classified in more than forty families (Tateno, 2010; Tateno et al., 2012). Interestingly, plant and animal lectins show no primary structural homology, yet they share similarities in their tertiary structures (Ghazarian et al., 2011; Sharon and Lis, 2004), suggesting that animal and plant lectin genes may have co-evolved, thus highlighting the importance of lectin-carbohydrate interactions in living systems (Ghazarian et al., 2011; Gorelik et al., 2001).

Structural studies conducted on animal lectins suggested that the carbohydrate binding activity of most lectins was generated by limited amino acid residues designated as the carbohydrate recognition domain (CRD) (Ghazarian et al., 2011; Sharon and Lis, 2004). Several highly conserved CRD amino acid sequences have been identified, thus allowing investigators to categorize the majority of these lectins into structurally related families and superfamilies (Sharon and Lis, 2004).

Several lectins have been associated with the pancreatic ZG (Parikh et al., 2012; Rindler et al., 2007; Sun and Jiang, 2013), but I will focus on a group of unusual pancreatic secretory proteins with carbohydrate-binding activities. Among them are a multifunctional family of secreted lectins containing CTL (C-type lectin) domains (Reg family) with known anti-inflammatory, antiapoptotic, and mitogenic action in multiple physiologic and disease contexts (Iovanna and Dagorn, 2005; Parikh et al., 2012) and the lectin ZG16p, a mannose-binding Jacalin-related lectin (mJRL), and the main subject of this dissertation.

Protein analysis of ZG (and pancreatic secretions) resulted in the identification of several unique proteins with carbohydrate-binding properties. Among them are the secretory lectin ZG16p and the structurally different C-type lectins regenerating gene (Reg) family.

The latter are supposed to exert anti-inflammatory, anti-apoptotic, proliferative, free radical scavenging and antibacterial effects (Iovanna and Dagorn, 2005; Moniaux et al., 2011), whereas the activity of ZG16p is largely unknown. Interestingly their expression is not restricted to the pancreas thus pointing to multifunctional properties and a broader (patho)physiological importance (Laurine et al., 2003). As lectins have been shown to be involved in various protein trafficking/sorting processes and in the maintenance of membrane polarisation (Delacour et al., 2009), the biochemical and functional analysis of the unusual secretory lectins is of great biological importance.

1.5.2. The regenerating gene family

The Reg family encodes a group of secreted proteins, RegI to RegIV, and each member has an N-terminal signal peptide linked to a conserved sequence motif homologous to the carbohydrate recognition domain (CRD) of C-type lectin (Cash et al., 2006; Ho et al., 2010). C-type lectins are the most abundant of all animal lectins, and the CTL superfamily is grouped into three families: selectins, collectins and endocytic lectins (Kerrigan and Brown, 2009; Sharon and Lis, 2004). A majority of CTLs are large, asymmetric, have one or more CRDs and exist as Ca^{2+} dependent proteins found in secreted or bound forms (Ghazarian et al., 2011; Gorelik et al., 2001; Sharon and Lis, 2004). The Reg proteins were discovered independently during pancreatitis and pancreatic islet regeneration (de Caro et al., 1979; Keim et al., 1984), but there is evidence of participation of Reg proteins in the proliferation and differentiation of many cell types. Currently, they are associated with various pathologies, including diabetes, pancreatitis, gastrointestinal cancer (Parikh et al., 2012), Alzheimer or Creutzfeldt-Jakob disease (Duplan et al., 2001; Laurine et al., 2003). These findings have led to the emergence of key roles for Reg proteins as anti-inflammatory, antiapoptotic, and mitogenic agents in multiple physiologic and disease contexts (Parikh et al., 2012).

Despite the initial association with the pancreas, most Reg proteins are expressed in multiple organs under normal and pathological conditions. At least one of the REG1α, REG1β, and REG3β is detected in human fetal and adult pancreas, brain, stomach, intestine, and pituitary gland (Bartoli et al., 1998). The latest addition to the Reg group, RegIV, was initially found to be significantly upregulated during mucosal injury due to active Crohn's disease or ulcerative colitis (Hartupee et al., 2001). It is overexpressed in colorectal

carcinomas (Violette et al., 2003) and is prominently expressed in the human gastrointestinal tract. RegIV expression is also linked to pancreatic cancer and malignancies of the stomach, intestine, colon, rectum, gallbladder, and urogenital tract (Hayashi et al., 2009; Nanakin et al., 2007; Oue et al., 2005; Tamura et al., 2009; Violette et al., 2003). But the expression patterns and relevance to diseases and/or tissue homeostasis of the Reg family remain unclear (Parikh et al., 2012). In addition, some of the Reg family members were associated with antibacterial activity, suggesting an extracellular function in host defence after secretion. RegI was found to bind and aggregate several bacterial strains, including Gram-positive and Gram-negative aerobic and anaerobic bacteria (Iovanna et al., 1993). Recently, mouse RegIIIγ and human RegIII were shown to be direct antibacterial proteins that bind to Gram-positive bacteria via interactions with peptidoglycan carbohydrate in a calcium-independent manner (Ho et al., 2010; Lehotzky et al., 2010). RegIV protein adopts a typical fold of C-type lectin but binds mannan, a polymer of mannose residues, with two calcium-independent sites (Ho et al., 2010). These proteins may play a vital role in maintaining host-bacterial homeostasis in the mammalian gut, which reveals a previously undiscovered biological function for animal lectins, and represent an evolutionarily primitive form of lectin-mediated innate immunity (Ho et al., 2010).

1.5.3. The secretory lectin ZG16p

1.5.3.1. Discovery and localization in ZG

Zymogen Granule protein 16 was first identified by immunoscreening of a rat pancreatic cDNA expression library with a polyspecific antiserum raised against purified ZGM (Cronshagen et al., 1994). It was considered to be a secretory lectin due to its sequence homology with the plant lectin Jacalin (Cronshagen et al., 1994). Most recently, the tertiary structure of ZG16p was solved by crystallography and it was shown to possess a Jacalin-related β-prism fold, the first to be reported among mammalian lectins (Kanagawa et al., 2011). After ZG16p discovery, Kleene and colleagues have shown that it is mainly associated with the luminal side of ZGM and that it is almost completely removed after bicarbonate treatment at pH 11.5 (Kleene et al., 1999b). Later, it was shown that ZG16p was found in cholesterol-glycosphingolipid-enriched microdomains together with GP2, syncollin and sulfated proteoglycans (Kalus et al., 2002; Schmidt et al., 2001). Furthermore, the

association of ZG16p with the luminal side of the zymogen granule membrane was confirmed by proteomics in several publications (Borta et al., 2010; Chen et al., 2006, 2008; Rindler et al., 2007).

Full length ZG16p has 167 amino acids (aa) where the first 16 aa represent a signal peptide that targets the protein to the ER (Cronshagen et al., 1994; Kanagawa et al., 2011) and it doesn't have any transmembrane domains (Borta et al., 2010; Cronshagen et al., 1994; Kanagawa et al., 2011, 2014). Residues 36-159 are classified as the jacalin-related domain based on sequence alignment in the Pfam database (http://pfam.xfam.org/protein/Q8CJD3).

1.5.3.2. 3D structure and binding motifs

The crystal structure of ZG16p was recently solved (Kanagawa et al., 2011) revealing a β-prism fold with 3 β-sheets, each consisting of 3-4 β-strands forming three Greek motifs (PDB: 3APA), similar to jacalin related mannose-binding type lectins (mJRL) (Kanagawa et al., 2011). Jacalin-related lectins (JRLs) derive their name from Jacalin, the first member to be identified from the seeds of jackfruit (Bunn-Moreno and Campos-Neto, 1981; Raval et al., 2004). They are further divided into two subgroups based on the sugar-binding specificities: galactose-binding-type (gJRLs) and mannose-binding-type (mJRLs) (Van Damme et al., 1996; Nakamura-Tsuruta et al., 2008; Tateno et al., 2012). Most JRLs identified so far belong to mJRL, which consists of the intact subunit of about 150 amino acids (Tateno et al., 2012). The gJRL subfamily consists of a short β-chain (2 KDa) and a long chain (13 KDa) as a result of post-translational processing (Nakamura-Tsuruta et al., 2008) and is a much smaller subgroup, in which only a few members have been identified, such as Jacalin (Sastry et al., 1986; Tateno et al., 2012). While gJRLs have been extensively used as tools to detect mucin-type O-glycans, (Nakamura-Tsuruta et al., 2008), an mJRL (BanLec) isolated from the fruit of bananas was recently shown to be a potent inhibitor of HIV-1 infection. BanLec inhibits entry of the virus into the cell by binding to the high mannose structures found on the heavily glycosylated envelope protein gp120 (Swanson et al., 2010; Tateno et al., 2012). The structural similarities between ZG16p and the mJRLs suggested that it possesses the same mannose-binding mode through three conserved exposed loops (GG loop, recognition loop and binding loop) at the top of the β-prism I fold. The binding loop is a common carbohydrate recognition domain (CRD), a glycine and an aspartic acid separated by a 3-amino-acid spacer (GXXXD) (Figure 4). This domain is

conserved in the majority of β-prism fold lectins (Kumazawa-Inoue et al., 2012; Raval et al., 2004; Sharma et al., 2007). In addition, it was shown by a glycoconjugate microarray, that ZG16p binds to polyvalent mannose via the carbohydrate recognition domain and, by frontal affinity chromatography, that ZG16p binds to high-density mannose and yeast mannan. It was further demonstrated that ZG16p binds to pathogenic *Candida* and *Malassezia* species heavily coated with mannan (Tateno et al., 2012). More recently, Kanagawa and colleagues characterized by crystallography the binding of ZG16p with α-O-methyl-mannose and concluded that ZG16p and mJRLs have the same mannose-binding mode (Kanagawa et al., 2014). On both cases mutation of the amino acid D151 abolished the binding of the carbohydrate recognition domain (GXXXD) to mannose-related probes (Kanagawa et al., 2014; Tateno et al., 2012). Interestingly, analysis of the crystal structures of BanLec (a mJRL) with carbohydrate ligands revealed that BanLec possesses two carbohydrate-binding sites including the signature motifs GG and GXXXD (Kumazawa-Inoue et al., 2012; Meagher et al., 2005; Singh et al., 2005), while ZG16p has only one mannose-binding site (Kanagawa et al., 2011, 2014). On the other hand, BanLec does not bind glycosaminoglycans (GAG) probably due to its negatively charged surface potential (Kanagawa et al., 2014).

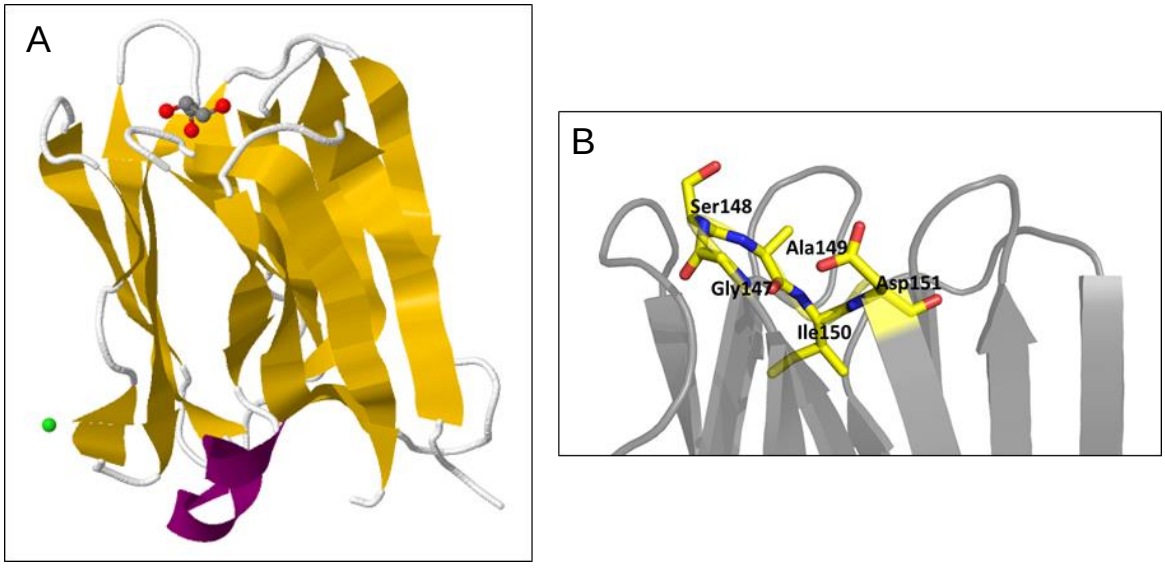

Figure 4. Tertiary structure and the carbohydrate recognition domain (CRD) of ZG16p. (A) 3D model obtained from Protein Database Bank (3APA). β-strands are coloured in yellow and a short α-helix is coloured in purple. A glycerol molecule is bound to the CRD at the top of ZG16p molecule. (B) Close-up view of the CRD of ZG16p.

Previously, ZG16p was suggested to bind to sulfated proteoglycans (Kanagawa et al., 2011; Kleene et al., 1999b; Schmidt et al., 2001; Schrader, 2004) but the characterization

of the proteoglycan binding sites was only accomplished recently by Kumazawa-Inoue and colleagues (Kumazawa-Inoue et al., 2012). ZG16p binds to proteoglycans through two positively charged basic patches, constituted by lysine and arginine residues on the surface of the protein, that interact with the negatively charged side chains of sulfated proteoglycans (Kanagawa et al., 2011; Kleene et al., 1999b; Kumazawa-Inoue et al., 2012). Point mutation of those sites (K33A, K36A, R37A and R55A, R58A) abolished the binding to heparin (Kumazawa-Inoue et al., 2012) (Figure 5).

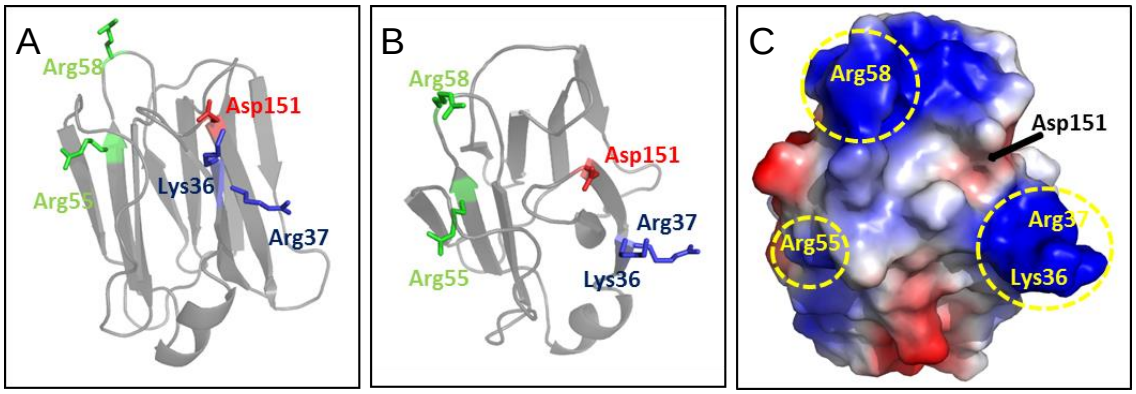

Figure 5. Localization of the amino acids at the surface of ZG16p subjected to point mutation. (A and B) Amino acids coloured in green and blue correspond to the proteoglycan binding motif (PGM) and the amino acid coloured in red is part of the carbohydrate recognition domain. (C) Surface model of ZG16p coloured according to the electrostatic surface potential (blue – positive, red – negative). Yellow circle shows localization of the PGM and the arrow points to CRD.

ZG16p is likely a unique lectin with dual specificity to sulfated glycosaminoglycans (proteoglycan binding motif) and to polyvalent mannose and short chain α-manno-oligosaccharides (carbohydrate recognition domain) (Figure 6) (Kanagawa et al., 2011, 2014; Kumazawa-Inoue et al., 2012; Tateno et al., 2012). Furthermore, the mannose binding site does not compete with the proteoglycan binding site on ZG16p (Kanagawa et al., 2014).

Figure 6. Domains of ZG16p. SP – Signal Peptide, PGM – ProteoGlycan binding Motif, CRD – Carbohydrate Recognition Domain.

1.5.3.3. ZG16 gene expression profile

ZG16p was first identified in the zymogen granules of the rat pancreas (Cronshagen et al., 1994) and it was shown that the expression of ZG16 mRNA in the pancreas was up-regulated by a hormonal treatment with cholecystokinin (CCK) or cerulein (Cronshagen et al., 1994). Both peptide hormones are known to evoke a complete release of zymogen

granules and to up-regulate expression and transport of most secretory enzymes (Cronshagen et al., 1994; Steinhilber et al., 1988; Vasiloudes et al., 1991; Wang and Cui, 2007). Furthermore, expression of ZG16 mRNA levels in a rat acinar carcinoma cell line (AR42J) treated with dexamethasone resulted in a 12-fold increase (Cronshagen et al., 1994). Treatment with the glucocorticoid dexamethasone induces both the differentiation of AR42J cells into acinar-like cells and the *de novo* formation of electron-opaque secretory granules, which contain the major pancreatic zymogens (Logsdon et al., 1985). In parallel, the presence of ZG16 mRNA was tested on several tissues by Northern blot and it was detected in pancreas, duodenum, colon and stomach (Cronshagen et al., 1994).

Interestingly, gene expression profiling in very diverse studies revealed new insights into the up or down regulation of ZG16 mRNA across different tissues. Implants of biomaterials into the rat stomach strikingly lead to the transient expression of several genes encoding pancreatic enzymes and ZG16 in the gastric wall (Löbler et al., 2002). The comparison of gene expression in response to treatment with known liver toxicants or inducers between rat liver slices and primary hepatocytes (*in vitro*) and rat liver (*in vivo*) also showed the regulation of ZG16 mRNA in the liver. In this case, treatment with ANIT (α-napthylisothiocyanate), an insecticide that gives rise to cholangiolitic hepatitis with necrosis of the bile duct epithelial cells and hepatic parenchymal cells (Fukumoto et al., 1980; Jessen et al., 2003), induced over a two fold increase of ZG16 mRNA on all tested systems (Jessen et al., 2003). In a study aiming at the identification of regulated genes in the lesion area as well as in the axotomized neurons following lesion of a central nervous system (CNS) fibre tract, ZG16 mRNA was in the 2.3% of the 1185 genes studied that showed significant changes (3 fold for ZG16 mRNA) in the lesion site, when compared with the control (Küry et al., 2004). This study also indicates, for the first time, the expression of ZG16 mRNA in the rat brain, while previously it was only associated with the digestive system. The gene expression profiling in the ileum in a rat ileal-augmented bladder model revealed that ZG16 mRNA was over two fold down-regulated in 1 and 3 months after surgery (Miyake et al., 2004). In a rat model for colon cancer induced by azoxymethane (AOM) it was evaluated the effect of lifetime ingestion of casein (control), soy and whey proteins on the gene expression profile of colons. ZG16p was determined to be over four fold down-regulated in rats fed with whey protein and no changes were observed when fed with soy protein (Xiao et al., 2005). Human ZG16 (hZG16) was shown, by Northern blot, to

be expressed in adult liver and colon and, by RT-PCR, in adult pancreas. But more significantly, hZG16 was down-regulated in hepatocellular carcinoma (Zhou et al., 2007). In a tissue screening of expression of human ZG16 mRNA by real-time PCR, ZG16 was strongly detected in liver, pancreas and small intestine (Tateno et al., 2012). A treatment of mice with supraphysiological doses of cerulein inducing acute pancreatitis, led to a rapid down regulation (12 h) of ZG16p mRNA in mouse pancreas with recovery of mRNA levels within 3 days (Neuschwander-Tetri et al., 2004). These studies reveal that ZG16 mRNA is found not only in the pancreas or intestine but several other organs like the stomach, liver or brain under normal or disease states. However, a more careful investigation of ZG16 expression in different tissues (in health and disease) is necessary, in order to better understand the relevance of ZG16 expression under (patho)physiological conditions.

1.5.3.4. ZG16 protein expression in different tissues

ZG16p was first identified in the pancreas and as outlined above it was shown to be associated with the ZGM (see Chapter 1.5.3.1). Additionally, there is evidence at the protein level (western blot, dot blot, immunohistochemistry and immunocytochemistry and MS identification) of ZG16p expression in different tissues from different species. Initially, Cronshagen and colleagues reported by immunohistochemistry the expression of ZG16p in pancreas, mucus-producing goblet cells and at the luminal surface of the duodenum and colon (Cronshagen et al., 1994). Later, ZG16p was found by dot blot analysis in human intestine and colon, and by immunohistochemistry in human liver (Zhou et al., 2007). More recently, Tateno and colleagues showed by immunohistochemistry the localization of ZG16p in human serum and in mucus-secreting cells of the digestive system: in acinar cells of pancreas, goblet cells of the small bowel, colon, appendix and rectum and in the serosanguineous acinar cells of the parotid gland (Tateno et al., 2012). ZG16p was first found to be part of the mucus proteome of the mouse colon (Johansson et al., 2008) and later to be part of the mucus proteome through all gastrointestinal tract (GIT) (Rodríguez-Piñeiro et al., 2013). The mouse GIT is protected by mucus that covers the epithelial surface from stomach to colon (Ermund et al., 2013; Rodríguez-Piñeiro et al., 2013). The stomach is covered by a two-layered mucus with an inner mucus layer that is adherent to the epithelium but fully penetrable, the colon is also constituted by two layers (an inner layer attached to the epithelium, impenetrable and devoid of bacteria and an outer layer, looser in structure and

colonized by bacteria), while the small intestine is covered by a loosely attached mucus layer (Ermund et al., 2013; Larsson et al., 2013; Rodríguez-Piñeiro et al., 2013). Muc5ac is one of the most abundant proteins of the mucus layer in the stomach, while Muc2 is most abundant in the intestine mucus samples (Rodríguez-Piñeiro et al., 2013). ZG16p was found as part of the mucus proteome in all sites of the GIT and, interestingly, both ZG16p and Muc2 were both shown, by mass spectrometry and immunohistochemistry, to increase quantitatively from the stomach to the colon, where MUC2 is the most abundant mucin and ZG16p is in the top 10 of most abundant proteins of the mucus proteome (Rodríguez-Piñeiro et al., 2013). Additionally, sulfation of mucin O-glycans shows a similar pattern, increasing from the stomach to the colon. Lastly, both Muc2 and ZG16p were found to be highly expressed in the mucus-producing goblet cells (Cronshagen et al., 1994; Rodríguez-Piñeiro et al., 2013). Altogether, these results indicate a close relation between the proteoglycan Muc2 and ZG16p.

Finally, the publication of the first draft of the Human proteome (Kim et al., 2014; Wilhelm et al., 2014) allowed access to a high coverage map (over 92% of human protein-coding genes) (Wilhelm et al., 2014) of proteins expressed in several human tissues and body fluids. ZG16p was successfully identified in several tissues by both publications but the expression patterns differ from each other and from other published data (e.g., pancreatic expression is not described on both drafts). In one publication, ZG16p was found in adult colon and rectum (Kim et al., 2014), and in the other, ZG16p was found in colon, colonic epithelial cells, ileum epithelial cells, rectum, proximal fluid (coronary sinus), urine and stomach (Wilhelm et al., 2014). With a different approach, the Human Protein Atlas aims at a systematic exploration of the human proteome using antibody-based proteomics, and detected ZG16p in duodenum, small intestine, appendix, colon and rectum. As also indicated by the analysis of the ZG16 gene expression, this further shows that the expression of the lectin ZG16p is not limited to the pancreas thus pointing to multifunctional properties and a broader (patho)physiological importance, resembling the Reg proteins, a distinct family of pancreatic lectins.

1.5.3.5. Proposed functions of ZG16p

ZG16p is predominantly associated with the luminal surface of ZGM, and can be removed in conjunction with proteoglycans/GAGs by carbonate-, chondroitinase- or

heparitinase-treatment (Kleene et al., 1999b; Kumazawa-Inoue et al., 2012; Schmidt et al., 2000; Schrader, 2004). Thus, it was suggested to represent a component of the submembranous granule matrix (see Chapter 1.4), where it interacts with sulfated proteoglycans. Interestingly, ZG16p has also been found to associate with cholesterol-glycosphingolipid-enriched microdomains in the ZGM together with GP-2 and sulfated proteoglycans (Schmidt et al., 2001). However, the ZGM association of ZG16p was not influenced in GP-2 knock-out mice (Yu et al., 2004). In line with this, a function as a linker/helper protein in the binding of aggregated zymogens to the granule membrane has been proposed from *in vitro* studies (Kleene et al., 1999b). Pretreatment of ZGM with anti-ZG16p antibody in an *in vitro* condensation-sorting assay (Dartsch et al., 1998) inhibited the binding of aggregated content proteins to the membrane by about 50% whereas pretreatment with anti-amylase antibody had no significant effect (Kleene et al., 1999b) . Furthermore, ZG16p was found to bind to heparin sulfate proteoglycans, present in the ZG, by recognizing their glycosaminoglycan chains through two positive patches constituted by basic amino acids on the surface of ZG16p (Kumazawa-Inoue et al., 2012). The recent structural data on ZG16p (Kanagawa et al., 2011, 2014; Kumazawa-Inoue et al., 2012; Tateno et al., 2012) resulted in the identification of a carbohydrate recognition domain (Kanagawa et al., 2011, 2014; Tateno et al., 2012) and two proteoglycan binding sites (Kumazawa-Inoue et al., 2012). Importantly, both carbohydrate and proteoglycan binding sites are independent from each other (Kanagawa et al., 2014), suggesting that ZG16p could aid in the formation of the submembranous matrix by functioning as a linker between the GAG chains and contribute to the sorting and packaging of zymogens during ZG biogenesis (Dartsch et al., 1998; Kalus et al., 2002; Kleene et al., 1999b; Kumazawa-Inoue et al., 2012; Leblond et al., 1993; Schrader, 2004).

In addition, the recent association of ZG16p with the mucus proteome and more specifically with expression of Muc2 (a sulphated proteoglycan and the main component of the mucus in the intestine) suggests that ZG16p might also have a function after secretion (e.g., in host defence). Quantitatively, ZG16p was shown to increase from the stomach to the colon (Rodríguez-Piñeiro et al., 2013) and it is known that the small intestine is designed to limit the growth and transport of bacteria distally, whereas the large intestine harbours the commensal bacteria (Johansson et al., 2013). Interestingly, the large intestine shows higher amounts of both Muc2 and ZG16p (Rodríguez-Piñeiro et al., 2013) in the mucus layer.

Furthermore, it was demonstrated that ZG16p binds to pathogenic *Candida* and *Malassezia* species heavily coated with mannan through its carbohydrate recognition domain (Tateno et al., 2012). The leading cause of candidiasis, *Candida albicans*, resides as a commensal of the mucosa and the intestinal tract (Arendorf and Walker, 1980; Tateno et al., 2012).

Thévenod and co-workers proposed an additional function for ZG16p in the regulation of a K^+ conductance in zymogen granules (Braun and Thévenod, 2000). In an approach to identify a ZGM protein involved in the regulation of an ATP-sensitive K+ and Cl^- conductance they used a dihydropyridine derivative in photoaffinity labeling experiments. To their surprise, they labeled and purified ZG16p as a high-affinity dihydropyridine binding protein of rat ZGM. They suggested a regulatory role for ZG16p in the direct coupling between granule fusion to the plasma membrane and the activation of channels in the ZGM (Thévenod, 2002). It had already been proposed that anion-cation channels might promote "flushing out" of the granule content (i.e., enzymes or mucins) during exocytosis in pancreatic acinar cells and in intestinal goblet cells (Guo et al., 1997; de Lisle and Hopfer, 1986). It is speculated that a similar mechanism may take place after an initial, fusion pore-mediated granule swelling by the granule matrix, including ZG16p (Thévenod, 2002; Thévenod et al., 1994). This intriguing possibility remains to be elucidated.

Taken together this suggests that ZG16p might have multiple functions at different locations, highlighted by its expression in different tissues, and points to a broader (patho)physiological importance.

1.6. Pancreatic diseases

Under physiological conditions, the pancreatic acinar cells are subjected to high levels of stress, mostly due to the high rate of protein synthesis and secretion. To prevent autodigestion, the pancreatic acinar cells normally synthesize proteolytic enzymes in the inactive zymogen form, but if prematurely activated those enzymes are capable of damaging the cells and consequently the pancreas itself. Pancreatic damage can be acute or chronic. Acute damage is associated with the generation of an inflammatory response, which can be mild and localized to the pancreas (acute pancreatitis), or severe and systemic. The systemic inflammation resulting from pancreatic disease can lead to multiple organ failure and mortality (Logsdon and Ji, 2013). Chronic damage to the pancreas results in chronic

pancreatitis with acinar cell destruction and replacement with fibrosis or fat, which if extensive, leads to exocrine insufficiency. It also increases the probability of genetic instability and thus the risk of developing pancreatic cancer, especially pancreatic ductal adenocarcinoma (PDAC) (Logsdon and Ji, 2013). The rate of pancreatic cancer in patients with chronic pancreatitis is greater than that in age-matched controls (Lowenfels et al., 1993), and the risk is especially high in patients with prolonged pancreatic inflammation due to hereditary pancreatitis (Lowenfels et al., 1997; Whitcomb and Beger, 2008). Currently, no effective treatments beyond surgery exist for either PDAC or pancreatitis, two diseases associated with severe pain (Logsdon and Ji, 2013).

1.6.1. New insights in the study of pancreatitis. The role of autophagy in pancreatitis

Chronic pancreatitis is a progressive inflammatory disorder in which the pancreatic secretory parenchyma is destroyed and replaced by fibrous tissue, eventually leading to malnutrition and diabetes. Traditionally, chronic pancreatitis has been classified as fundamentally different from acute pancreatitis, which is usually characterised by restoration of normal pancreatic histology after full clinical recovery (Sarles, 1986). However, acute, recurrent acute, and chronic pancreatitis are now regarded as a disease continuum (Braganza et al., 2011; Mitchell et al., 2003; Whitcomb, 2004). Pathologic responses arising from the pancreatic acinar cell appear to have a central role in initiating acute pancreatitis. Activation of zymogens within the acinar cell and an inhibition of secretion are critical, but poorly understood, early pancreatitis events. Additionally, stimulation of acinar cell autophagy has been a recognized feature of acute pancreatitis for years, although its role remains to be clarified (Gorelick and Thrower, 2009). Mice deficient in the ability to form autophagosomes are resistant to acute pancreatitis (Hashimoto et al., 2008), suggesting that formation of autophagosomes is also an important step to develop pancreatitis (Feng et al., 2012). It is thought that autophagy might have multiple roles in acute pancreatitis. For example, distinct autophagic events could modulate zymogen activation (leading to pancreatitis) *vs* the degradation of active zymogens in the acinar cell (protecting from pancreatitis) (Gorelick and Thrower, 2009).

Recent studies have suggested that impaired autophagic flux due to deficient lysosomal degradation is an important mechanism that contributes to intra-acinar trypsin

activation and pancreatitis (Feng et al., 2012; Fortunato and Kroemer, 2009; Gukovsky and Gukovskaya, 2010; Mareninova et al., 2009). Autophagy encompasses several intracellular pathways of lysosome-driven degradation and recycling of organelles and long-lived proteins (Gukovskaya and Gukovsky, 2012). Impaired autophagy mediates two key pathological responses of pancreatitis: accumulation of vacuoles in acinar cells and the abnormal, intra-acinar activation of digestive enzymes such as trypsinogen (Gukovsky et al., 2011). The lysosomal function is impaired in pancreatitis through at least two mechanisms, which both cause retarded autophagic flux: (1) deficient lysosomal proteolytic activity and (2) pathologic alterations in lysosomal membrane proteins, such as LAMPs. For example, LAMP-2 genetic ablation causes autophagy impairment in pancreas (Tanaka et al., 2000), with accumulation of large autolysosomes containing poorly degraded material. The decreased activity of proteolytic activity is a result from impaired maturation of hydrolases and consequent defective activation. The delivery of hydrolases to the lysosome is a multistep process controlled by the Golgi and the endosomal system (Gukovskaya and Gukovsky, 2012). During trafficking, cathepsins undergo proteolytic processing (maturation) to become active enzymes: first, in endosomes, this process generates an intermediate, “single-chain” form of cathepsins, and then, mainly in the lysosome, a fully mature “double-chain” active form. Therefore, the lysosomal/autophagic dysfunction may be a manifestation of a more general phenomenon, indicating disordering of endo-lysosomal traffic in pancreatitis (Gukovskaya and Gukovsky, 2012).

OBJECTIVES

2. Objectives

To understand the molecular machinery required for granule biogenesis, sorting and secretion in exocrine cells, a better molecular characterization of the components of the ZGM is required. Clearly, these components have a central function in granule formation at the TGN, in protein sorting, apical exocytosis and membrane fusion as well as regulation of exocytosis. The disturbance of these regulated processes (incorrect compartmentalization, premature activation of the zymogens, uncontrolled and unspecific fusions) can cause pathological changes of the pancreas, e.g. during acute pancreatitis. The identification of membrane components of ZG, their molecular characterization and the unravelling of their functions in granule biogenesis and regulated secretion are therefore highly relevant for both cell biologists and clinical research developments.

We favour a model, in which a predicted submembranous matrix composed of high molecular weight components and associated proteins attached to the luminal side of the ZGM fulfils important functions during the sorting and packaging of secretory proteins. Furthermore, the submembranous matrix might have protective and mechanical properties, e. g., to maintain membrane curvature, granule shape and stability (Borta et al., 2010; Schrader, 2004). Since specific membrane receptors or sorting signals have not yet been identified in exocrine cells, the concept of the submembranous matrix offers an interesting alternative to understand the packaging and sorting of zymogens in ZG. Once in the intestinal tract matrix proteins such as ZG16p, syncollin, or GP2 are also supposed to fulfil important protective functions, e.g. in host defence (Bach et al., 2006; Hase et al., 2009; Tateno et al., 2012). Our main goal is to understand the molecular machinery required for granule biogenesis, using the pancreatic acinar cell as a model system, with the specific aims:

a) Isolation and identification of membrane-associated proteins of the predicted submembranous granule matrix.

b) Characterization of the biochemical properties and function (by mutational analyses) of the secretory lectin ZG16p, a membrane-associated protein.

c) Explore the potential of ZG16p as a new tool for labelling the endo-lysosomal compartment.

MATERIAL AND METHODS

3. Material and Methods

3.1. Frequently used buffers and solutions

Blocking solution for immunofluorescence:

1% (w/v) BSA in PBS

Blocking solution for immunoblots:

5% (w/v) milk powder in PBS

Cell culture medium for COS-7, AR42J and HepG2 cells:

DMEM, high glucose (4.5 g/l) with L-glutamine; 10% (v/v) FBS; 100 U/ml Penicillin; 100 µg/ml Streptomycin

Equilibration buffer (2D-GE)

6 M urea, 75 mM Tris-HCl pH 8.8, 34.5% Glycerol (87%), 2% SDS, 0.002% bromophenol blue and 1.5 mM DTT

Fixative for immunofluorescence:

4% (w/v) Paraformaldehyde in PBS, pH 7.4

HBS – HEPES buffered saline, pH 7.15, for electroporation:

5 g/l HEPES; 8 g/l Sodium chloride; 0.37 g/l Potassium chloride; 0.1 g/l Sodium phosphate dibasic; 1.08 g/l D(+)Glucose

LB medium:

2.5% (w/v) LB-Broth Miller

LB plates:

2.5% (w/v) LB-Broth Miller; 1% (w/v) Agar

Mounting medium for immunofluorescence:

3 volumes Mowiol stock; 1 volume n-propylgallat stock

Mowiol stock:

12 g Mowiol 4-88; 40 ml PBS, 20 ml Glycerol

n-propylgallate stock (antifading):

2.5% (w/v) Propylgallate in PBS; 50% (v/v) Glycerol

PBS – phosphate buffered saline, pH 7.35:

140 mM Sodium chloride; 2.5 mM Potassium chloride; 6.5 mM Sodium phosphate dibasic; 1.5 mM Potassium phosphate dibasic

Permeabilization for immunofluorescence:

0.2% (v/v) Triton X-100 in PBS

Protease inhibitor mix (final concentrations):

0.1 mM PMSF; 0.01 mM FOY 305; 0.25% (v/v) Trasylol

Rehydration Buffer (2D-PAGE)

8 M Urea; 2 M Thiourea; 1% CHAPS; 12.9 mM DTT; 0.1% Pharmalyte 3-10 (IPG buffer); 0.01% Bromophenol Blue

SDS loading buffer (Laemmli 1970):

60 mM Tris, pH 6.8; 2% (w/v) SDS; 10% (v/v) Glycerol; 0.005% (w/v) Bromophenol blue; 20 mM DTT; 5% (v/v) β-Mercaptoethanol (fresh)

SDS-PAGE running buffer:

25 mM Tris-HCl; 190 mM Glycine; 0.1% (w/v) SDS

Semidry blotting buffer:

48 mm Tris-HCl; 39 mM Glycine; 0.4% (w/v) SDS; 20% (v/v) Methanol

TAE – Tris-Acetate-EDTA (50x), pH 8.0:

40 mM Tris; 20 mM Acetic acid; 1 mM EDTA

Tris buffer separation gel (pH 8.8):

2 M Tris-HCl

Tris buffer stacking gel (pH 6.8):

1 M Tris-HCl

Zymogen Granule homogenization buffer:

0.25 M sucrose; 5 mM 2-N-morpholino-ethanesulfonic acid (MES), pH 6.25; 0.1 mM $MgSO_4$; 10µM Foy 305; 2.5 mM Trasylol; 0.1 mM phenylmethylsulfonyl fluoride (PMSF).

3.2. Lists of antibodies, plasmids and primers used

Table 1. List of primary antibodies and corresponding dilutions

Antibody	Source / Reference	Dilution	
		IMF	WB
Amylase (rabbit pc)	Sigma-Aldrich	1:200	1:2000
BiP (mouse mc)	BD Biosciences		1:1000
Calnexin (rabbit pc)	Stressgen		1:1000
Carboxypeptidase A (rabbit pc)	Rockland, Immunochemicals	1:800	1:5000
Chymase (goat pc)	LB Schwarz, Virginia Commonwealth University		1:1000
CEL (chicken pc)	Borta, Aroso et al. 2010		1:88
Chymotrypsin (sheep pc)	Eigene Herstellung, Marburg	1:400	1:2000
EEA1 (rabbit pc)	Abcam	1:500	
GFP (rabbit pc)	Invitrogen, Molecular Probes		1:2000
GP2 (4AS9 mouse mc)	A. Lowe, Stanford University, USA		1:2000
Myc (mouse mc)	Santa Cruz Biotechnology	1:200	
p115 (mouse mc)	BD Biosciences	1:200	
PDI R-707 (rabbit pc)	HD Sölling, Max-Planck Institute for Biophysical Chemistry	1:500	
PpiB (rabbit pc)	Abcam	1:100	1:1000
RNaseA (rabbit pc)	Sigma-Aldrich	1:1000	
TGN38 (guinea pig-pc)	H. F. Kern (ref 1995)	1:100	
Tryptase β1 (mouse pc)	R&D Systems		1:1000
ZG16p N1d1 (rabbit pc)	Cronshagen, Voland et al. 1994	1:200	1:2000

Abbreviations: pc, polyclonal; mc, monoclonal; IMF, immunofluorescence; WB, Western blot

Table 2. List of secondary antibodies and corresponding dilutions

Antibody	Source	Dilution	
		IMF	**WB**
TRITC Donkey anti Mouse	Dianova	1:200	
TRITC Donkey anti Rabbit	Dianova	1:200	
TRITC Donkey anti Sheep	Dianova	1:400	
Alexa 488 Goat anti Mouse	Invitrogen	1:400	
Alexa 488 Goat anti Rabbit	Invitrogen	1:400	
HRP Rabbit anti Chicken	Sigma-Aldrich		1:2000
HRP Donkey anti Goat	Dianova		1:2000
HRP Goat anti Mouse	Bio Rad		1:5000

Antibody	Source	Dilution	
		IMF	WB
HRP Goat anti Rabbit	Bio Rad		1:5000

Abbreviations: pc, polyclonal; mc, monoclonal; IMF, immunofluorescence; WB, Western blot

Table 3. Plasmids used in this study

Name	Source
pDsRed2-ER	Clontech
pET-28b	Novagen
pCMV-Tag 3A	Stratagene
pcDNA3	Invitrogen
pEGFP-C1	Clontech
Lamp1-GFP	Steve Caplan, University of Nebraska, USA

Table 4. Plasmids cloned during this study

Name	Vector	Primer	Template
H-ZG16dSP	pET-28b	UpHis-Zg16 & ZG16down	Myc-ZG16dSP
HMyc-ZG16dSP	pET-28b	UpHisMycZG16 & ZG16down	Myc-ZG16dSP
ER-Myc-ZG16dSP	pDsRed2-ER	ER-Myc-Up & ZG16down	Myc-ZG16dSP
ER-Myc-ZG16dSP_K	pDsRed2-ER	K33A.K36A.R37Afw & K33A.K36A.R37Arv	ER-Myc-ZG16dSP
ER-Myc-ZG16dSP_R	pDsRed2-ER	R55A.R58Afw & R55A.R58Arv	ER-Myc-ZG16dSP
ER-Myc-ZG16dSP_D	pDsRed2-ER	D151Afw & D151Arv	ER-Myc-ZG16dSP
ER-Myc-ZG16dSP_K_R	pDsRed2-ER	R55A.R58Afw & R55A.R58Arv	ER-Myc-ZG16dSP_K
ER-Myc-ZG16dSP_K_D	pDsRed2-ER	D151Afw & D151Arv	ER-Myc-ZG16dSP_K
ER-Myc-ZG16dSP_R_D	pDsRed2-ER	D151Afw & D151Arv	ER-Myc-ZG16dSP_R
ER-Myc-ZG16dSP_KRD	pDsRed2-ER	D151Afw & D151Arv	ER-Myc-ZG16dSP_K_R
ER-Myc-ZG16dBM	pDsRed2-ER	ER-Myc-Up & ZG16part1down & ZG16part2up & ZG16down	Myc-ZG16dSP
ER-Myc-ZG16d21	pDsRed2-ER	ER-Myc-Up & ZG16d24down	Myc-ZG16dSP
Myc-ZG16dSP	pCMV-Tag 3A	ZG16up & ZG16down	Rat cDNA
Myc-ZG16dSP_K	pCMV-Tag 3A	K33A.K36A.R37Afw & K33A.K36A.R37Arv	Myc-ZG16dSP

Name	Vector	Primer	Template
Myc-ZG16dSP_R	pCMV-Tag 3A	R55A.R58Afw & R55A.R58Arv	Myc-ZG16dSP
Myc-ZG16dSP_D	pCMV-Tag 3A	D151Afw & D151Arv	Myc-ZG16dSP
GFP-ZG16dSP[γ]	pEGFP-C1	UpGFPZG16 & DownGFPZG16	Myc-ZG16dSP
GFP-ZG16dSP_K	pEGFP-C1	K33A.K36A.R37Afw & K33A.K36A.R37Arv	GFP-ZG16dSP
GFP-ZG16dSP_R	pEGFP-C1	R55A.R58Afw & R55A.R58Arv	GFP-ZG16dSP
GFP-ZG16dSP_D	pEGFP-C1	D151Afw & D151Arv	GFP-ZG16dSP
ZG16dSP[γ]	pcDNA3	ZG16-dSP_f2 & ZG16down	Myc-ZG16dSP

[#] KDEL (ER retention signal) sequence was removed during cloning; [γ] Cloned by María Gómez Lázaro (Centre for Cell Biology, University of Aveiro)

Table 5. Primer sequences used for cloning in this study

Name	Sequence	Enzyme
UpHis-Zg16	CTA GCT AGC AAT TCC ATT CAG TCC AGG TCC TCC	NheI
ZG16down	CCG CTC GAG TCA ACA AGT GTT GCA GTG GCT AG	XhoI
UpHisMycZG16	CTA GCT AGC ATG GAG CAG AAA CTC ATC TCT GAA G	NheI
ER-Myc-Up	T TAC CGG TCC ATG GAG CAG AAA CTC ATC TCT GAG G	AgeI
K33A.K36A.R37Afw[¥]	GGA GAG TAT GGC GGT *GCA* GGA GGA *GCG GCA* TTC TCT CAC TCT GG	–
K33A.K36A.R37Arv[¥]	CCA GAG TGA GAG AA*T GCC GC*T CCT CC*T GC*A CCG CCA TAC TCT CC	–
R55A.R58Afw[¥]	CT GCC ATC CGG ATC *GCT* GTC AAC *GCA* TAC TAC ATA ATA GGT CTC C	–
R55A.R58Arv[¥]	G GAG ACC TAT TAT GTA GTA *TGC* GTT GAC *AGC* GAT CCG GAT GGC AG	–
D151Afw[¥]	CGA TCT GGC TCT GCC ATA *GCT* GCT ATC AGC CTG CAC	–
D151Arv[¥]	GTG CAG GCT GAT AGC *AGC* TAT GGC AGA GCC AGA TCG	–
ZG16part1down[λ]	GCA GGC TGA TAG CAG ATC GGC CAC TAA TGA AAC GG	–
ZG16part2up[λ]	GTG GCC GAT CTG CTA TCA GCC TGC ACT GGG ATA C	–
ZG16d24down	CCG CTC GAG TCA GTA GGT ATC CCA GTG CAG	XhoI
ZG16up	AA CTG CAG AGC TCG CAA TTC CAT TCA GTC CAG GTC CTC C	PstI
ZG16down	CCG CTC GAG TCA ACA AGT GTT GCA GTG GCT AG	XhoI
UpGFPZG16	CCC AAG CTT TGA ATT CCA TTC AGT CCA GGT CCT	Hind III
DownGFPZG16	GG GGT ACC TCA ACA AGT GTT GCA GTG GCT A	KpnI
ZG16-dSP_f2	CCC AAG CTT ACC ATG AAT TCC ATT CAG TCC AGG TCC	HindIII

[¥] Primers used for the QuikChange site-directed mutagenesis method. [λ] Primers used for deletion of ZG16p carbohydrate recognition domain (CRD)

3.3. Molecular biology techniques

3.3.1. Cloning of DNA plasmids

The PCRs performed for cloning in this study are listed with template, primer pair and target vector in Table 4, and primer sequences and restriction endonuclease cutting sites, in Table 5. PCRs were performed with KOD DNA polymerase (Novagen, Darmstadt, Germany). PCR products and other DNA samples were separated by agarose gel electrophoresis. Routinely 0.8 to 1% (w/v) gels were used. Agarose was dissolved in TAE buffer (3.1) by boiling in a microwave. The solution was cooled down until being hand-hot and ethidium bromide was added (0.5 µg/ml). DNA samples were mixed with 6x DNA loading dye (Thermo Scientific) and a co-migrating DNA ladder (ruler DNA ladder mix) (Fermentas) was used to mark DNA sizes. Gene Separation was performed at maximal 5 V per cm electrode distance (60 to 130 V) for 30 to 60 minutes. Digital images were taken using AlphaImager HP (ProteinSimple, California, USA) and quantification was done with the provided software. The PCR product and the target vector were isolated from agarose gels using a gel extraction kit (Nucleospin gel and PCR clean Up, Macherey-Nagel, Duren, Germany). The DNA bands visible with UV light were cut with a scalpel and transferred to a microtube. Agarose was melted at 50°C in the supplied buffer and the DNA was extracted with spin columns. Elution was performed using 30 µl of distilled water. PCR product extracted from the agarose gel and the target vector were digested with the same two enzymes. Routinely, preparative digestions were performed at 37°C overnight. Afterwards, successful digestion was checked on an agarose gel, the DNA was isolated and the vector was incubated with 1 µl Antarctic phosphatase in the provided buffer for 30 minutes at 37°C. Subsequently, phosphatase was inactivated at 65°C for 10 minutes. For ligation, DNA concentrations of vector and insert were determined by comparing each gel band intensity with the intensity of the bands of co-migrated DNA ladder with known quantity on an agarose gel. The molecule ratios chosen between vector and insert were mostly between 1:3 and 1:5 following the estimated calculation:

$$mass_{insert}\ (ng) = \frac{5 \times mass_{vector}\ (ng) \times length_{insert}\ (kb)}{lenght_{vector}\ (kb)}$$

Ligation was assembled by preparing a 20 µl reaction with T4 Ligase (400 U/µl), 50 ng of vector and the corresponding amount of insert, and incubated at 16°C overnight. The plasmid formed was transformed and amplified in *E. coli* (3.6.4) and screened for correct

ligations by analytical RE digestion (3.6.5.1). A control reaction without insert was performed side-by-side. The PCR products were cloned in frame into cloning vectors (Table 4) and all constructs were verified by sequencing (Eurofins Genomics, Ebersberg Germany).

Table 6. PCR programme for cloning

Construct	PCR programme				
		30 Cycles			
	Denaturation & activation	Denaturation	Annealing	Elongation	Elongation (final)
Myc-ZG16dSP ER-Myc-ZG16dSp H-ZG16dSp HMyc-ZG16dSP GFP-ZG16dSp ZG16dSP ER-Myc-ZG16d21	2 min	95˚C 20 s	55˚C 10 s	70˚C 10 s	70˚C 2 min

3.3.2. Bacterial culture

For cloning and amplification of DNA plasmids *Escherichia coli* (DH5α or XL1-Blue) cultures were used. The bacteria were cultured in LB medium containing a selective antibiotic (100 mg/ml Ampicillin or 30 µg/ml Kanamycin) at 37˚C and 200 rpm in an incubator shaker. Long-time storage of *E. coli* cultures was performed as 15% glycerol mixtures at –80˚C. For single-cell colonies bacteria were spread on LB agar plates and incubated overnight in a 37˚C incubator. Plates were short-term stored at 4˚C and the bacterial colonies were used for inoculation of liquid cultures (3 to 5 ml).

3.3.3. Preparation of competent bacterial cells

5 ml of an *E. coli* DH5α culture grown overnight were diluted in 500 ml LB medium and shaken at 37˚C for 2 to 3 hours until an optical density of OD_{600} = 0.4 was reached. The culture was chilled on ice for 15 minutes and centrifuged at 3000 rpm, 4°C for 15 minutes. The pellet was resupended in 40 ml ice-cold 0.1 M calcium chloride ($CaCl_2$) solution and incubated on ice for 30 minutes. The bacteria were re-centrifuged, the pellet was resuspended in 20 ml ice-cold 0.1 M calcium chloride solution and 20% (v/v) glycerol was added. After

incubation on ice for 2 hours aliquots of 100 µl were frozen in liquid nitrogen and stored at –80˚C.

3.3.4. Chemical transformation

100 µl competent *E. coli* cells were mixed with the plasmid DNA (e.g. from a ligation reaction) and incubated on ice for 30 minutes. After a 90 seconds heat shock at 42˚C the bacteria were chilled on ice and 700 µl LB medium without antibiotics was added, followed by 1 hour shaking incubation at 37˚C. A cell pellet was formed by centrifugation (3 minutes at 5000 rpm) and resuspended in 25 - 50 µl LB medium. The suspension was spread on a LB agar plate containing a selective antibiotic using sterile glass beads and grown overnight at 37˚C.

3.3.5. Plasmid isolation

3.3.5.1. Analytical restriction endonuclease (RE) digestion

Plasmid isolation for screening for correct plasmid ligation by analytical RE digestion was done as follows: 3 ml *E. coli* cultures inoculated from single colonies were grown overnight and sedimented twice by centrifugation at 5000 rpm for 3 minutes. The supernatant was carefully removed and the pellet was completely resuspended in 100 µl cold solution I. 200 ml solution II were added and mixed by inverting the tube five times (maximal 5 minutes). After addition of 150 µl cold solution III and mixing by inverting the lysate was incubated on ice for 3 to 5 minutes. The precipitate formed was removed by centrifugation at 13000 rpm, 4°C for 10 minutes and the supernatant was transferred to a new tube. The DNA was precipitated by addition of 2 volumes 96% ethanol, incubation at room temperature for 2 minutes and centrifugation at 13000 rpm, 4°C for 5 minutes. The pellet was washed with 1 ml 70% ethanol and centrifuged for 5 minutes at 13,000 rpm, 4°C. After air-drying the pellet was resuspended in 50 ml water supplemented with 20 µg/ml RNase, if the RNase has not been added to solution I.

Solution I: 50 mM glucose; 25 mM Tris; 10 mM EDTA; (100 µg/ml RNase), pH 8.0, autoclaved

Solution II: 0.2 M sodium hydroxide; 1% (w/v) SDS

Solution III: 3 M potassium acetate; 11.5% v/v glacial acetic acid, pH 4.8

3.3.5.2. Mini-prep

Plasmid isolation for sequencing was done with the Nucleospin® plasmid kit (Macherey-Nagel). 3 ml *E. coli* cultures were grown overnight and sedimented twice by centrifugation at 5,000 rpm for 3 minutes. The supernatant was carefully removed and the pellet was completely resuspended in 250 µl of buffer A1. Then, 250 µL of buffer A2 were added, the tube was mixed gently by inverting 6-8 times and incubated at room temperature for up to 5 min. 300 µL of buffer A3 were added, the tube was mixed gently by inverting 6-8 times and centrifuged for 5 min, 11000×*g* at room temperature. The column was placed in a collection tube (2 ml), the supernatant was decanted to the column and centrifuged for 1 min at 11000×*g*. The flow-through was discarded. The silica membrane was washed with 600 µL buffer A4 and dried by centrifugation for 2 min at 11000×g. The column was placed on a 1.5 mL microcentrifuge tube, 30 µl of sterile distilled water were added to the column and incubated for 1 min at room temperature. The DNA was eluted with centrifugation for 1 min at 11000×*g*. To increase the elution yield the last step was repeated with 20 µl of sterile distilled water.

3.3.5.3. Midi-prep

For isolation of larger quantity of plasmids the Nucleobond® Xtra Midi (Macherey-Nagel) was used. 200 ml *E. coli* cultures were grown overnight and sedimented by centrifugation at 6000×*g* for 15 minutes. The supernatant was carefully removed and the pellet was completely resuspended in 8 ml of buffer RES. Then, 8 ml of buffer LYS were added, the tube was mixed gently by inverting 6-8 times and incubated at room temperature for up to 5 min. 8 ml of buffer NEU were added and the tube was mixed gently by inverting 6-8 times. The column together with the filter were equilibrated with 12 ml of buffer EQU and the lysate was loaded on the Nucleobond® Xtra column filter. The column was washed with 5 ml of buffer EQU and the Nucleobond® Xtra column filter discarded. The column was washed again with 8 ml of buffer WASH the DNA eluted with 5 ml of buffer ELU. The DNA was precipitated with 3.5 ml of isopropanol and centrifuged at 15000×*g* for 30 min at 4˚C. The DNA pellet was washed with 2 ml of 70% ethanol and centrifuged at 15000×g for

5 min at 4˚C. After drying the DNA was reconstituted in 200-300 µl of sterile distilled water and frozen at –20°C until usage.

3.3.6. Measurement of DNA concentrations

1 µl of a DNA preparation was diluted 1:500 (midi-prep) or 1:200 (mini-prep) in water and measured in a quartz cuvette with water as blank at 260 and 280 nm. A clean DNA preparation should have an OD_{260}/OD_{280} ratio of 1.8

3.3.7. *In vitro* site-directed mutagenesis

Mutant plasmids were generated using the QuickChange site-directed mutagenesis kit (Agilent Technologies, California, USA). The mutagenic oligonucleotide primers were designed individually according to the desired mutation (Table 5) and they anneal at the same sequence on opposite strands of the plasmid. Typically, 20 ng of double-stranded DNA (dsDNA) was used and sample reactions were prepared with KOD DNA polymerase and 125 ng of each primer. Cycling parameters were set as indicated on Table 7. Then, the amplification products were digested with 1 µl of the *Dpn* I restriction enzyme (10 U/µl) at 37˚C for 1 hour. Transformation of XL1-Blue was performed as described in 3.6.4 with 1 µl of the *Dpn* I treated DNA. All constructs were verified by sequencing (Eurofins Genomics).

Table 7. PCR programme for the QuickChange site-directed mutagenesis method

Cycles	Temperature	Time
1	95˚C	30 sec.
16	95˚C	30 sec.
	55˚C	1 min.
	68˚C	5 min

3.4. Biochemical Methods

3.4.1. Cellular subfractionation

3.4.1.1. Isolation of Zymogen Granules

ZG were isolated from the pancreas of male Wistar rats (200-230 g) (Charles River, Sulzfeld, Germany) which were fasted overnight. Tissue homogenization was performed in zymogen granule homogenization buffer. 4-6 Pancreata were individually minced with a scissor on 1 ml of homogenization buffer. Then the total volume was made up to 10 ml with homogenization buffer and it was further homogenized on ice using a brendle type homogenizer (Yellow line, OST20 Digital, Imlab, Belgium). The homogenate was transferred to conical glass tubes, centrifuged for 10 min, 4°C at 500×*g*, and the resulting post nuclear supernatant was further centrifuged for 10 min, 4°C at 2000×*g* to sediment ZG. The brownish layer of mitochondria on top of the pellet was removed by resuspending in homogenization buffer. The white zymogen granules in the bottom were collected in homogenization buffer. Tissue homogenization was repeated 2-3 times. The collected ZG fractions were combined and centrifuged for 20 min, 4 °C at 2000×*g*. The final ZG pellet was resuspended (2-3 ml) in HEPES buffer and frozen at -20˚C. All centrifugation steps were performed in an Eppendorf centrifuge 5810R (Eppendorf, Hamburg, Germany) with a swinging bucket rotor.

3.4.1.2. Zymogen Granule Subfractionation

Isolated granules (in HEPES buffer) were carefully lysed by freezing and thawing and separated into zymogen granule content (ZGC) and membrane (ZGM) fractions by centrifugation at 100000×*g* for 30 min in a swinging-bucket rotor (SW50.1) (Beckman Coulter, Fullerton, USA). The membranes were rinsed and resuspended in HEPES buffer and treated with 150 mM Na_2CO_3, pH 11.5 for 2 h on ice. Treated membranes (ZGMcarb) were recovered by centrifugation at 100000×*g* for 30 min and thereby separated from peripheral membrane proteins (Wash). Isolated ZGMcarb were resuspended in 50 mM HEPES, pH 8.0.

Alternatively, purified ZG were resuspended in HEPES buffer with 80 mM KCl, carefully lysed by freezing and thawing and centrifuged through a 0.3/1 M sucrose step

gradient for 1 h, 4°C at 200000×*g* (Beckman 80 Ti rotor). ZGM were recovered at the interface and washed twice in HEPES buffer or in 100 mM $NaHCO_3$, pH 8.1. After each washing step, ZGM were recovered by centrifugation for 1 h, 4°C at 150000×*g* (Beckman 80 Ti rotor). Finally, membranes were rinsed and resuspended in HEPES buffer.

A microsome-enriched fraction was obtained from a pancreas homogenate after subcellular fractionation and ultracentrifugation (100000×*g* for 1 h, 4°C; Beckman SW50.1).

3.4.2. Determination of protein concentration

Protein concentrations were determined using the Bradford assay (Bradford 1976). Standards containing 1 to 20 µg BSA, blank, and samples (1 to 10 µl) were filled up to 100 µl with 0.1 M NaOH. Protein assay solution (Bradford) (Biorad, California, USA) was diluted 1:5 with distilled water and 1 ml of the solution was added to each sample. All standards and samples were prepared as triplicates. After 15 minutes of incubation at room temperature the absorption at 595 nm compared to the blank was measured. Using the standard curve prepared from the mean values, the protein concentration of the samples was calculated. Assays were run with a recording spectrophotometer (Ultraspec 100 pro, Amersham Biosciences, Uppsala, Sweden).

3.4.3. Protein precipitation

Routinely, precipitation was performed using trichloroacetic acid (TCA) by mixing (1:1) the sample (if below 100 µl the volume was completed with distilled water) and 20% (w/v) TCA. The mixture was then incubated on ice for 15-20 min and centrifuged for 5 min at 13000 rpm, 4˚C and the supernatant was discarded. The resulting pellet was washed with 5% TCA, centrifuged for 2 min at 13000 rpm, 4˚C and the supernatant was discarded. The pellet was re-washed with distilled water and centrifuged as before. Finally, the pellet was washed with 500 µl of ice-cold acetone, centrifuged for 15 min at 13000 rpm, 4˚C and the supernatant was discarded. Samples were then air-dried and resuspended in the suitable buffer (e.g. SDS-PAGE loading buffer).

3.4.4. Enterokinase assay

Isolated ZG or ZG fractions (ZGM, ZGC, Wash) with concentration of 5 µg/µl were incubated with and without Enterokinase (0.02 units) (Sigma-Aldrich, Karlsruhe, Germany) in HEPES buffer (pH 8.0), 37˚C for 24 h or 48 h. After digestion, 40 µg of total protein were analysed by SDS-PAGE on 15% acrylamide gels

3.4.5. Digestion of HMyc-ZG16dSP and H-ZG16dSP with trypsin

3 µg of recombinant protein were mixed with 30 ng of sequence grade modified porcine trypsin (Promega, Madison, USA) prepared in 25 mM ammonium bicarbonate and incubated overnight at 37˚C. Then the sample was mixed with SDS-PAGE loading buffer, analysed by SDS-PAGE gel and stained with Coomassie blue. The Wash subfraction from ZG (40 µg) was used as endogenous ZG16p control. For immunoblot analysis 1/10 of the sample was separated by SDS-PAGE.

3.4.6. Sodium-dodecyl sulphate polyacrylamide gel electrophoresis (SDS-PAGE)

Standard SDS-PAGE was performed with 15% polyacrylamide (PA) separating and 5% PA stacking gels. Gel electrophoresis in mini gel chambers was conducted for approximately 1 h at 180 V until the running front (bromophenol blue) reached the bottom of the gel. The gel chambers were filled with 1x SDS running buffer (3.1). Several protein molecular weight markers were used according to final application of the gel: for Coomassie blue staining the BenchMark™ protein ladder (Invitrogen, Carlsbad, USA) was used; for immunoblotting the Precision Plus Protein™ Kaleidoscope™ standards (BioRad) were applied.

3.4.7. Sample preparation for SDS-PAGE

Typically samples were prepared with SDS-PAGE loading buffer (3.1), heated at 95˚C for 5 min and loaded on the SDS-PAGE gel. Alternatively, samples were prepared on SDS-PAGE loading buffer, heated at 37˚C or 65˚C for 5 min or heated at 95˚C for 10 min, previous to gel loading.

3.4.8. Bidimensional gel electrophoresis (2D-GE)

The first dimension of 2D-GE was performed in a horizontal apparatus (Ettan IPGphor, GE Healthcare, San Francisco, USA). Granule subfractions were precipitated with TCA (3.2.2). Protein samples (300 µg) were solubilized for 30 min at 30 °C in rehydration buffer (3.1). The samples were then applied onto IPG strips (11 cm, pH 3-11) and isoelectric focusing was conducted at 20 °C with 50 µA, for a minimum of 10 h at 50 V, 1 h at 500 V, 1 h at 1000 V and 110 min at 8000 V. The strips were afterwards incubated for 15 min in equilibration buffer (3.1) and then applied on top of a SDS-PAGE gel (14 cm by 14 cm, 15% PAA). Proteins were separated according to molecular weight in a Hoefer 600 SE RUBY chamber (GE Healthcare, Connecticut, USA), 200 V for 3-4 hours.

3.4.9. Staining with Colloidal Coomassie Brilliant Blue G-250

Gels were fixed agitating for 30 min in 10% (v/v) acetic acid and 40% (v/v) methanol, followed by a washing step in distilled water. Staining was performed for 2 h in 0.32% (w/v) Coomassie G250 in 20% (v/v) methanol. To wash out unbound Coomassie-G250 and visualize protein bands, gels were destained by washing in dH_2O for 1-2 min followed by several times washing in destaining solution containing 25% (v/v) methanol. Gels were then kept in dH_2O and scanned with a Bio-Rad GS-710 Calibrated Imaging Densitometer.

3.4.10. Alcian Blue Staining

Gels were fixed and stained overnight with 0.5% (w/v) alcian blue in 2% (v/v) acetic acid and destained with distilled water. Gels were then kept in dH_2O and scanned with a Bio-Rad GS-710 Calibrated Imaging Densitometer.

3.4.11. Immunoblotting

Protein transfer from SDS-PAGE gels to the membrane was performed by semidry Western blotting (Trans-Blot SD, Biorad) (Kyhse-Andersen 1984). The nitrocellulose membrane and two Whatman filter papers (3 mm) were soaked with semidry blotting buffer (3.1) and a stack of Whatman filter, membrane, gel, and Whatman filter was formed. Air bubbles in between the layers had to be removed to guarantee complete transfer. The stack

was put into a semidry transfer chamber and the proteins were blotted for 45 minutes at 12 V. Next, the membrane was blocked by incubation with 5% low fat powdered milk in PBS for 1 h. For incubation with the primary antibody the membrane was sealed into a plastic bag with the respective antibody dilution in PBS and incubated with shaking over night at 4°C or for 2 to 3 h at room temperature. Afterwards the membrane was washed three times for 10 minutes to remove excess (unbound) antibody. The incubation with the secondary antibody was performed for 1 to 2 h at room temperature. For the ECL (Amersham, New Jersey, USA) reaction, ECL 1 (containing luminol) and ECL 2 (phenol-containing enhancer) solutions were mixed (ratio 1:1) and the membrane was incubated for 1 min. Film exposure (1 to 30 minutes), development and fixation (Carestream® Kodak® autoradiography GBX developer/fixer, Sigma-Aldrich**)** were performed in a light protected environment. For presentation and quantification the films were scanned with a Bio-Rad GS-710 Calibrated Imaging Densitometer and densitometric analysis for quantification was done using Bio-Rad Laboratories Quantity One software.

3.4.12. Reprobing of immunoblots

Reprobing of immunoblots was done after inactivation of peroxidase activity of the secondary antibody as described by Sennepin et al. 2009. Typically, the irreversible HRP inhibition was performed by incubating the membrane (48 cm^2) for 30 min with 2 ml of 30% H_2O_2 (Sigma-Aldrich) at 37˚C.

3.4.13. Co-Immunoprecipitation

Usually, two confluent 100 mm dishes of COS-7 cells transfected with GFP-ZG16dSP_K, GFP-ZG16dSP or GFP by electroporation (3.4.6) were used. The cells were washed with PBS and carefully harvested in a total volume of 3 ml PBS by scraping. All further steps were performed on ice. A cell pellet was prepared by centrifugation (5 min, 500×*g*) and resuspended in 500 µl lysis buffer containing protease inhibitors. The cells were lysed by passing ten times through a 26 G needle followed by overhead rotation for 30 minutes at 4°C. In order to remove DNA and cell debris the lysate was cleared by centrifugation at 13000 rpm and 4°C for 15 minutes. Co-immunoprecipitation was

performed either by using Pureproteome™ magnetic beads (Merck Millipore, Darmstadt, Germany) or the GFP-Trap® (Chromotek, Munich, Germany).

Incubation of GFP-ZG16dSP_K and GFP with HMyc-ZG16p before co-immunoprecipitation was done by adding 2 µg of recombinant protein to cell lysate and incubating on ice for 2 h with gentle mixing every 10 min.

Lysis buffer, pH 7.5: 25 mM Tris-HCl; 50 mM Sodium chloride; 0.5% (w/v) Sodium deoxycholate; 0.5% (w/v) Triton X-100

Dilution/Wash buffer, pH 7.5: 10 mM Tris-HCl; 150 mM NaCl; 0.5 mM EDTA

3.4.14. Pureproteome™ magnetic beads

The cell lysate was diluted with 750 µl of dilution buffer in order to keep the final concentration of detergent below 0.2%. An aliquot of 50 µl of the lysate was saved to use as expression control in immunoblot analysis (SN1). Then, 2 µl of the anti-GFP antibody (2 mg/ml) was added to the lysate and incubated at 4˚C with over-head rotation for 2-3 h. PureProteome protein G magnetic beads were gently mixed to be uniformly resuspended and 25 µl of suspended beads were washed twice with 500 µl of PBS, added to the lysate and incubated for 30 min with over-head rotation at 4˚C. The beads were magnetically separated until the supernatant was clear. 50 µl of the supernatant were saved to use in immunoblot analysis (SN2). The beads were washed twice with 500 µl of dilution buffer. The beads were resuspended in 50 µl of 2x SDS-PAGE loading buffer and boiled for 10 min at 95˚C. 25 µl were loaded in a SDS-PAGE gel and analysed by immunoblotting.

3.4.15. GFP-Trap®

The cell lysate was diluted with 750 µl of dilution buffer in order to keep the final concentration of detergent below 0.2%. An aliquot of 50 µl of the lysate was saved to use as expression control in immunoblot analysis (SN1). GFP-Trap®_M beads were gently mixed to be uniformly resuspended and 20 µl of suspended beads were washed twice with 500 µl of PBS, added to the lysate and incubated for 30 min with over-head rotation at 4˚C. The beads were magnetically separated until the supernatant was clear. 50 µl of the supernatant were saved to use in immunoblot analysis (SN2). The beads were washed twice with 500 µl

of dilution buffer. The beads were resuspended in 50 µl of 2x SDS-sample buffer and boiled for 10 min at 95˚C. 25 µl were loaded in a SDS-PAGE gel and analysed by immunoblotting.

3.4.16. Cross-linking

4 mg of DSP (dithiobis[succinimidyl propionate]) were freshly dissolved in DMSO (dimethyl sulfoxide) and added drop-wise to 10 ml of PBS resulting in a final concentration of 400 µg/ml. Before harvesting the cells (see Chapter 3.4.13) they were incubated with DSP solution for 30 minutes at room temperature. DSP reactivity was quenched by incubation with 1 ml of 500 mM of Tris-HCl, pH 7.4 for 15 min.

3.4.17. Purification of His-tagged proteins

DNA fragments encoding rat ZG16p (amino acid residues 17-167) and rat Myc-ZG16p (amino acid residues 17-167) were subcloned in pET28b vector. The plasmid constructs were transformed into *Escherichia coli* Rosetta (DE3) and colonies were screened for protein expression. Plasmids from selected colonies were verified by sequencing.

For protein expression and purification bacteria were grown overnight in 5 ml of LB medium at 37˚C. Then 250 ml of fresh LB medium was inoculated with 2.5 ml of the grown culture and incubated with agitation at 37˚C until the OD_{600} reached ~0.6. Protein expression was induced with 1 mM of IPTG and culture was further incubated at 37˚C with shaking for 3 h. The bacteria were collected by centrifugation at 6000×*g* for 15 min, 4˚C. The pellet was resuspended in 5 ml of lysis buffer and the cells were lysed by sonication (15 s pulses, 50% amplitude per cycle) with an ultrasonic probe sonicator. The lysate was cleared by centrifugation at 12000×*g* for 30 min, 4˚C. The supernatant was collected and used for protein purification with the Talon® single step column (5 ml). The resin was first washed with 5 ml of distilled water and then equilibrated with 5 ml of equilibration buffer. The bottom closure was placed on the column and 5 ml of the supernatant were loaded in the column. The column was closed with the top cap and the suspension was mixed by overhead rotation for 30 min, 4˚C. The resin was allowed to settle, the top cap and the bottom closure were removed and the liquid allowed to drain by gravity flow. Then, the resin was washed twice with 5 ml of washing buffer 1, followed by washing with 5 ml of washing buffer 2. The purified protein was eluted with 5 ml of elution buffer. 500 µl fractions of the second

wash and the elution were collected for protein analysis. The most pure fractions of recombinant proteins were selected, combined and dialyzed against PBS, pH 7.4.

Lysis buffer / equilibration buffer / washing buffer 1: 50 mM sodium phosphate; 300 mM NaCl; pH 8.0
Washing buffer 2: 50 mM sodium phosphate; 300 mM NaCl; 10 mM imidazole; pH 8.0
Elution buffer: 50 mM sodium phosphate; 300 mM NaCl; 150 mM imidazole; pH 8.

3.4.18. Tryptic Digestion

The protein spots were excised from the gels and washed three times with 25 mM ammonium bicarbonate/50% acetonitrile (ACN), one time with ACN and dried. 25 µL of 10 µg/mL sequence grade modified porcine trypsin in 25 mM ammonium bicarbonate were added to the dried gel pieces and the samples were incubated overnight at 37 °C. Extraction of tryptic peptides was performed by adding 10% formic acid (FA)/50% ACN (3x) being lyophilized in a SpeedVac (Thermo Fisher Scientific, Asheville, NC). Tryptic peptides were resuspended in 13 µL of a 50% acetonitrile/0.1% formic acid solution.

3.4.19. Mass Spectrometry

Aliquots of samples (0.5 µL) were spotted onto the MALDI sample target plate and mixed (1:1) with a matrix consisting of a saturated solution of α-cyano-4-hydroxycinnamic acid (5 mg/mL) prepared in 50% acetonitrile/0.1% formic acid. Peptide mass spectra were obtained on a MALDI-TOF/TOF mass spectrometer (4800 Proteomics Analyzer, Applied Biosystems, Europe) in the positive ion reflector mode. Spectra were obtained in the mass range between 800 and 4500 Da with *ca.* 1500 laser shots. For each sample spot, a data dependent acquisition method was created to select the six most intense peaks, excluding those from the matrix, trypsin autolysis, or acrylamide peaks, for subsequent MS/MS data acquisition. Trypsin autolysis peaks were used for internal calibration of the mass spectra, allowing a routine mass accuracy of better than 20 ppm. Spectra were processed and analyzed by the Global Protein Server Workstation (Applied Biosystems, Foster City, CA), which uses internal Mascot (Matrix Science Inc., Boston, MA) software for searching the

peptide mass fingerprints and MS/MS data. Searches were performed against the NCBI non redundant protein database.

3.4.20. Liquid Chromatography

Analyses were performed using an Ultimate 3000 ‘‘LcPackings’’ (Thermo Scientific, California, USA). 20 µl of each sample (3 µg of peptide extract) were injected onto a C18 trapping column (Zorbax 300SB-C18, 5 µm particle size, 5 x 0,3 mm, Agilent Technologies) using an autosampler. The sample was washed over the trapping column for 3 min with 95% buffer A (water, 0.1% TFA), 5% Buffer B (acetonitrile, 0.1% TFA) at a flow rate of 30 µl/min. Flow was then reversed over the trapping column, and sample was eluted onto a 150 mm × 75 µm Zorbax 300SB capillary analytical C18 column with 3.5-µm particle size (Agilent Technologies) at a flow rate of 0.3 µl/min. A linear gradient of 5% Buffer B to 55% Buffer B was run over a period of 35 min. The column was then washed with a 3 min gradient from 55% to 90% Buffer B, followed by a 5-min hold at 90% Buffer B. The column was then re-equilibrated in 5% Buffer B prior to future analyses. The peptides eluting off the monolithic capillary column were directly deposited onto 384-well MALDI plates at 20 s intervals for each spot using Probot (LcPackings) adding 170 nl of α-CHCA (α-Cyano-4-hydroxycinnamic acid) (Sigma-Aldrich) matrix solution (prepared by diluting saturated α-CHCA with 70% acetonitrile/0.1% TFA with the addition of 10 fmol of Glu-Fib as internal standard).

3.5. Cell Culture and Transfection Experiments

3.5.1. Cell lines

COS-7

Source: ATCC (Rockville, USA) no. CRL-1651

Cercopithecus aethiops (African green monkey), kidney

SV40 transformed, produce large T antigen,

Adherent, fibroblast morphology

HepG2

Source: ATCC (Rockville, USA) no. HB-8065

Homo sapiens (human), liver

Hepatoblastoma cells

Adherent, epithelial morphology

AR42J

Source: ATCC (Rockville, USA) no. CRL-149

Rattus norvegicus (Wistar strain), pancreas

Pancreatic exocrine tumor

Adherent when plated on matrigel coated surfaces. Differentiation into acinar-like cells with formation of zymogen granules can be induced with dexamethasone

3.5.2. Cell culture

COS-7, AR42J, and HepG2 cells were cultured in Dulbecco's modified Eagle medium (DMEM) high glucose (4.5 g/l) supplemented with fetal bovine serum and (FBS) penicillin (100 U/mL)/streptomycin (100 µg/mL) (PAA Laboratories GmbH, Linz, Austria) at 37 °C in a 5% CO_2-humidified incubator. Cell culture work was performed in a sterile laminar flow safety cabinet and all materials and solutions were sterilized by filtration, autoclaving or heat sterilization. Routinely, cells were grown in 100 mm in diameter dishes and seeded on coverslips in 60 mm in diameter dishes for immunofluorescence experiments. To improve cell adherence of AR42J cells, the culture dishes were coated with an extract of Engelbreth-Holm-Swarm tumour (Kleinman, H. 1979). To induce differentiation and zymogen granule formation, cells were incubated with 10 nM dexamethasone for 2-3 days.

3.5.3. Cell passage

Routinely, passaging or splitting of cell was performed twice per week, after the cells reached confluency (~$1.7x10^4$ cells/cm²). Cells were washed with PBS and incubated with 2 ml trypsin EDTA solution (0.5 mg/ml trypsin and 0.22 mg/ml EDTA) for 3-5 minutes at 37°C. Cells were resuspended in 8 ml medium containing FBS and pelleted by centrifugation for 5 minutes at 500×*g*. The pellet was resuspended in medium and cells were seeded as single cell suspension in a dilution of 1:10 (10^4 cells/ml).

3.5.4. Cell freezing

For long term storage, cells were frozen and stored in the vapour phase of liquid nitrogen. Cell pellets prepared as described above (3.4.3) were resuspended in freezing medium containing 20% FBS and 10% DMSO to avoid crystal formation. Cell suspension aliquots of 1 ml were filled into cryovials, slowly frozen overnight at -80˚C and subsequently transferred into the liquid nitrogen storage tank. For unfreezing, cells were thawed quickly in a water bath (37˚C) or by mixing with pre-warmed culture medium, and the cells were seeded with pre-warmed medium in a regular dish. After adhesion of the cells to the bottom of the dish, the medium was changed to remove DMSO and debris.

3.5.5. PEI transfection

For morphological experiments, like immunofluorescence studies, COS-7 cells were usually transfected using PEI (polyethylenimine) (Sigma). 24 hours before transfection cells were seeded on coverslips in 60 mm dishes. 10 µg DNA were diluted in 750 µl 150 mM sodium chloride, and 100 µl PEI (0.9-1 mg/ml in water) were diluted with 650 µl sodium chloride solution. After 15 minutes of incubation at room temperature the PEI solution was added drop-wise to the DNA solution and the mixture was incubated for additional 15 minutes. 500 µl of the mixture were added drop-wise to 2.5 ml medium into the cell dish and the cells were incubated for 3 to 6 hours at 37°C. Afterwards cells were washed with PBS and incubated for 24 to 48 hours in fresh medium before fixation and processing for immunofluorescence (3.5.1).

3.5.6. Electroporation

A confluent dish of cells was trypsinized as described in 3.4.3. The cell pellet was washed by resuspension in 5 ml HBS buffer (3.1) and re-centrifuged. The cell pellet was resuspended in 1 ml HBS buffer and 0.5 ml of this cell suspension was mixed with DNA (10 µg) in a 4 mm gap electroporation cuvette. Electroporation of COS-7 cells was performed at 230 V, 1500 µF, and 125 Ω. Subsequently, the cells were mixed quickly with 1 ml of complete medium and seeded in dishes prepared with pre-warmed medium.

3.5.7. Turbofect™ transfection

For morphological experiments like immunofluorescence studies in AR42J and HepG2 cells were usually transfected using Turbofect™ (Fermentas). 24 hours before transfection cells were seeded on coverslips in 60 mm dishes. 4 µg DNA were diluted in 400 µl DMEM and 6 µl of Turbofect™ were added. After 20 minutes of incubation at room temperature the mixture was added drop-wise into the cell dish with 3.6 ml of DMEM and the cells were incubated for 3 to 6 hours at 37°C. Afterwards cells were washed with PBS and incubated for 24 to 48 hours in fresh complete medium before fixation and processing for immunofluorescence (3.5.1).

3.6. Microscopic techniques

3.6.1. Immunofluorescence

Cells grown on coverslips were washed twice with PBS to remove residual medium and fixed with 4% paraformaldehyde (PFA) (3.1) for 20 minutes at room temperature. The cells were washed tree times with PBS and washing was performed in between all further incubation steps. Cellular membranes were permeabilized using 0.2% Triton X-100 for 10 minutes. Afterwards unspecific binding sites were blocked by incubation with 1% BSA for 10 minutes. Incubation with the primary antibodies (Table 1) was performed for 1 hour in a humid and dark environment to avoid drying of the cells, followed by incubation with the secondary antibodies (Table 2) in the same way. If a set of several (primary or secondary) antibodies was used, the incubation occurred simultaneously. The coverslips were washed with distilled water to avoid crystal formation of the salts present in PBS, mounted on glass slides using Mowiol and dried overnight before microscopic examination.

3.6.2. Fluorescence microscopy

For morphological studies an Olympus BX-61 microscope (Olympus Optical Co. GmbH, Hamburg, Germany) equipped with the appropriate filter combinations and a 100× objective (Olympus Plan-Neofluar; numerical aperture, 1.35) was used. Digital images were acquired with an F-view II CCD camera (Soft Imaging System GmbH, Munster, Germany) driven by Soft imaging software.

3.6.3. Confocal microscopy

Confocal images were acquired on a Zeiss LSM510 confocal microscope (CarlZeiss, Oberkochen, Germany) using a Plan-Apochromat 63X or 100X /1.4 oil objective. Images were processed and quantified using LSM- 510 software (Carl Zeiss MicroImaging, Inc.). Background noise was minimal when optimal gain/offset settings for the detectors were used.

3.6.4. Live cell imaging

The Zeiss LSM-510 confocal microscope was equipped with a closed chamber which was aerated with 5% warm (37°C) CO_2 to create normal culture conditions. Cells growing in glass bottom dishes in medium without phenol red were placed in a heated chamber and live cell time-lapse imaging was performed. Images were taken in time intervals of 13 seconds.

3.6.5. TexasRed-transferrin

COS-7 cells grown on coverslips were incubated in serum-free medium for 2 hours, 37˚C. The medium was replaced by DMEM with 20 mM HEPES buffer and the cells were incubated for 30 min at 37˚C. Then the medium was replaced with DMEM with 1% BSA and 100 nM of TexasRed-transferrin (TexasRed-tf) and the cells were incubated for 30 min at 37˚C. The cells were cooled to 4˚C, washed twice with ice-cold PBS and fixed with 4% PFA. The coverslips were washed with distilled water to avoid crystal formation of the salts present in PBS, mounted on glass slides using Mowiol and dried overnight before microscopic examination.

RESULTS

4. Results

Zymogen granules (ZG) are specialized storage organelles within the acinar cells of the exocrine pancreas. Their main cargo is constituted by pancreatic digestive enzymes as inactive precursors which are released by regulated apical secretion, triggered by an external stimulus. ZG formation is initiated at the trans-Golgi network (TGN) where the regulated secretory ZG proteins co-aggregate at the mildly acidic pH and high Ca^{2+} levels and condensing vacuoles/immature secretory granules are formed (Colomer et al., 1996; Dartsch et al., 1998; Freedman and Scheele, 1993; Leblond et al., 1993). Their maturation involves further concentration of the cargo proteins with selective removal of components not destined for regulated secretion, and a reduction in granule size (Arvan and Castle, 1998; Borgonovo et al., 2006; Tooze et al., 2001). The mature ZGs are transported to the apical domain of the acinar cell, where they are stored until a neuronal or hormonal stimulus (e.g., acetylcholine and cholecystokinin) releases intracellular calcium stores, thus triggering the fusion of ZGs with the plasma membrane and with neighbouring granules (compound exocytosis). Fusion results in exocytosis of digestive enzymes into the apical lumen and the pancreatic duct system (Wasle and Edwardson, 2002; Williams, 2006). Although the ZG has long been a model for the understanding of secretory granule biogenesis and functions, the molecular mechanisms required for ZG formation at the TGN, for packaging and sorting of cargo proteins, as well as for granule fusion and exocytosis are still poorly defined (Borgonovo et al., 2006; Borta et al., 2010; Schrader, 2004; Williams, 2006). According to recent models, part of the molecular machinery required for digestive enzyme sorting, granule trafficking and exocytosis is supposed to be associated with the zymogen granule membrane (ZGM). The submembranous matrix model predicts high molecular mass components (e.g. a proteoglycan scaffold and associated (glyco)proteins) attached to the luminal side of the granule membrane which fulfil important functions during the sorting and packaging of secretory proteins (Scheele et al., 1994; Schrader, 2004). The glycoconjugate scaffold underneath the ZGM is supposed to serve as the backbone of a complex submembrane matrix, and a bridge between the ZGM and the zymogens. In addition to basic research interests, ZG play important roles in pancreatic injury and disease (Gaisano and Gorelick, 2009; Parikh et al., 2012). Thus, there is currently great interest in the identification and characterization of ZG and ZGM components by conducting antibody

screens, raft analyses and proteomic studies (Borta et al., 2010; Faust et al., 2008; Rindler et al., 2007; Schmidt et al., 2000, 2001; Sun and Jiang, 2013).

In the first part of the work I have focused on the identification of a "basic" group of peripheral granule membrane proteins from rat exocrine pancreas (4.1). In the second part I have discovered and characterized new biochemical properties of the lectin ZG16p (a component of the submembranous matrix) (4.2). The last section presents functional analyses of ZG16p by expression and mutational studies in mammalian cells (4.3).

4.1. Identification of peripheral membrane proteins of zymogen granules

To understand the biogenesis and further processing of pancreatic ZG as well as their role in disease a deep analysis of their proteome is required. We focused on the analysis of membrane-associated ZG proteins by applying a suborganellar proteomics approach to identify peripheral membrane-associated ZG proteins (Figure 7 A-D). Zymogen granules were isolated from rat pancreas according to a standardized protocol (Dartsch et al., 1998; Faust et al., 2008; Schmidt et al., 2000). The purity of the isolated ZG fractions (≥ 90%) was controlled by electron microscopy and immunoblotting (Faust et al., 2008; Gómez-Lázaro et al., 2010). Intact granules were gently lysed and further separated in a membrane (ZGM) and content fraction (ZGC). The isolated membranes (ZGM) were treated with carbonate to liberate membrane-associated proteins and separated in a pellet (ZGMwashed) and supernatant fraction (Wash) (see Chapter 3.4.1.2). To characterize the ZG peripheral membrane-associated proteins, 2D gel maps were generated for the supernatant fraction (Wash) of carbonate-washed ZGM. For comparison typical 2D gel patterns of the Wash and the content subfractions (ZGC) separated under equal conditions are shown in Figure 7.

Note that the representative gels exhibit unique spot patterns for the two different subfractions. In a representative gel for the Wash fraction about 104 spots were reproducibly visualized, which represent an acidic and more basic group of ZG protein spots (Figure 7 B and D). We focussed on the analysis of the spots from the "basic" group (pH range 6.2-11). In this region, 46 spots were visualized among which 44 were identified by tandem mass spectrometry (Figure 7 D, Supplementary Table 1).

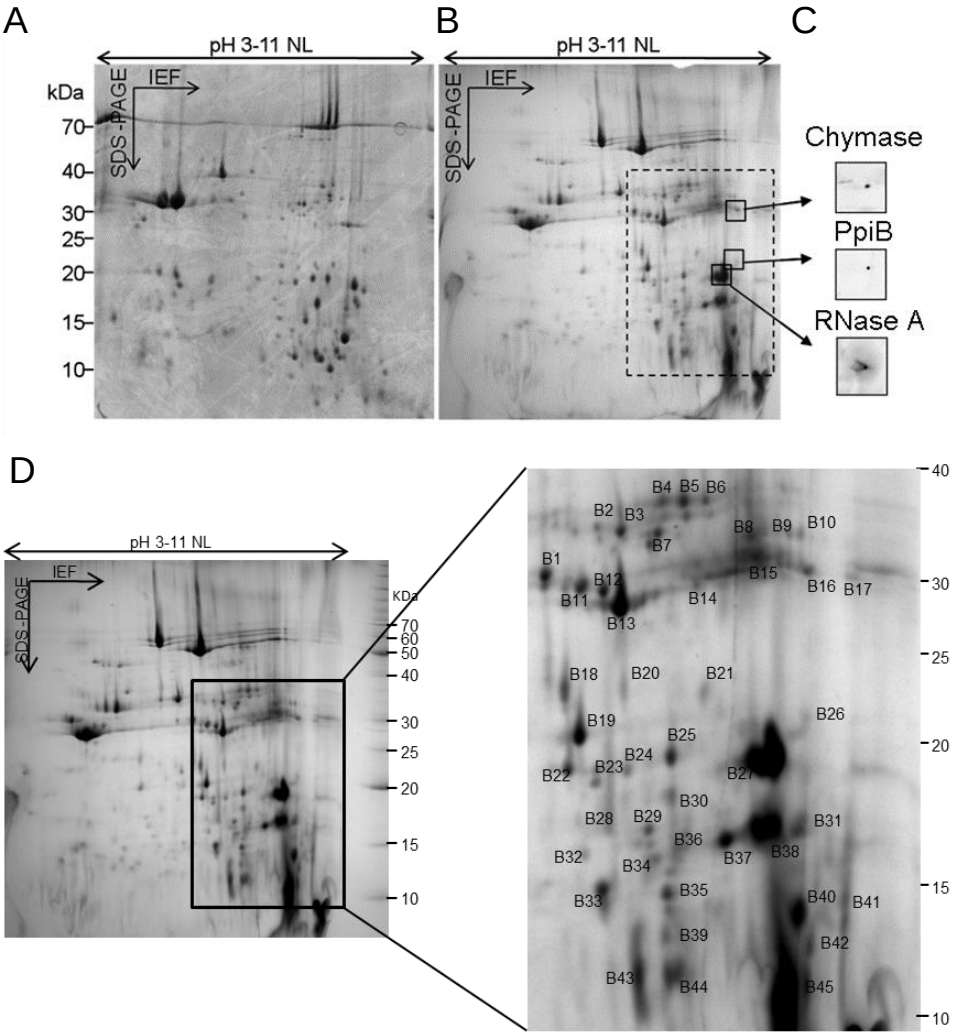

Figure 7. Separation of rat ZG content and ZGM Wash subfractions by two-dimensional IEF/SDS-PAGE. The whole complement of ZGC (A) and the supernatant fraction (Wash) (B, D) of carbonate-treated ZGM were subjected to 2D-PAGE followed by Coomassie blue staining. For IEF, 300 µg of protein were separated on 11 cm IPG strips (pH 3-11NL) and on 15% polyacrylamide gels in the 2nd dimension. Note the differences in the spot pattern of ZGC (A) and the Wash fraction (B). The boxed areas in (B, C) highlight basic protein spots (chymase, PpiB, RNase A) which have been selected for further analysis and are verified by immunoblotting (C) using specific antibodies to rat mast cell chymase, PpiB, and RNase A. The boxed region (D) highlights the basic protein spots (B1-46) analysed by MS.

The identified spots corresponded to 16 unique proteins (Figure 8 A), which were categorized in 6 groups based on their known subcellular localization: ZGC (n=6; 38%) and ZGM (n=6; 38%) proteins, mast cell proteins (n=1; 6%), ER resident proteins (n=1; 6%), and proteins with other localizations (n=2; 12%) (Figure 8 B). Considering their predicted biological functions we identified 12 enzymes including 9 digestive enzymes (usually attributed to the ZGC), 2 matrix proteins (ZG16p, syncollin) and 3 slightly acidic glycoproteins (CEL, pancreatic lipase related protein 1 and 2). Based on literature and the Protein Knowledgebase (UniProtKB), all of the identified proteins are soluble or peripheral

membrane proteins, and no transmembrane or membrane-anchored proteins have been identified in the Wash fraction. Furthermore, except for two cytosolic proteins (vinculin (fragment), an actin-binding protein, and ubiquitin carrier protein involved in ubiquitination/quality control) all identified proteins are supposed to be components of the secretory pathway. This further confirms the applicability of the carbonate and gel-based proteomic approach.

A

UniProtKB	Protein name	Localization	Function
LIPR1_RAT	Pancreatic lipase related protein 1	ZGM	Lipid degradation
LIPP_RAT	Pancreatic triacylglycerol lipase	ZGM	Lipid degradation
AMYP_RAT	Pancreatic alpha-amylase	ZGC	Carbohydrate metabolism
CEL_RAT	Bile salt-activated lipase	ZGC	Lipid degradation
MCPT1_RAT	Mast cell protease I (RMCP-1) (Chymase)	Mast Cell Granules	Serine-type endopeptidase activity
CELA1_RAT	Chymotrypsin-like elastase family member 1	ZGC	Serine-type endopeptidase activity
VINC_RAT	Vinculin	Cell Membrane	Cell Adhesion
TRY3_RAT	Cationic trypsin-3	ZGC	Serine-type endopeptidase activity
RNS1B_RAT	Ribonuclease pancreatic beta-type	ZGC	RNA Endonuclease
PPIB_RAT	Peptidyl-prolyl cis-trans isomerase B	Endoplasmic Reticulum	Protein Folding
ZG16_RAT	Zymogen granule membrane protein 16	ZGM	Lectin – Sugar binding
SYCN_RAT	Syncollin	ZGM	Compound exocytosis
B2RZA9_RAT	Ubiquitin carrier protein	Cytoplasm	Protein Modification
LIPR2_RAT	Pancreatic lipase-related protein 2	ZGM	Galactolipid catabolic process
COL_RAT	Colipase	ZGM	Cofactor of pancreatic lipase
Q9EQZ8_RAT	Chymopasin	ZGC	Serine protease

B

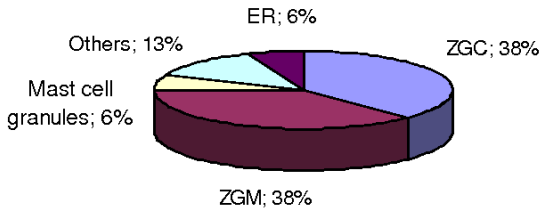

Figure 8. (A) Proteins identified from the "basic group" of a ZGM carbonate Wash fraction. Functional annotation and organelle assignments were made using the UniprotKB database, additional annotation was incorporated from literature search. Extra information supporting the identification of the potential ZGM proteins is summarized in Supplementary Table 1. (B) Diagram illustrating the intracellular distribution of the identified proteins of the Wash fraction. On the basis of published data, annotations in databases or predictions based on similarity to related proteins, the identified proteins are grouped in a pie chart according to their subcellular distribution and function.

In addition, some classical content proteins such as amylase, elastase, colipase and triacylglycerol lipase were identified in the Wash fraction (Figure 8, Supplementary Table 1). This can be due to a cross-contamination of the subfractions or due to the fact that the

interactions established between the proteins from the different subfractions are not completely disrupted in the separation procedure. The identification of some abundant theoretical acidic proteins within the "basic" group (e.g., CEL, lipase related protein 1) is likely to be a result of protein degradation and/or glycosylation.

To validate our suborganellar proteomic data, we selected three proteins for further characterization: chymase, PpiB and RNase A. Chymase (RMCP-1) and peptidyl-prolyl cis-trans isomerase B (PpiB; cyclophilin B) are likely to be previously unknown genuine membrane-associated ZG proteins. Chymase was initially identified as a proteoglycan-associated serine protease in granules of mast cells (Pejler and Berg, 1995; Pejler and Maccarana, 1994). In support of our findings, chymase was also identified in ZGM fractions in a proteomic study combining two-dimensional LC and tandem mass spectrometry (Chen et al., 2008). PpiB has been reported to be an ER-resident enzyme with proteoglycan-binding properties (Hanoulle et al., 2007; Iwai and Inagami, 1990). Furthermore, we selected RNase A originally known as a typical content protein of ZG, but prominently present in our Wash fraction. Based on the spot size, chymase and PpiB appear to be low abundant components of ZGM (Figure 7 D). To confirm their presence in our 2D gels and thus, their correct identification, immunoblotting was performed with the 2D-gels of the Wash fraction. As shown in Figure 7, the corresponding chymase, PpiB and RNase A spots identified by tandem mass spectrometry were recognized by specific antibodies after immunoblotting (Figure 7 C).

4.1.1. Chymase and PpiB are novel peripheral ZGM proteins

To compare the distribution of chymase and PpiB among granule subfractions, equal amounts of protein from the four granule subfractions (ZGC, ZGM, ZGMwashed and Wash) were separated on 12.5% acrylamide gels and immunoblotted using antibodies directed to chymase and PpiB (Figure 9). Furthermore, antibodies to the granule marker proteins amylase, CEL, RNase A, GP2, and ZG16p were used to monitor proper granule subfractionation. As shown in Figure 3, amylase was mainly present in the ZGC fraction, whereas GP2, a major GPI-anchored glycoprotein of ZG, was predominantly found in the ZGM fraction. The secretory lectin ZG16p, a peripheral ZGM protein (Cronshagen et al., 1994), was concentrated on isolated ZGM, and a major portion was liberated by carbonate

treatment (Figure 3). Interestingly, chymase and PpiB showed a similar distribution pattern to ZG16p. Both enzymes were associated with isolated ZGM, but barely detectable in the ZGC fraction. Upon carbonate-treatment the majority of chymase and PpiB was removed from the ZGM and detected in the Wash fraction indicating that both proteins are peripheral components of the ZGM. Furthermore, we investigated the distribution of CEL and RNase A within the granule subfractions. Remarkably, the majority of CEL appears to be associated with the ZGM (Figure 9). However, only a small portion can be removed from the ZGM by carbonate treatment indicating that the enzyme is more tightly associated with the ZGM. This might be due to its affinity to lipid surfaces (Bruneau and Lombardo, 1995; Bruneau et al., 2000; Lombardo, 2001; Lombardo and Guy, 1980). In the case of RNase A, the majority of the enzyme is located in the ZGC fraction, but a surprisingly high amount (about 40%, Figure 9) is associated with the ZGM and can be liberated by carbonate treatment. Note that the ZGM associated portion of RNase A is much higher than that of membrane-associated amylase (13%, Figure 9).

To exclude a contamination of the ZG subfractions with granules from mast cells (e.g., from pancreatic tissue), an antibody to tryptase β1, a prominent mast cell marker, was applied. A lysate of rat tongue, which is rich in mast cells containing chymase, was used as a positive control. In contrast to chymase, tryptase β1 was absent from the ZG subfractions. However, both tryptase β1 and chymase were detected in lysates of rat tongue. To check for contamination of the ZG subfractions with ER or ER-resident proteins, specific antibodies directed to the ER marker proteins BiP (GRP78, 78 kDa glucose regulated protein), PDI (protein disulfide isomerase) and calnexin (an abundant ER transmembrane protein) were applied. PpiB, BiP, PDI and calnexin were all detected in a microsome-enriched fraction which was used as a positive control. In contrast to PpiB, which was prominently labeled in the ZGM and Wash fractions, BiP and calnexin were below the detection level in all ZG subfractions. Interestingly, a small amount of PDI was detected in the ZGC fraction, but PDI was not detectable in all other ZG subfractions. This is consistent with morphological studies where small amounts of PDI have been detected in the ZG content. The presence of PDI is supposed to be due to occasional escape from the ER (Yoshimori et al., 1990). PpiB was as well identified in ZGM fractions in a recent proteomics report using 2D-GEP and LC-MS/MS (Rindler et al., 2007). As PpiB is selectively enriched in the ZG or ZGM fraction, but calnexin, BiP and PDI are not (or are barely detectable), a contamination with ER appears

unlikely. In addition, other major microsomal proteins were not identified in our 2D gel analyses. These findings support the notion that PpiB is a bona fide ZG protein and not the result of a contamination.

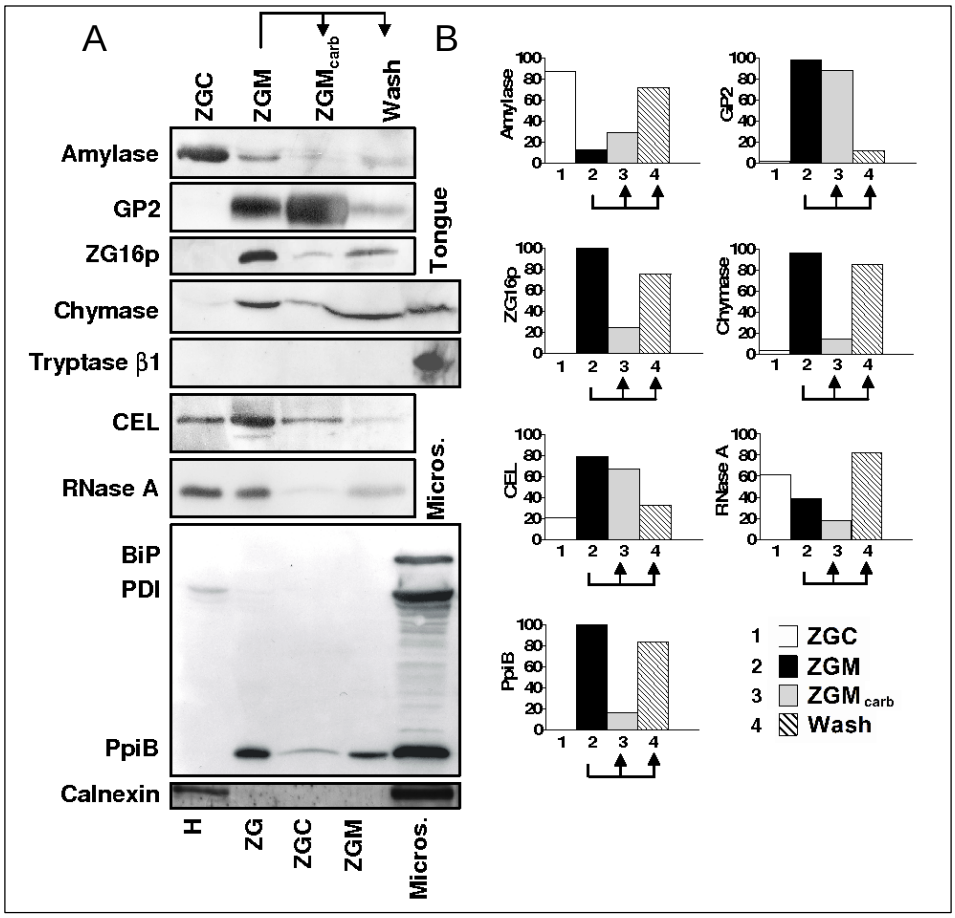

Figure 9. Chymase and PpiB represent peripheral membrane proteins of rat ZG. (A) Lysed granules were separated into a content (ZGC) and membrane fraction (ZGM). In addition, isolated membranes were treated with Na_2CO_3 at pH 11.0 and separated into pellet (ZGMcarb) and supernatant (Wash) fractions. Equal amounts of protein (20 µg) were run on 12.5% acrylamide gels, blotted onto nitrocellulose membranes and incubated with antibodies to amylase (ZGC marker protein), GP2 (ZGM marker protein), ZG16p (peripheral ZGM marker protein), chymase, tryptase β1 (mast cell control), carboxyl ester lipase (CEL), RNase A, BiP and PDI (ER control) and PpiB. (B) Densitometric quantification of immunoblots shown in (A). The distribution to ZGC and ZGM (% of total ZGC + ZGM) as well as the distribution to ZGMcarb and Wash (% of total ZGM) is depicted (see also Supplementary Table 3). Note that the distribution of chymase and PpiB resembles that of ZG16p, a peripheral ZGM marker protein. A lysate from rat tongue and a microsome-enriched fraction (Micros.) served as controls for the detection of mast cell proteins and ER resident proteins, respectively.

To exclude a contamination of the ZG subfractions with granules from mast cells (e.g., from pancreatic tissue), an antibody to tryptase β1, a prominent mast cell marker, was applied. A lysate of rat tongue, which is rich in mast cells containing chymase, was used as a positive control. In contrast to chymase, tryptase β1 was absent from the ZG subfractions. However, both tryptase β1 and chymase were detected in lysates of rat tongue. To check for

contamination of the ZG subfractions with ER or ER-resident proteins, specific antibodies directed to the ER marker proteins BiP (GRP78, 78 kDa glucose regulated protein), PDI (protein disulfide isomerase) and calnexin (an abundant ER transmembrane protein) were applied. PpiB, BiP, PDI and calnexin were all detected in a microsome-enriched fraction which was used as a positive control. In contrast to PpiB, which was prominently labeled in the ZGM and Wash fractions, BiP and calnexin were below the detection level in all ZG subfractions. Interestingly, a small amount of PDI was detected in the ZGC fraction, but PDI was not detectable in all other ZG subfractions. This is consistent with morphological studies where small amounts of PDI have been detected in the ZG content. The presence of PDI is supposed to be due to occasional escape from the ER (Yoshimori et al., 1990). PpiB was as well identified in ZGM fractions in a recent proteomics report using 2D-GEP and LC-MS/MS (Rindler et al., 2007). As PpiB is selectively enriched in the ZG or ZGM fraction, but calnexin, BiP and PDI are not (or are barely detectable), a contamination with ER appears unlikely. In addition, other major microsomal proteins were not identified in our 2D gel analyses. These findings support the notion that PpiB is a bona fide ZG protein and not the result of a contamination.

To confirm that all of the content is solubilized and that aggregated zymogens do not sediment with the membranes, we have isolated ZG in a high salt buffer and recovered ZGM in a 0.3 M/1 M sucrose gradient without pelleting. The ZGM were as well more extensively washed either in 50 mM Hepes, pH 8.0 or in 100 mM $NaHCO_3$, pH 8.1 (Figure 10).Whereas amylase was more efficiently removed from the ZGM fractions after extensive washing, the distribution of CEL, chymase and PpiB was not grossly altered by the different isolation procedures. The minor amount of amylase found in the ZGM fractions is as well an indicator for complete ZG lysis and solubilization of the granule content (at least of amylase-containing complexes). Furthermore, membrane-association of some content proteins was also observed by others after more stringent washing/purification conditions and gradient centrifugation (Chen et al., 2006; Rindler et al., 2007).

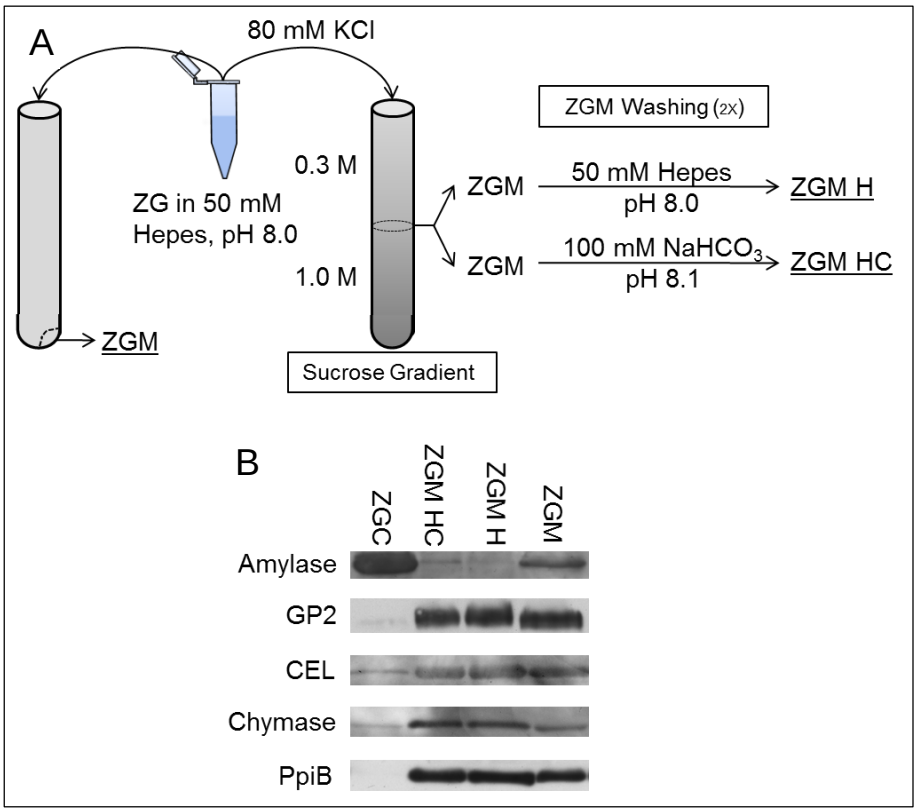

Figure 10. Distribution of granule proteins after isolation of ZGM by sucrose gradient centrifugation. (A) Purification scheme. Purified ZG were resuspended in 50 mM Hepes, pH 8.0, 80 mM KCl, gently lysed by freezing and thawing and centrifuged through a 0.3 M/1 M sucrose step gradient. ZGM were recovered at the interface and washed twice in 50 mM Hepes, pH 8.0 (ZGM H) or in 100 mM $NaHCO_3$, pH 8.1 (ZGM HC). After each washing step, ZGM were recovered by centrifugation. Alternatively, ZGM were obtained by sedimentation as described in 3.4.1.2. (B) Equal amounts of protein (20 µg) were run on 12.5% acrylamide gels, blotted onto nitrocellulose membranes and incubated with antibodies to amylase, GP2, carboxyl ester lipase (CEL), chymase, and PpiB. Note that amylase is more efficiently removed from the ZGM fractions after extensive washing, whereas the distribution of CEL, chymase and PpiB is not grossly altered by the different isolation procedures.

In summary, a 2D-gel approach combined with tandem mass spectrometry led to the identification of membrane-associated proteins including classical ZG content proteins, lipid binding proteins as well as previously unknown low abundant proteins such as chymase, a serine protease earlier described in mast cell granules, and peptidyl-prolyl cis-trans isomerase B (PpiB), a known ER-resident enzyme. As we identified several peripheral ZGM proteins with proteoglycan-binding properties (e.g. ZG16p, chymase, PpiB, RNase A), our findings may help to unveil the possible role of proteoglycans in the sorting and packaging of zymogens. Furthermore, proteoglycans may also fulfil an important additional function after secretion. For example, the interaction of mast cell chymase with proteoglycans after

degranulation has been shown to affect the kinetics of substrate cleavage and to protect chymase from several macromolecular protease inhibitors (Rönnberg et al., 2012).

According to recent models, part of the molecular machinery required for digestive enzyme sorting, granule trafficking and exocytosis is supposed to be associated with the granule membrane (ZGM). In addition to basic research interests, ZG play important roles in pancreatic injury and disease (Gaisano and Gorelick, 2009). Thus, there is currently great interest in the identification and characterization of ZG and ZGM components.

4.2. Development and application of an Enterokinase assay

Zymogen granules are specialized organelles in packaging, storage and regulated secretion of a complex mixture of digestive enzymes and isoenzymes. ZG contain a cocktail of proteases with five functional groups of hydrolytic enzymes: endoproteases (e.g., trypsin) and exoproteases (e.g., carboxypeptidase A), lipases (e.g., CEL), glycosidases (e.g., amylase) and RNases (e.g., RNase A). Those enzymes are released into the small intestine, where conversion of trypsinogen to trypsin is mediated by proteolytic cleavage via enterokinase (EK) (Gómez-Lázaro et al., 2010; Zheng et al., 2009). Enterokinase is a type II transmembrane serine protease, localized to the brush border of the duodenal and jejunal mucosa. Enterokinase converts trypsinogen to trypsin by cleavage of the specific trypsinogen activation peptide and then trypsin subsequently activates other digestive zymogens (Figure 11) in the lumen of the gut (Zheng et al., 2009).

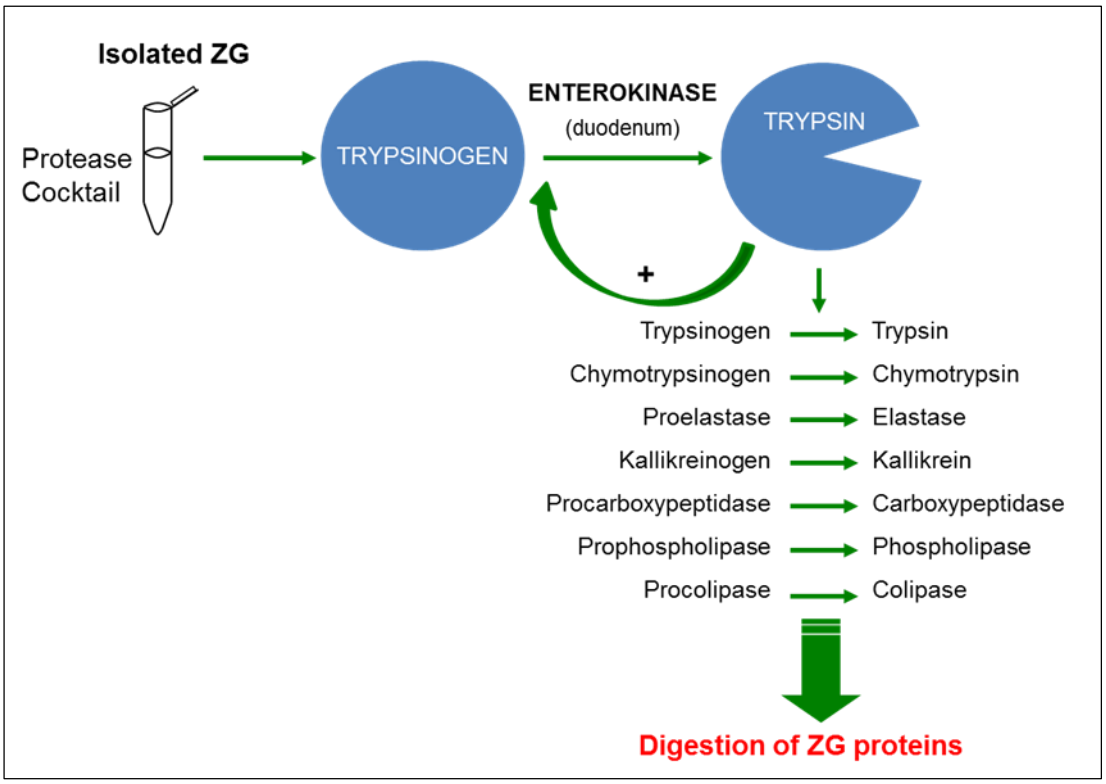

Figure 11. Scheme of protease activation by enterokinase (EK) of isolated zymogen granules (ZG). Enterokinase was added to isolated zymogen granules after being lysed by freezing and thawing. This enzyme converts trypsinogen into trypsin that subsequently activates the other proenzymes leading to a rapid chain activation of proteases and to digestion of the zymogen granule proteins.

Bottom-up proteomics largely relies on tryptic peptides for protein identification but tryptic digestion often results in limited coverage of protein sequence due to problems such

as peptide length, ionization efficiency or posttranslational modification (PTM). One approach to increase sequence coverage is to use, in combination or alone, other proteases than trypsin for digestion (Guo et al., 2014). Thus, the number of identified peptides and proteins should improve significantly by the use of multiple enzymes in parallel, especially in whole proteome sequencing (Swaney et al., 2010; Switzar et al., 2013). To take advantage of the ZG protease cocktail and easy activation of the zymogens by enterokinase we developed a "bottom-up" proteomics approach with the objective of creating and identifying as many peptides as possible in order to uncover the ZG proteome. In brief, EK is added to lysed ZG leading to activation of the zymogens and consequent digestion of ZG proteins under native conditions by multiple enzymes.

4.2.1. Activation of digestive enzymes from pancreatic zymogen granules by enterokinase uncovers several protease-resistant proteins

Isolated zymogen granules were lysed by freezing and thawing and the zymogens were activated by addition of enterokinase (3.4.4). Samples with or without enterokinase (ZG_EK and ZG_control respectively) were incubated at 37˚C and aliquots were taken from 5 min up to 48 h (Figures 12). Several time-points (0 h, 5 min, 1 h and 24 h) were analysed by LC-MS/MS but, contrary to what we expected, only the most abundant proteases were identified by this approach (Supplementary Table 2). ZG have a high concentration of active proteases that might lead to an over-digestion of the sample. So, to visualize the rate of digestion the samples from different time points were separated by SDS-PAGE. At 5 min after protease activation a prominent degree of digestion was observed when compared with the control (Figure 6 B and D). On the other hand, it was also observed that several bands did not change over time indicating that those proteins are protease resistant. The proteins present in those bands were identified by MS as: carboxypeptidase A (1), chymotrypsin C (2), elastase (3) and the lectin ZG16p (4) (Figure 12).

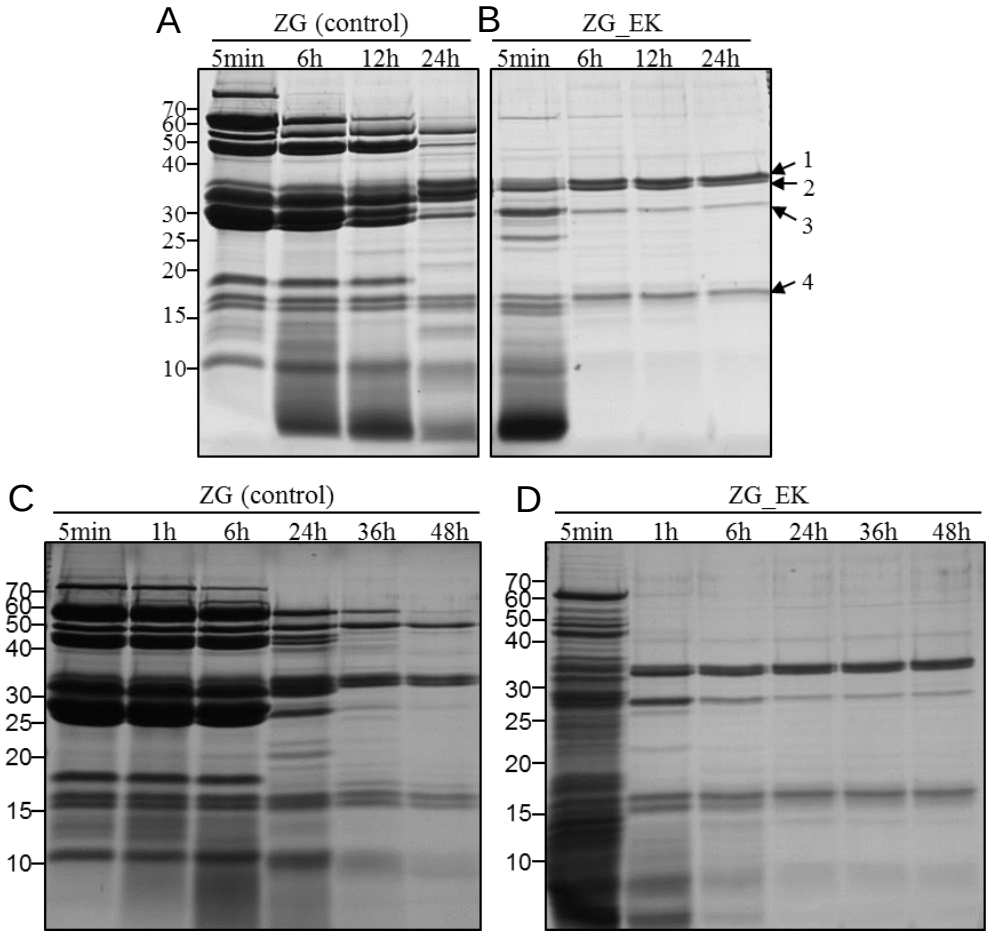

Figure 12. Digestion of lysed zymogen granules (ZG) reveals several protease resistant proteins. Isolated ZG were lysed by freezing and thawing and incubated at 37ºC without enterokinase (control) or with enterokinase (ZG_EK). Digestion was monitored by 15% SDS-PAGE and gels were stained with Coomassie blue. (A, C) In controls a slight digestion of ZG proteins is detected at 6 h indicated by the reduction of high molecular weight bands and the increase of low molecular weight bands. Digestion of proteins increases slowly over time. (B, D) In ZG_EK already after 5 minutes a prominent digestion of ZG proteins is observed when compared with the control. Several bands are protease resistant as they persist overtime and were identified by MS as: carboxypeptidase A (1), chymotrypsin C (2), elastase (3) and the lectin ZG16p (4).

The exocrine pancreas secretes digestive enzymes and mucins immersed in a bicarbonate (HCO^{3-}) rich fluid (pancreatic juice) to neutralize acid and provide optimal pH environment (slightly basic) for enzymatic digestion (Lee et al., 2012). On the other hand, digestive enzymes are stored in ZG under acidic pH (Lebel et al., 1988). To compare the extent of ZG protein digestion at different pH values (from acidic to basic), we induced the activation of zymogens by enterokinase at pH 6.0, 7.5, 8.0 and 9.0 (Figure 13). As expected, at basic pH (similar to the pancreatic juice, pH 8.0) protein digestion was fast and extensive, slowing down with the decrease of the pH. At basic pH, digestion is almost complete immediately after 1 h of incubation and only the identified protease resistant proteins remain.

In contrast, at an acidic pH of 6.0, ZG protein digestion is incomplete, as it can be observed by the band profile that is mostly similar from 1 h to 24 h of incubation (Figure 13 C). At neutral pH of 7.5, on the other hand, the digestion is still incomplete but more pronounced than at acidic pH (Figure 13 D). This is in accordance with physiological conditions since the acinar cells have several mechanisms to prevent premature intracellular activation of the zymogens under physiological conditions that include low concentrations of intracellular Ca^{2+}, the presence of protease inhibitors and low pH within the zymogen granules (Weiss et al., 2008).

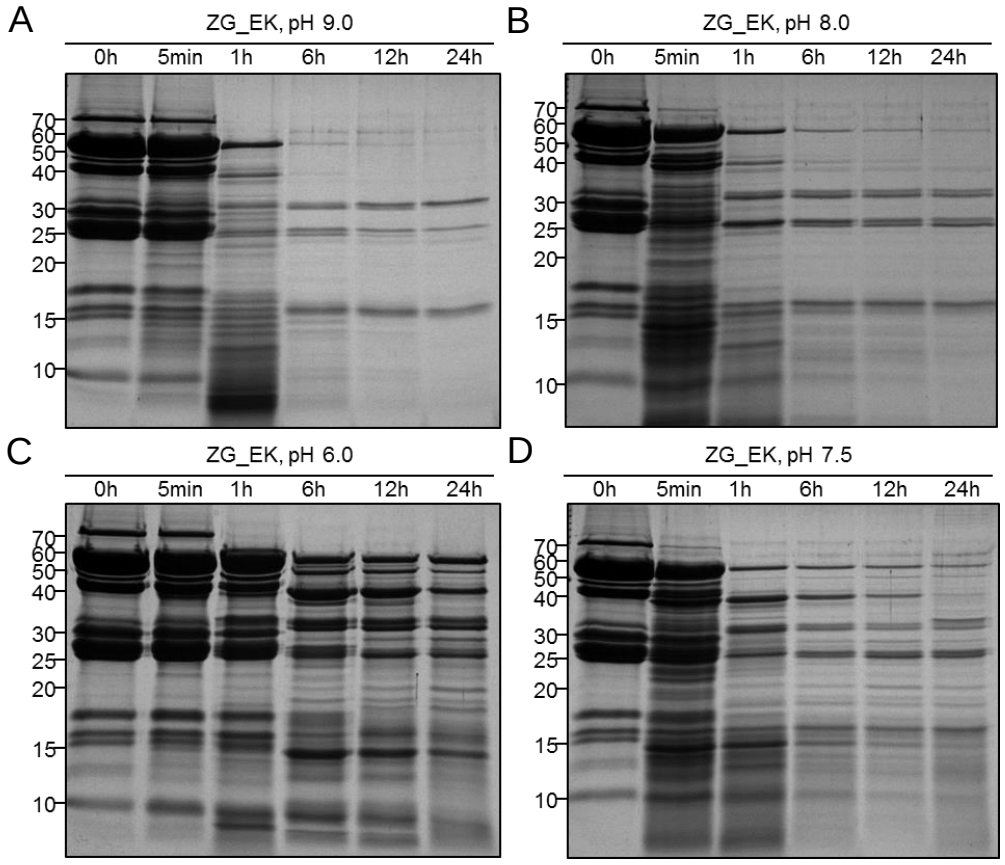

Figure 13. Digestion of ZG is pH-dependent. Isolated ZG were lysed by freezing and thawing. The pH of the samples was adjusted to (A) pH 9.0, (B) pH 8.0, (C) pH 6.0 and (D) pH 7.5 before incubation at 37ºC with enterokinase (ZG_EK). Samples were analysed by 15% SDS-PAGE and stained with Coomassie blue.

It is known that some of the pancreatic enzymes have a certain degree of protease resistance to each other (Szmola and Sahin-Tóth, 2007) what might explain their presence even at 48 h after protease activation. On the other hand, the presence of a small (16 kDa) non-enzymatic protein with no previous reference to protease resistance was quite intriguing. To confirm the MS identification of the lectin ZG16p and its resistance to protease digestion we performed an immunoblot with anti-ZG16p and anti-amylase antibodies. The digestion

of ZG (ZG_EK) was followed over a period of 24 h after enzymatic activation and it was possible to observe that amylase was completely digested after 2 h but the band corresponding to ZG16p remained constant over time (Figure 14).

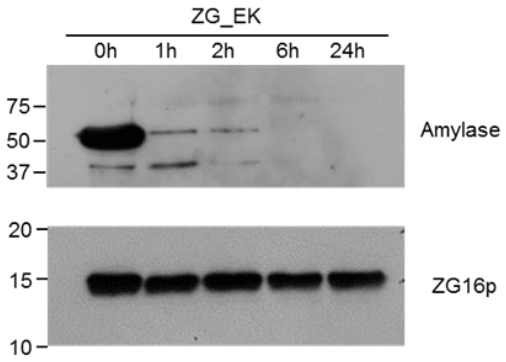

Figure 14. The lectin ZG16p is a protease resistant ZG protein. Isolated ZG were lysed by freezing and thawing and incubated at 37ºC with enterokinase (ZG_EK). 40 µg of protein were separated by 15% SDS-PAGE and analysed by immunoblotting with anti-amylase and anti-ZG16p antibodies.

ZG16p is predominantly associated with the luminal surface of ZGM, and can be removed in conjunction with proteoglycans/GAGs by carbonate-, chondroitinase- or heparitinase-treatment (Kleene et al., 1999b; Kumazawa-Inoue et al., 2012; Schmidt et al., 2000; Schrader, 2004). Interestingly, ZG16p was described to mediate the binding of aggregated secretory proteins to the submembranous matrix by associating with the dense granule core and the ZGM at acidic pH (Kleene et al., 1999b). ZG16p is likely a unique lectin with dual specificity to sulfated glycosaminoglycans (proteoglycan binding motif) and to polyvalent mannose and short chain α-manno-oligosaccharides (carbohydrate recognition domain) (Figure 15) (Kanagawa et al., 2014).

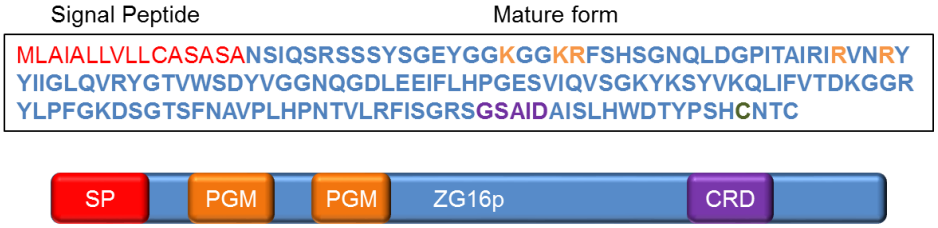

Figure 15. Amino acid sequence of rat ZG16p and its protein domains. Same colour was used to highlight the amino acids and corresponding domain. SP - Signal Peptide; PGM – Proteoglycan Binding Motif; CRD – Carbohydrate Recognition Domain.

Furthermore, ZG16p might have a protective function in the gut since it was identified as a prominent component of the mucus proteome, the first defence line of the gastrointestinal tract (Pelaseyed et al., 2014). In addition, ZG16p binds to pathogenic *Candida* and *Malassezia* species, heavily coated with mannan, through the carbohydrate recognition domain (see Chapter 1.5.3.5). Therefore, ZG16p is an interesting candidate to

play a major role in the sorting process in acinar cells and may also have a regulatory and/or a protective function after secretion.

4.2.2. Preparation of recombinant rat ZG16p

To investigate the protease resistant properties of the lectin ZG16p we prepared a recombinant protein. ZG16p has 167 amino acids (aa) where the first 16 aa represent a signal peptide that targets the protein to the ER (Cronshagen et al., 1994; Kanagawa et al., 2011). The signal peptide is removed upon entry into the ER, giving rise to the mature form of ZG16p (Kanagawa et al., 2011) (Figure 15). To purify the recombinant rat ZG16p by affinity chromatography, we generated two plasmids encoding ZG16p without the signal peptide to mimic the mature form of the protein (Figure 16).

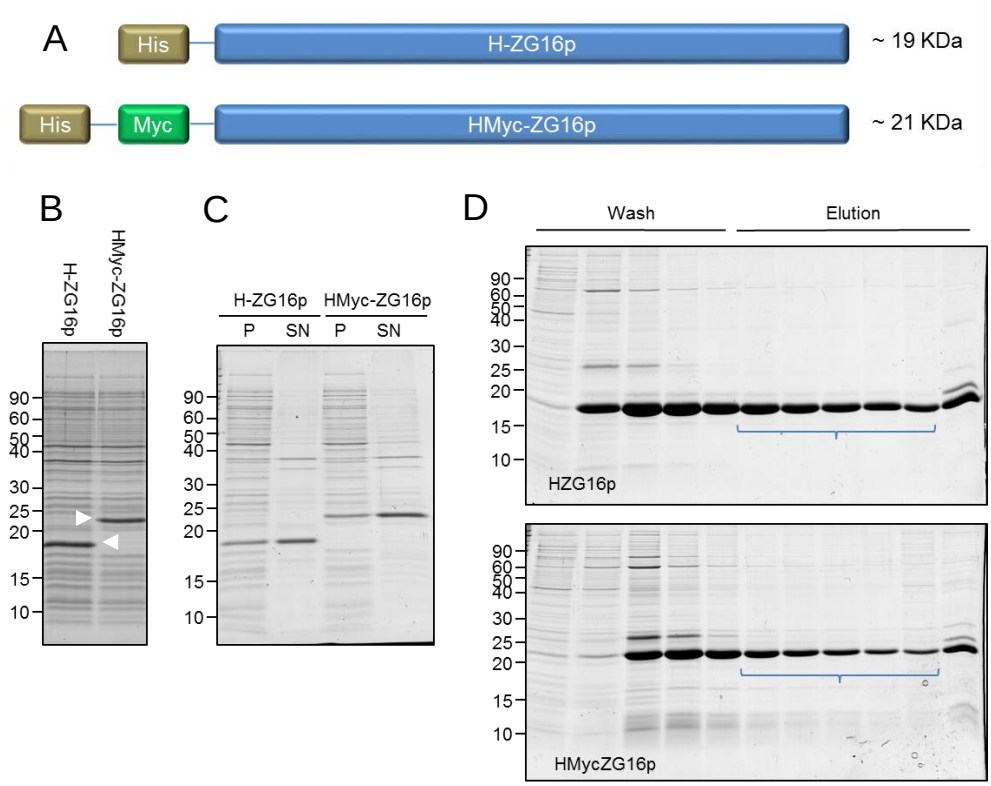

Figure 16. Purification of recombinant rat ZG16p. (A) Two ZG16p constructs with different tags were generated; a His-tagged version with 19 kDa (H-ZG16p) and a His-Myc-tagged construct with 21 kDa (HMyc-ZG16p). (B) *E. Coli* Rosetta were transformed with each construct and protein expression was induced with IPTG. Bacterial lysates were separated by 15% SDS-PAGE and stained with Coomassie blue. The recombinant ZG16p corresponds to the higher intensity band on each lane (arrow heads). (C) Bacterial lysate was centrifuged at 16000 rpm, 5 min. and the pellet (P) and supernatant (SN) fractions were separated on a 15% SDS-PAGE and stained with Coomassie blue. Both recombinant proteins are enriched in the supernatant showing that it is soluble. (D) Recombinant proteins were purified in a TALON His-Tag column. After loading the supernatant in the column, the fractions of the washing and the elution step were collected. The wash and elution were separated by 15% SDS-PAGE and stained with Coomassie blue. The fractions indicated (blue bracket) were collected and combined, constituting the purified ZG16p.

In addition, two tags were added to the N-terminus of ZG16p: a hexahistidine (His) tag to aid in the purification of the protein (H-ZG16p) in one case and a His plus a Myc tag to help in differentiating both recombinant proteins (HMyc-ZG16p) in the other case. Plasmids were transformed into *E. coli* Rosetta, and production of recombinant proteins was induced by addition of IPTG. After sonication of the bacteria, recombinant proteins were purified by affinity chromatography on a Cobalt (Co^{2+}) sepharose column (Figure 16). After purification, the recombinant proteins were used to characterize ZG16p by accessing resistance to digestion, formation of dimers and migration in polyacrylamide (PA) gels.

4.2.3. Protease resistance is an intrinsic property of ZG16p

We have shown (4.2.1) that endogenous ZG16p is a protease resistant protein. We now aimed to elucidate if this is an intrinsic property of ZG16p or the result of the interaction between ZG16p and other components of zymogen granules (e.g., submembranous matrix). The enzyme trypsin is normally used in proteomics to digest proteins in solution and in gel (Guo et al., 2014; Zhang et al., 2013). To investigate the protease resistance of ZG16p we incubated the recombinant proteins (H-ZG16p and HMyc-ZG16p) and the endogenous ZG16p (from the ZG subfractions – Wash) was used as a control, with and without trypsin at 37˚C for 16 h. If the recombinant proteins were not digested in the presence of trypsin it would mean that ZG16p resistance to proteases is an intrinsic property of the protein and if they were digested it would mean that the protease resistance depends on an external factor (e.g., binding to proteoglycans). Samples were separated by SDS-PAGE and stained with Coomassie blue or blotted and probed with an anti-ZG16p antibody (Figure 17 A and B). Although H-ZG16p, HMyc-ZG16p and the endogenous ZG16p have different molecular weights, due to the different protein tags, it was observed that after trypsin digestion all proteins migrate the same distance in the PA gel, indicating that they have the same molecular weight as a result of partial digestion of the recombinant proteins (Figure 17 A and B). Thus, the digestion of recombinant ZG16p resulted in a 3 kDa and 5 kDa shift (H-ZG16p and HMyc-ZG16p, respectively) in the protein size. Interestingly, this difference in the protein size corresponds to the size of the added tags to each recombinant protein (Figure 16 A). To investigate if the N-terminal tags are removed by trypsin digestion we used specific antibodies to His and Myc tags (Figure 17 C). As expected, before trypsin digestion

the His tag is detected in both recombinant proteins and the Myc tag is only detected on HMyc-ZG16p by western blot. However, after digestion both tags are no longer detected by immunoblotting suggesting that they were removed by trypsin. Since the molecular weight of both recombinant proteins, before and after digestion, only differs in the size that corresponds to the protein tags and the size after digestion is similar to the endogenous ZG16p, it indicates that ZG16p is not digested. These results show that resistance to digestion is an intrinsic property of ZG16p.

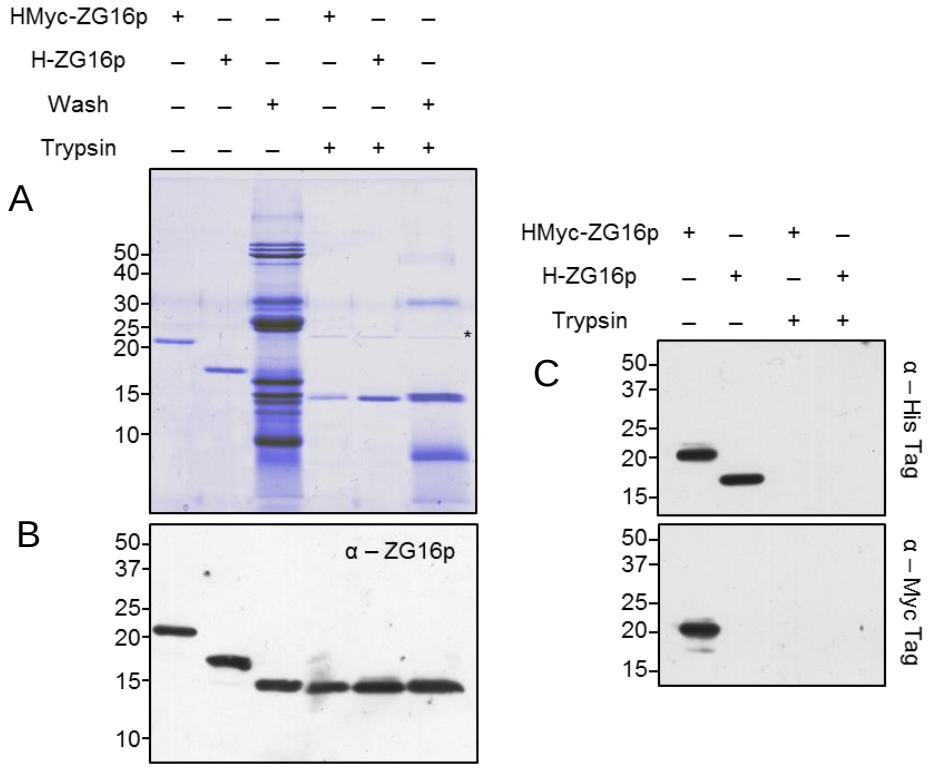

Figure 17. Recombinant ZG16p is protease resistant. (A) The purified recombinant proteins (HMyc-ZG16p and H-ZG16p) and the Wash fraction of the ZG with (first three lanes) and without (last three lanes) trypsin digestion were separated by 15% SDS-PAGE. The gel was stained with Coomassie blue. (B) Immunoblot of a gel similar to (A) probed with an anti-ZG16p antibody. After trypsin digestion the recombinant and endogenous proteins have the same protein size. (C) Immunoblot of recombinant ZG16p with and without trypsin digestion probed with an anti-histidine tag and anti-Myc tag antibodies. Note that both tags are removed after trypsin digestion.

4.2.4. Migration of ZG16p in SDS-PA gels is temperature sensitive

The lectin ZG16p, a resistant protein to pancreatic proteases, interacts with highly sulfated GAGs of proteoglycans present at the ZGM (Kumazawa-Inoue et al., 2012). Sulfated proteoglycans have previously been identified as constituents of pancreatic

zymogen granules (see Chapter 1.4). The glycosaminoglycans (GAGs) of the proteoglycans should resist the digestion after protease activation by enterokinase since no endoglycosidases (e.g., heparitinase, chondroitinase) were identified in ZG. To investigate if ZG16p is bound to proteoglycan GAGs after digestion of ZG subfractions the samples were analysed by immunoblotting with different temperature treatment before loading to the PA gel (see Chapter 3.4.7). In brief, the ZG subfractions digested after protease activation by enterokinase were heated at 95˚C or prepared at room temperature (RT) with SDS-PAGE loading buffer. The objective was to compare the migration of ZG16p of both samples, where the treatment at RT should not disrupt the interaction of ZG16p with the GAGs resulting in a shift of the molecular weight (correspondent to the size of ZG16p and the GAGs) observed in the immunoblotting. Remarkably, ZG16p was found by immunoblotting at the top of the gel (Figure 18) when the sample was prepared at RT. However, when the sample was prepared at 95˚C, ZG16p was identified at the expected size by immunoblotting. This indicates that ZG16p is present in a high molecular weight complex that is not able to enter the PA gel. The submembranous matrix model predicts high molecular weight components (e.g., a proteoglycan scaffold and associated (glyco)proteins) attached to the luminal side of the granule membrane and might be the responsible for retaining ZG16p on top of the gel.

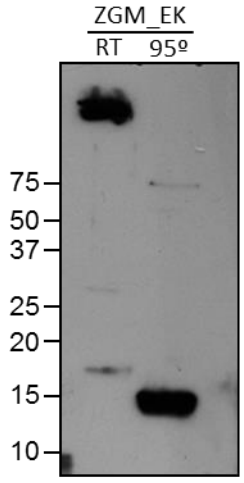

Figure 18. Migration of ZG16p in SDS-PAGE is temperature dependent. Digested ZGM (ZGM_EK) was prepared with or without boiling (95˚C or RT respectively) in SDS loading buffer before analysis by immunoblotting. An anti-ZG16p antibody was used. Note that ZG16p is detected at the top of the stacking gel (4% PA) when the sample is processed at RT and at the expected molecular weight after heating at 95˚C. RT, room temperature.

In support of the hypothesis that ZG16p interacts with the submembranous matrix and is thus retained on top of the PA gel, we repeated the same assay with several ZG subfractions. The submembranous matrix is localized at the luminal surface of the ZGM and is released by carbonate treatment, thus it is present in the ZGM fraction and constitutes most of the Wash fraction (obtained after carbonate treatment of the ZGM) and is absent in

the ZGC fraction. By comparing the ZGM and the Wash fractions it should be possible to rule out the presence of lipids and membrane proteins as the responsible for the formation of a high molecular weight complex that interferes with the migration of ZG16p in SDS-PAGE. We digested the ZG and the ZG subfractions (ZGM, Wash and ZGC) by addition of enterokinase and prepared the samples in SDS sample buffer at RT or 95˚C before immunoblotting analysis. The recombinant protein HMyc-ZG16p was used as a control to show that purified ZG16p migrates to the expected size in the PA gel when the sample is prepared at RT. As expected ZG16p was identified by immunoblotting at the top of the gel in different ZG subfractions when the samples were prepared at RT (Figure 19). However, HMyc-ZG16p was always found at the correct size showing that it is not the biochemical characteristics of ZG16p that disturb the migration of the protein in SDS-PAGE. This also indicates that the recombinant protein does not bind to the potential proteoglycans present in the high molecular weight complex probably because the binding sites are occupied by endogenous ZG16p. Several bands corresponding to the recombinant protein (HMyc-ZG16p) were observed due to partial protein digestion (Figure 19) by the proteases present in the samples. Interestingly, when the ZG and ZG subfractions were not digested, a fraction of endogenous ZG16p was also observed at the correct size (first lane in Figure 19 A, B and D) when prepared at RT in SDS-PAGE loading buffer. In addition, there was no observable difference between the ZGM and Wash subfractions allowing us to exclude the presence of the ZG membranes as the responsible for ZG16p retention on top of the gel (Figure 19 B and D). Taken together, these data is in favour of the presence of a high molecular weight complex associated with the ZGM.

In fact, the interaction of ZG16p with proteoglycans at the ZGM was already suggested. It was proposed that ZG16p mediates the binding of aggregated secretory proteins to the submembranous matrix at acidic pH and that impairment of *in vitro* condensation-sorting results in removal of both ZG16p and the proteoglycans from ZGM (Kleene et al., 1999b; Schmidt et al., 2000). Most recently Kumazawa-Inoue and colleagues identified two positive patches in the protein surface constituted by basic amino acids (lysine and arginine) that are responsible for the interaction of ZG16p with highly sulfated GAGs of proteoglycans present at the ZGM (Kumazawa-Inoue et al., 2012). Those GAGs were successfully digested with heparitinase II (HPRT).

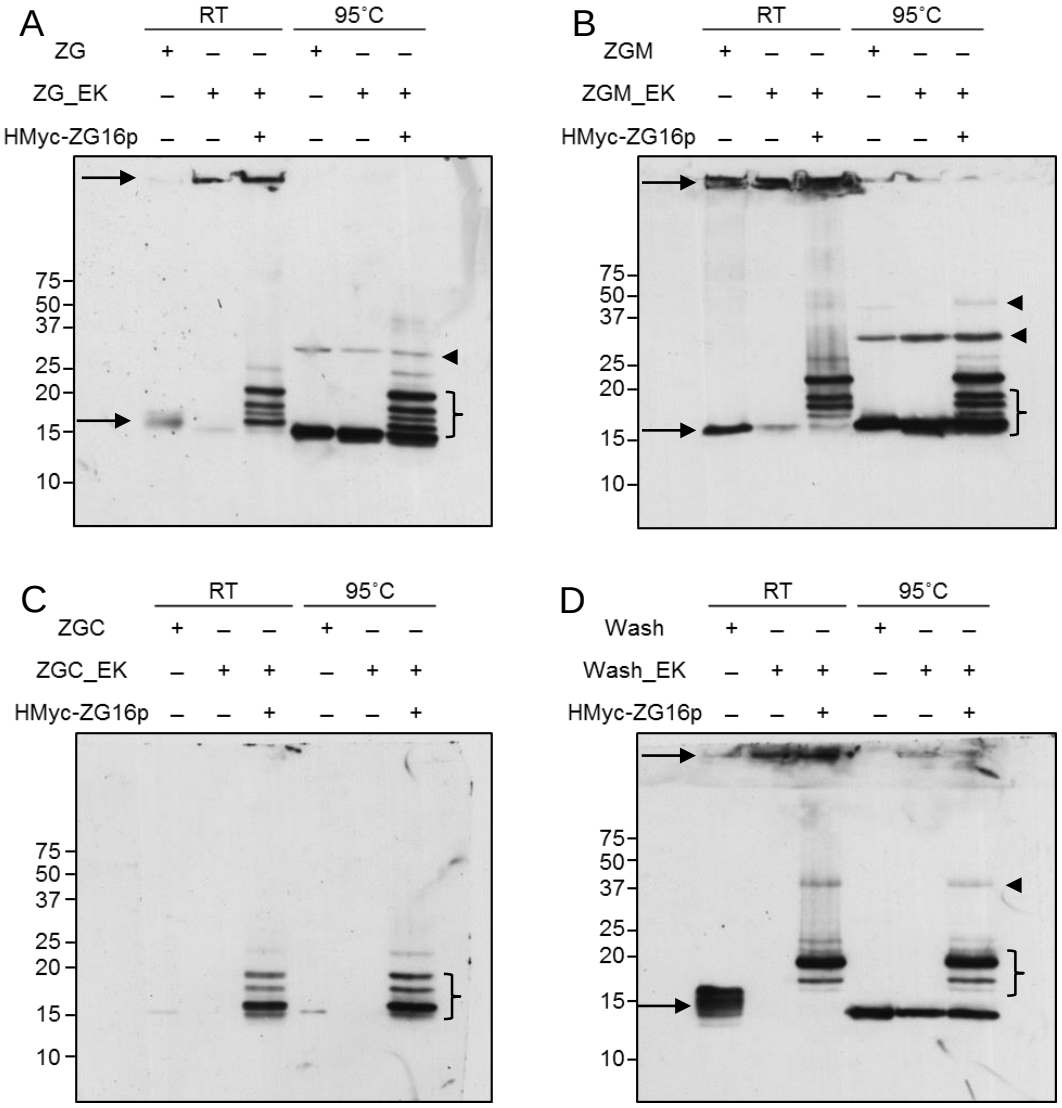

Figure 19. Migration of ZG16p in SDS-PAGE is temperature dependent and is observed in different ZG subfractions. ZG fractions were prepared with or without enterokinase and recombinant ZG16p (HMyc-ZG16p) was added to the sample with enterokinase right before loading. All samples were processed at room temperature (RT) or at 95˚C before analysis by immunoblotting with an anti-ZG16p antibody. Endogenous ZG16p is detected at the top of the stacking gel (4% PA) when is prepared at RT and at the expected molecular weight after heating at 95˚C (A, B and D) except for ZGC (C). On the other hand, the migration of recombinant ZG16p shows the same pattern at RT or 95˚C therefore it is independent of the sample treatment temperature. Arrows indicate endogenous ZG16p and brackets indicate recombinant ZG16p. Arrowheads indicate potential ZG16p dimers.

To test whether the interaction of ZG16p with GAGs prevents ZG16p from entering the PA gel we incubated the digested ZG fractions (ZG_EK and ZGM_EK) with the enzyme HPRT overnight at 30˚C (Figure 20). HPRT should be able to digest the GAG chains of the proteoglycans, disrupting the high molecular weight complex and allowing ZG16p to enter the PA gel. As a control we used ZG_EK without HPRT incubated under the same conditions. Samples were separated in 15% PA gel with (+) or without (-) heating at 95˚C

(Figure 20). To test if the enzyme HPRT was active at the conditions used we included a solution of heparin. The band corresponding to heparin is degraded after HPRT incubation, confirming that the enzyme is active (Figure 20 A, C, D and E). Under these experimental conditions, we did not observe differences between the samples with and without HPRT. Contrary to what was expected ZG16p did not enter the PA gel in the samples containing HPRT and prepared SDS-PAGE loading buffer without heating at 95˚C (-). Moreover, several bands appeared in the samples with and without HPRT that were not observed before (e.g., Figure 20).

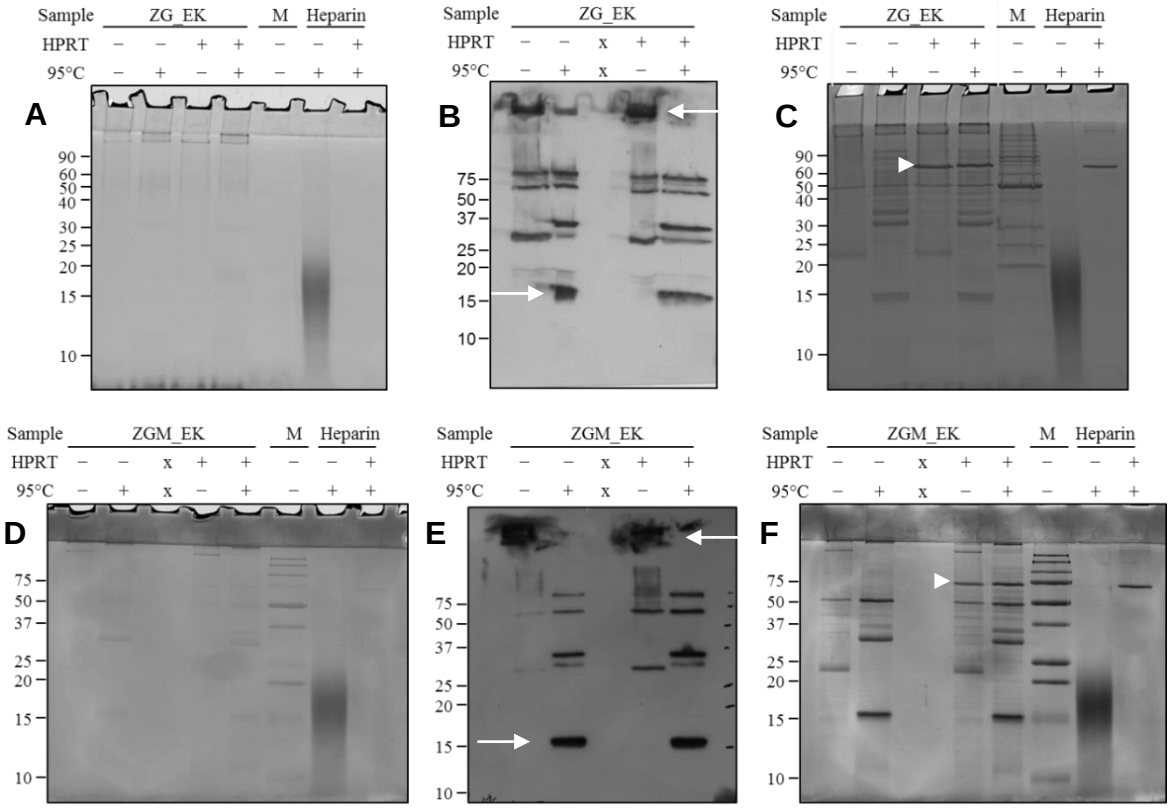

Figure 20. Digestion of ZG_EK and ZGM_EK with heparitinase II (HPRT). ZG_EK was incubated with (+) or without (-) HPRT overnight at 30°C. After incubation the samples were prepared for SDS-PAGE with (+) or without (-) heating at 95°C. As a control for HPRT activity a solution of heparin with a concentration of 1 mg/ml was used. (A and D) The gel was stained with Alcian Blue (specific for proteoglycans). The same pattern of bands is observed with or without HPRT incubation of ZG_EK or ZGM_EK. On the other hand, heparin is digested in the presence of HPRT confirming that this enzyme is active. (B and E) Immunoblotting of ZG_EK and ZGM_EK samples with or without HPRT incubation and probing with a ZG16p antibody. The same pattern of bands is observed in the presence or absence of HPRT. "x" indicates that no sample was loaded in the gel. (C and F) The same gel as in A and D respectively but stained with Coomassie blue. Again, there is no observable alteration in the band pattern. White Arrow indicates known ZG16p bands. Arrowhead indicates added HPRT. M, Marker.

These results indicate that either the binding of ZG16p to GAGs is not the responsible for retaining ZG16p at the top of the gel or that denaturation of the sample before addition of HPRT is required to provide access of the enzyme to the GAGs in order to accomplish the digestion. This may happen due to conformation of the GAGs that avoid binding of HPRT and/or due to binding of ZG16p to the GAGs protecting them from digestion by HPRT. Previously, ZG proteoglycans were successfully digested by HPRT after denaturation of the proteoglycans by boiling for 5 min (Kumazawa-Inoue et al., 2012).

4.2.5. ZG16p forms highly stable homodimers

Recently, it was suggested that ZG16p is a monomeric protein based on analysis by size exclusion chromatography, even though contact areas between ZG16p molecules were observed in crystals prepared for structure determination (Kanagawa et al., 2011). On the other hand, due to the observation of a band double the size (32 kDa) of ZG16p on immunoblots prepared with an anti-ZG16p antibody it was previously suggested that ZG16p might form dimers (Kalus et al., 2002; Kleene et al., 1999b). We have made a similar observation on immunoblots (e.g., Figure 19 B), despite the denaturing conditions used in the preparation of such immunoblots. To confirm the presence of ZG16p dimers we performed immunoblots prepared with endogenous and recombinant ZG16p with different molecular weights (ZG16p – 16 kDa, H-ZG16p – 19 kDa and HMyc-ZG16p – 21 kDa). This way, the resulting dimers should also differ between them (32, 38 and 42 kDa, respectively). Digested ZG (ZG_EK) were used as a source of endogenous ZG16p to reduce the complexity of the sample and to rule out unspecific binding of the antibody to other ZG proteins. The samples were prepared in SDS-PAGE loading buffer and heated at 65˚C for 5 min, 95˚C for 5 min or 95˚C for 10 min, separated by SDS-PAGE, blotted and probed with an anti-ZG16p antibody (Figure 21). Two bands were detected in all lanes, one corresponding to the monomeric form of ZG16p and the other, double the size, corresponding to the dimeric form. Furthermore, the intensity of the dimeric band decreased with increasing temperature and time, indicating that disruption of the dimer occurs only after prolonged exposure to high denaturing temperature. These results confirm that ZG16p forms dimers that are highly stable and resistant to denaturation.

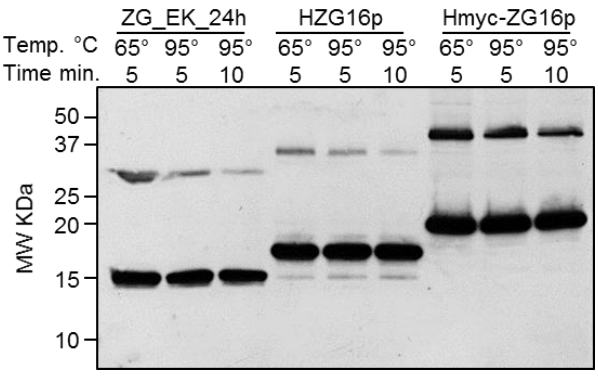

Figure 21. ZG16p is a dimeric protein. Endogenous (ZG_EK) and recombinant ZG16p (H-ZG16p, HMyc-ZG16p) were heated at 65˚C, at 95˚C for 5 minutes and at 95˚C for 10 minutes and analysed by immunoblotting with an anti-ZG16p antibody. In all lanes a monomeric (arrow) and a dimeric form (arrowhead) of ZG16p is detected. The intensity of the band that corresponds to the dimeric form decreases with both temperature and heating time.

We have generated several plasmids (see Table 4 and Chapter 4.3.1) to study the targeting of ZG16p to ZG in AR42J cells, a pancreatic model system. The cloning process involved two steps: first step was the addition of a Myc tag to the N-terminus of ZG16p and the second step was the addition of an ER targeting signal to the N-terminus of the Myc-tag. Surprisingly, when we tested the first plasmid (Myc-ZG16dSP) in COS-7 cells we discovered that when ZG16p is in the cytoplasm it binds to spherical and elongated tubular organelles (see Chapter 4.3.4). To further investigate this feature, we generated a GFP-tagged version of ZG16p (GFP-ZG16dSp) along with plasmids with point mutations in the proteoglycan and glycan binding motifs. We discovered that only the fusion protein with a mutation in one of the proteoglycan binding motifs (GFP-ZG16_K) lost its binding to the endo-lysosomal compartment (see Chapter 4.3.7) and was evenly distributed through the cytoplasm.

To demonstrate the formation of dimers by ZG16p we incubated the recombinant protein HMyc-ZG16p and the lysate of COS-7 cells expressing GFP-ZG16_K and performed a co-immunoprecipitation (co-IP) with an anti-GFP antibody (see Chapter 3.4.13). We expected to be able to co-immunoprecipitate GFP-ZG16p with HMyc-ZG16p, proving that both proteins were interacting due to the capacity of ZG16p to form dimers. A plasmid encoding for GFP alone was used as a control. We succeeded at co-immunoprecipitating GFP-ZG16p with HMyc-ZG16p (Figure 22 A and C) suggesting that both proteins were interacting, but a similar result was obtained when the GFP protein was used instead of GFP-ZG16_K. The co-immunoprecipitation was performed with two different systems: the GFP-Trap® and the PureProteome™ protein G magnetic beads coupled with an anti-GFP antibody. The use of two different antibodies allowed use to avoid a false positive result that could arise from the unspecific interaction between the antibody and HMyc-ZG16p resulting in the co-immunoprecipitation of the recombinant protein.

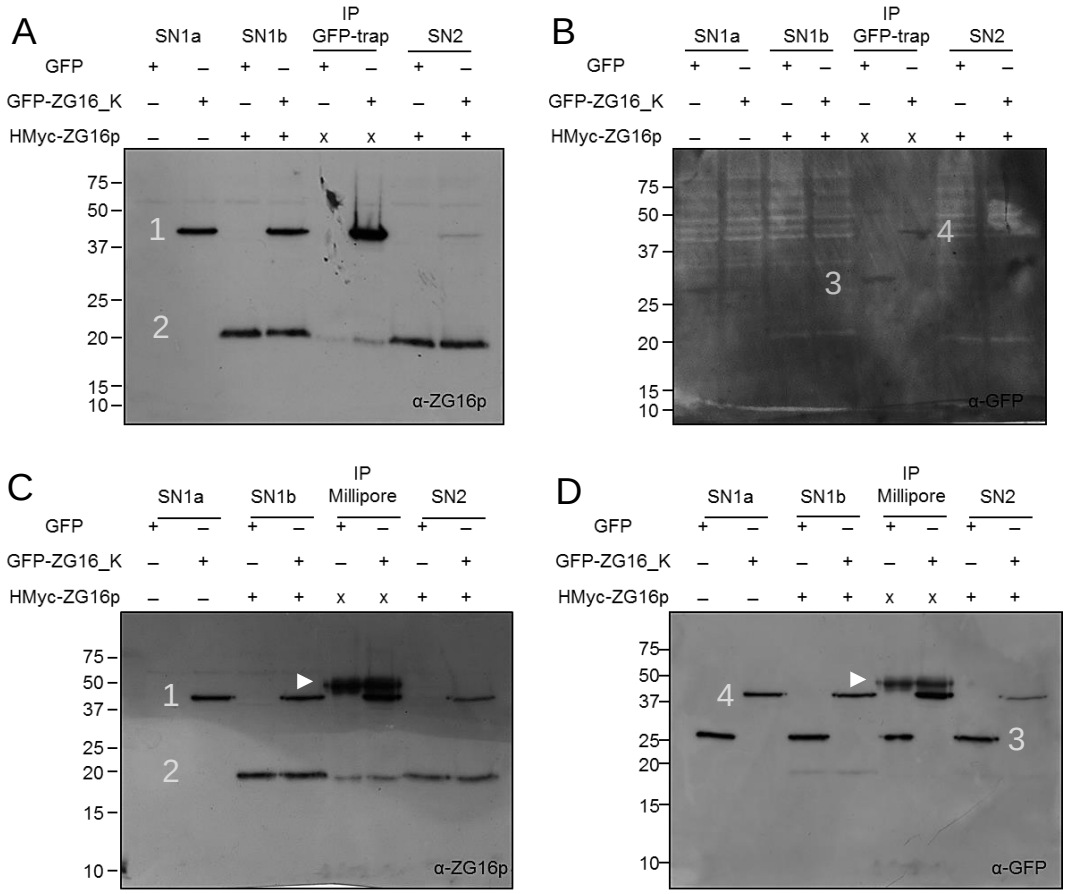

Figure 22. Co-immunoprecipitation (co-IP) of COS-7 cells transfected with GFP or GFPZG16_K via the GFP-Trap® magnetic beads or PureProteome™ protein G magnetic beads (Millipore) with an anti-GFP antibody. HMyc-ZG16p was added to the cell lysate before the co-IP in order to perceive the formation of dimers with GFP-ZG16_K. SN1a corresponds to the cell lysate. SN1b is the cell lysate after supplementation with HMyc-ZG16p and before addition of magnetic beads and SN2 is the supernatant after the co-IP. (A and C) Immunoblot with an anti-ZG16p antibody in which only GFP-ZG16_K (46 kDa) (1) and HMycZG16 (21 kDa) (2) are labelled. Note that HMyc-ZG16p was pulled-down in both samples (co-IP of GFP and GFP-ZG16_K). "x" indicates that HMyc-ZG16p was not added to the sample and the presence of the recombinant protein indicates interaction with GFP and GFP-ZG16_K. (B and D) Same membrane as in (A and C) but probed with an antibody to GFP. In this case only GFP (27 kDa) (3) and GFP-ZG16_K (4) bands are observed. Arrowheads indicate the bands corresponding to the heavy chain of the GFP antibody used in the co-IP with the PureProteome™ beads.

We were able to co-immunoprecipitate GFP-ZG16_K with HMyc-ZG16p by using both systems (Figure 22 A and C). However, co-immunoprecipitation of HMyc-ZG16p was also observed together with the GFP protein, indicating that the recombinant protein might interact with GFP (Figure 22 B and D). Thus, we could not confirm the dimerization of ZG16p based on this method because the co-immunoprecipitation of HMyc-ZG16p could be the result from interaction of the recombinant protein with "ZG16_K" (GFP-ZG16_K) or with GFP (GFP-ZG16_K or GFP protein).

These findings demonstrate that ZG16p is highly protease resistant and has the capacity to form dimers. Furthermore, we have shown that ZG16p is part of a high molecular weight complex associated with the ZGM (submembranous matrix). Since specific membrane receptors or sorting signals have not yet been identified in exocrine cells, the concept of the submembranous matrix offers an interesting alternative to understand the packaging and sorting of a complex mixture of proteins in an exocrine system. ZG16p is a unique lectin with dual specificity to sulfated glycosamynoglycans and to α-mannose-related glycans and might mediate the binding of the submembranous matrix and the aggregated zymogens. In the next chapter I have addressed if those binding domains are involved in the targeting of ZG16p to ZG in AR42J cells.

4.3. Functional analysis of ZG16p by expression and mutational studies in mammalian cells

ZG within acinar cells of the exocrine pancreas have long served as model organelles to understand regulated secretion. While the selective aggregation of ZG proteins has been well documented (see Chapter 1.2), their interaction with the TGN/ZG membrane is poorly understood at the molecular level, and neither a common sorting signal nor a sorting receptor has been identified so far. Although the application of proteomics has largely contributed to the identification of novel ZG proteins (Borta et al., 2010; Chen et al., 2006; Gómez-Lázaro et al., 2010; Rindler et al., 2007; Sun and Jiang, 2013) it was not yet accompanied by a better characterization of their functions. Since specific membrane receptors or sorting signals have not yet been identified in exocrine cells, the concept of the submembranous matrix offers an interesting alternative to understand the packaging and sorting of a complex mixture of proteins in an exocrine system. In support of this concept, we have identified novel ZG proteins, associated with the ZGM, with proteoglycan-binding properties (Chapter 4.1). Furthermore, it was suggested that ZG16p mediates the binding of aggregated secretory proteins to the submembranous matrix by associating with the dense granule core and the ZGM at acidic pH, and by impairment of *in vitro* condensation-sorting after removal of both ZG16p and the proteoglycans from ZGM (Kleene et al., 1999b; Schmidt et al., 2000). Surprisingly, using an *in vitro* digestion assay we discovered that ZG16p is highly protease-resistant and appears to be part of a high molecular weight complex within ZG, which might be as well protease-resistant. Furthermore, ZG16p is likely a unique lectin with dual specificity to sulfated glycosaminoglycans (proteoglycan binding motif) and to α-mannose-related glycans (carbohydrate recognition domain) (Figure 15) (Kanagawa et al., 2011, 2014; Kumazawa-Inoue et al., 2012; Tateno et al., 2012). Moreover, the glycan binding site does not compete with the heparin binding site on ZG16p (Kanagawa et al., 2014) (see Chapter 1.5.3.2).

In this chapter, we generated ZG16p constructs to be expressed in AR42J cells, a pancreatic cell model system, and screened, by mutational studies of the binding motifs, for alterations in ZG16p targeting/sorting into ZG. Pancreatic AR42J cells have been used as a model system for granule formation and pancreatic exocrine secretion. They were originally derived from a rat pancreatic tumour following exposure to azaserine (Longnecker et al., 1979). Treatment with the synthetic glucocorticoid dexamethasone induces the

differentiation of AR42J cells into exocrine, acinar-like cells and the *de novo* formation of electron-opaque secretory granules, which contain the major pancreatic zymogens. However, when compared to acinar cells from rat pancreas, AR42J cells are non-polarized, do not express all rat ZG proteins and exhibit smaller ZG (Logsdon et al., 1985; Rinn et al., 2012). The generation of wild type and mutated versions of ZG16p aimed at examining if the proteoglycan and/or the carbohydrate recognition motifs of ZG16p are essential for its sorting into ZG. Additionally, several constructs targeting ZG16p to the cytoplasm were generated and expressed in COS7 cells. Although ZG16p is not targeted to the cytoplasm under normal conditions it might escape from the ZG into the cytoplasm under disease conditions (e.g., pancreatitis).

4.3.1. Cloning of ZG16p with a Myc-tag at the N-terminus for expression in mammalian cells

ZG16p has 167 amino acids (aa) where the first 16 aa represent a signal peptide that targets the protein to the ER (Cronshagen et al., 1994; Kanagawa et al., 2011) and it does not have any transmembrane domains (Borta et al., 2010; Cronshagen et al., 1994; Kanagawa et al., 2011, 2014). Additionally, the residues 36-159 correspond to the jacalin-related domain. In order to investigate the targeting of ZG16p to ZG in AR42J cells we generated a plasmid with a Myc tag at the N-terminus of the mature form of ZG16p (16-167 aa). This was achieved in two steps: the first step was to insert ZG16p without the signal peptide (ZG16dSP) in the vector pCMV-tag3A in order to add a Myc tag at the N-terminus of ZG16dSP (Myc-ZG16dSP). And the second step consisted in the amplification of Myc-ZG16dSP and insertion in the vector pDsREd2-ER (Supplementary Figure 1) in order to add an ER signal (calreticulin) at the N-terminus of the Myc tag (ER-Myc-ZG16p) (Figure 23). The DsRed2 sequence and KDEL retention signal were removed from the pDsREd2-ER plasmid during the cloning procedure (Supplementary Figure 1).

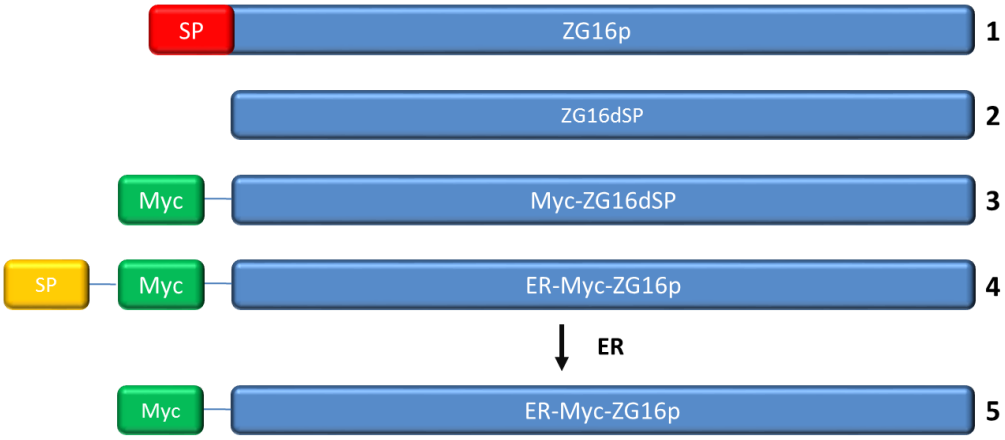

Figure 23. Cloning strategy for expression of ZG16p in mammalian cells. 1 – ZG16p; 2 – removal of the signal peptide (SP) from ZG16p; 3 – Addition of a Myc tag to the N-terminus of ZG16p; 4 – Addition of a SP to the N-terminus of the Myc tag. 5 – Removal of the SP after entering the ER and processed ZG16p N-terminally tagged.

Expression of ER-Myc-ZG16p in mammalian cells targets ZG16p to the ER, where the ER signal is removed giving rise to the mature form of the protein with a Myc tag at the N-terminus (Figure 24).

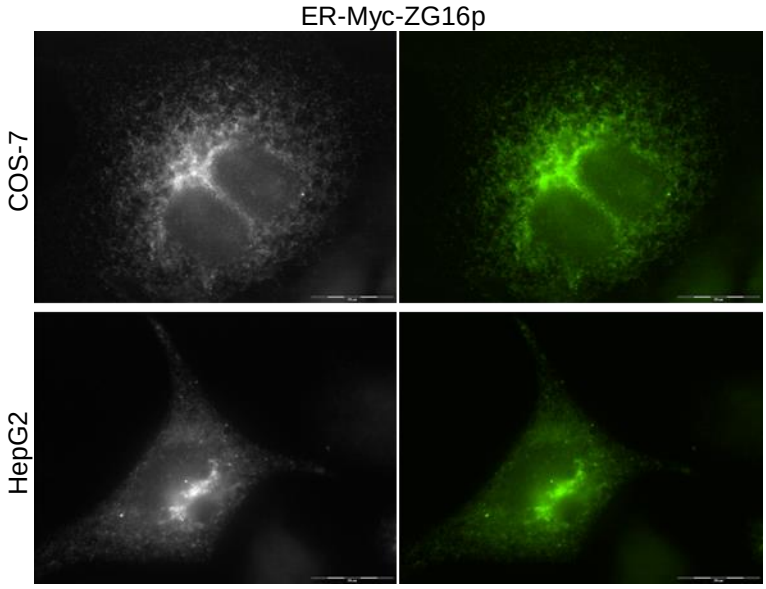

Figure 24. Expression of ER-Myc-ZG16p in COS-7 and HepG2 cells. Cells were transfected with ER-Myc-ZG16p construct and fixed after 24 h with 4% paraformaldehyde. Immunostaining was performed with an anti-Myc antibody. In both cell lines an ER like staining is observed. Bars, 20µm.

4.3.2. Deletion of the carbohydrate recognition domain inhibits ZG16p targeting to ZG in AR42J cells

While the selective aggregation of ZG proteins has been well documented, their interaction with the TGN/ZG membrane is poorly understood at the molecular level, and neither a common sorting signal nor a sorting receptor has been identified so far. ZG16p has a carbohydrate recognition domain (CRD) that is conserved in the majority of β-prism fold

lectins (Kumazawa-Inoue et al., 2012; Raval et al., 2004; Sharma et al., 2007). It is composed by 5 amino acids with a glycine and an aspartic acid separated by a 3-amino-acid spacer (GXXXD). In order to investigate if this domain is responsible for the targeting of ZG16p to ZG we generated a mutant protein by removing the CRD (aa 147-151) (ER-Myc-ZG16dCRD). AR42J cells were transfected with the wild type plasmid (ER-Myc-ZG16p) and the mutant (ER-Myc-ZG16dCRD) (Figure 25) and stimulated for granule formation with dexamethasone. After 2-3 days, cells were processed for indirect immunofluorescence with antibodies directed to carboyxpeptidase A (CBP, ZG marker), to the Myc tag and the Golgi markers TGN38 and p115. Colocalization between CBP and Myc was observed in dexamethasone stimulated AR42J cells transfected with ER-Myc-ZG16p (Figure 25 A-C) showing that the wild type ZG16p is targeted to ZG. On the other hand, cells transfected with ER-Myc-ZG16dCRD only showed limited colocalization between CBP and Myc indicating that the mutant protein is not targeted to ZG. Nevertheless, normal granule formation was not affected in transfected cells (Figure 25 D). Furthermore, immunostaining with anti-Myc antibody of transfected cells revealed absence of labelling in the Golgi region (Figure 25 E), supporting the idea that the mutant ZG16p fails to enter the secretory pathway. We then used two Golgi markers (TGN38 and p115) to further confirm if the mutant ZG16p was present in the Golgi complex. We did not observe colocalization between the Golgi markers TGN38 (Figure 25 J-L) and p115 (Figure 25 P-R) with the mutant ER-MycZG16dCRD. On the other hand, the wild type protein colocalized with the TGN38 (Figure 25 G-I) and with the p115 (Figure 25 M-O) proteins.

The zymogens are synthesized by ribosomes, associated with ER membranes, and inserted into the lumen of the rough ER. In the supranuclear region, the Golgi complex receives the products of the rough ER and starts the sorting of proteins into forming ZG. These results suggest that the mutant ER-Myc-ZG16dCRD is not transported to the Golgi complex and is most probably retained in the ER. This may happen because the CRD is essential for the sorting of ZG16p into the Golgi complex or the removal of the 5 amino acids interferes with the correct folding of the protein and inhibits the transport to the Golgi complex. The involvement of the CRD domain on targeting of ZG16p to ZG in AR42J cells was further investigated by mutational analyses.

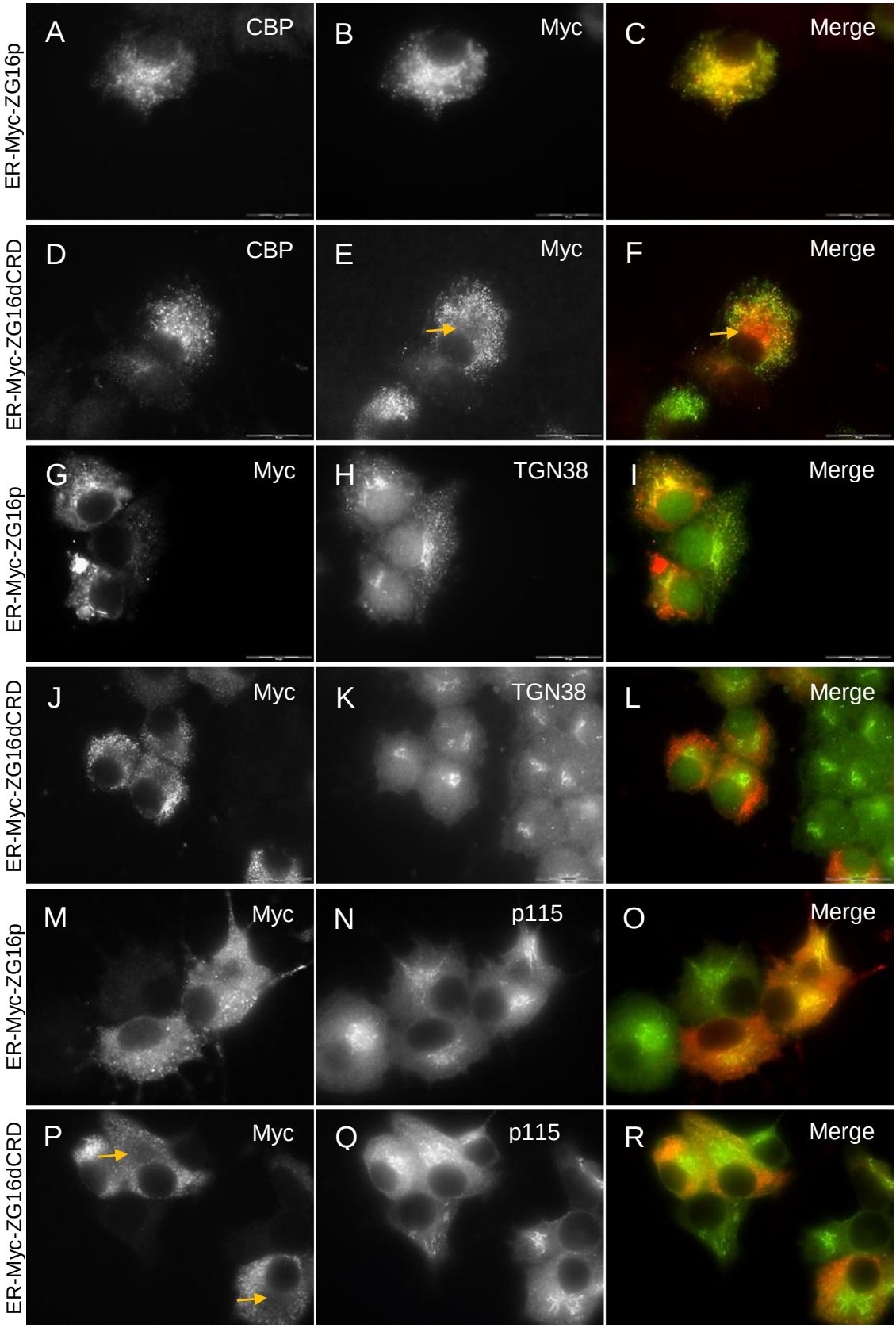

Figure 25. The ER-Myc-ZG16dCRD mutant is not target to ZG in pancreatic acinar AR42J cells. AR42J cells were transfected with a ER-Myc-ZG16p construct (A-C, G-I and M-O) or with the ER-Myc-ZG16dCRD

mutant (D-F, J-L and P-R) stimulated for granule formation and processed for indirect immunofluorescence 72 h after transfection using antibodies directed to carboxypeptidase A (CBP) (A and D), the Myc tag (B, E, G, J, M, P) and the Golgi markers TGN38 (H and K) and p115 (N and Q). Overlays (Merge) of (A-B; D-E; G-H; J-K, M-N and P-Q) are shown in (C, F, I, L, O and R). The ER-Myc-ZG16p colocalizes with the ZG marker (CBP) (C) and the Golgi markers TGN38 and p115 (I and O respectively). The ER-Myc-ZG16dCRD mutant does not colocalize completely with CBP (F). Yellow arrow points to an area devoided of ER-Myc-ZG16dCRD. Additionally, ER-Myc-ZG16dCRD does not colocalize neither with the TGN38 (L) or the p115 (R). Bars, 20µm.

4.3.3. Sorting of ZG16p into ZG is independent of the proteoglycan and glycan binding motifs

The concept of the submembranous matrix (a putative proteoglycan/glycoprotein scaffold at the luminal side of the ZGM) offers an interesting alternative to understand the packaging and sorting of a complex mixture of proteins in an exocrine system. ZG16p is a component of the submembranous matrix where it interacts with sulfated proteoglycans (Kleene et al., 1999b; Kumazawa-Inoue et al., 2012; Schmidt et al., 2000; Schrader, 2004) through two positively charged basic patches, constituted by lysine and arginine residues on the surface of the protein that interact with the negatively charged side chains of sulfated proteoglycans (Kanagawa et al., 2011; Kleene et al., 1999b; Kumazawa-Inoue et al., 2012). Point mutation of those sites (K33A, K36A, R37A and R55A, R58A) abolished the binding to heparin (Kumazawa-Inoue et al., 2012). In addition, ZG16p binds to polyvalent mannose and short chain α-manno-oligosaccharides via the carbohydrate recognition domain (GXXXD) and mutation of the amino acid D151A abolished the binding (Kanagawa et al., 2014; Tateno et al., 2012).

Although the removal of the CRD inhibited the targeting of ZG16p to ZG in AR42J cells we were not able to confirm if that inhibition was due to the absence of the CRD or to interference with the correct folding of the protein. Thus, we decided to address this by point mutation of the amino acids involved in the binding of ZG16p to proteoglycans and to glycans. We generated several constructs with point mutations (see Chapter 3.3.7) to investigate if inhibition of the proteoglycan and glycan binding motifs inhibits sorting of ZG16p to ZG in AR42J cells, namely: ER-Myc-ZG16_K (K33A, K36A, and R37A), ER-Myc-ZG16_R (R55A and R58A) and ER-Myc-ZG16_D (D151A) (Figure 26). AR42J cells were transfected with the wild type plasmid (ER-Myc-ZG16p) and the mutants (ER-Myc-ZG16_K, ER-Myc-ZG16_R and ER-Myc-ZG16_D) (Figure 27) and stimulated for granule

formation with dexamethasone. After 2-3 days, cells were processed for indirect immunofluorescence with anti-Carboyxpeptidase A (CBP, ZG marker) and anti-Myc antibodies. Colocalization between CBP and Myc was observed in transfected and dexamethasone stimulated AR42J cells (Figure 27), showing that the three mutants were targeted to ZG in AR42J cells.

MLAIALLVLLCASASANSIQSRSSSYSGEYGGKGGKRFSHSGNQLDGPITAIRIRVNRYYIIGLQVRYG
TVWSDYVGGNQGDLEEIFLHPGESVIQVSGKYKSYVKQLIFVTDKGGRYLPFGKDSGTSFNAVPLHP
NTVLRFISGRSGSAIDAISLHWDTYPSHCNTC

Figure 26. ZG16p amino acid sequence. Amino acids subjected to point mutation are highlighted. K33A, K36A, and R37A corresponds to mutant "K"; R55A, R58A corresponds to mutant "R" and D151A corresponds to mutant "D".

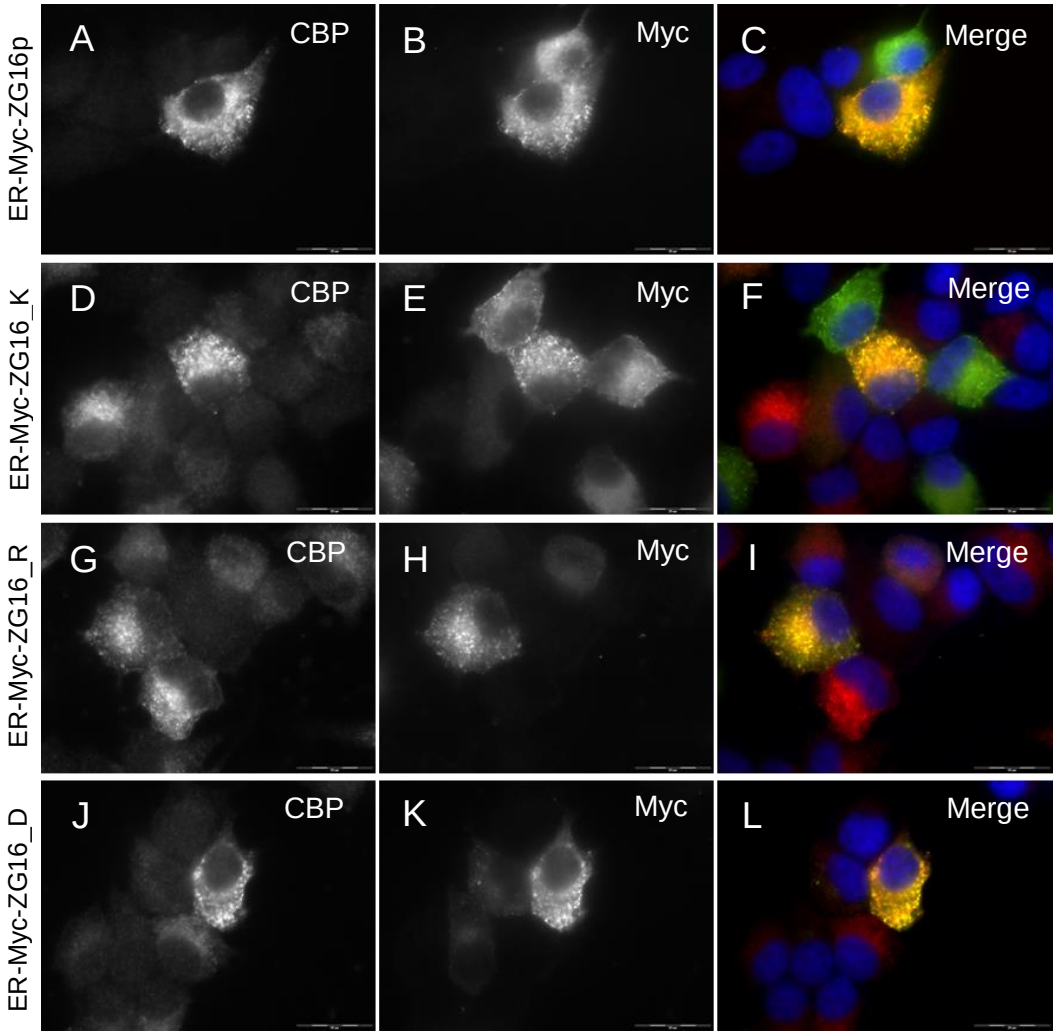

Figure 27. ER-Myc-ZG16p and ER-Myc-ZG16p mutants are targeted to ZG in pancreatic acinar AR42J cells. AR42J cells were transfected with a ER-Myc-ZG16p construct (A-C) or with the mutants: ER-Myc-ZG16_K (D-F), ER-Myc-ZG16_R (G-I) or ER-Myc-ZG16_D (J-L); stimulated for granule formation and processed for indirect immunofluorescence 72 h after transfection using antibodies directed to carboxypeptidase A (CBP) (A, D, G and J) and the Myc tag (B, E, H and K). Overlays (Merge) of (A-B; D-E; G-H; J-K) are shown in (C, F, I, L). Yellow dots represent colocalization of the transfected protein (green) with the ZG marker, carboxypeptidase A (red). Nuclei are stained with Hoechst (blue). Bars, 20µm.

Double and triple mutants (ER-Myc-ZG16_K_R, ER-Myc-ZG16_K_D, ER-Myc-ZG16_R_D and ER-Myc-ZG16_KRD, respectively) were also generated and all of them were targeted to ZG in AR42J cells after dexamethasone stimulation (Figure 28). Thus, mutation of the proteoglycan or glycan binding motifs, either alone or in parallel, did not inhibit the targeting of ZG16p to ZG in AR42J cells.

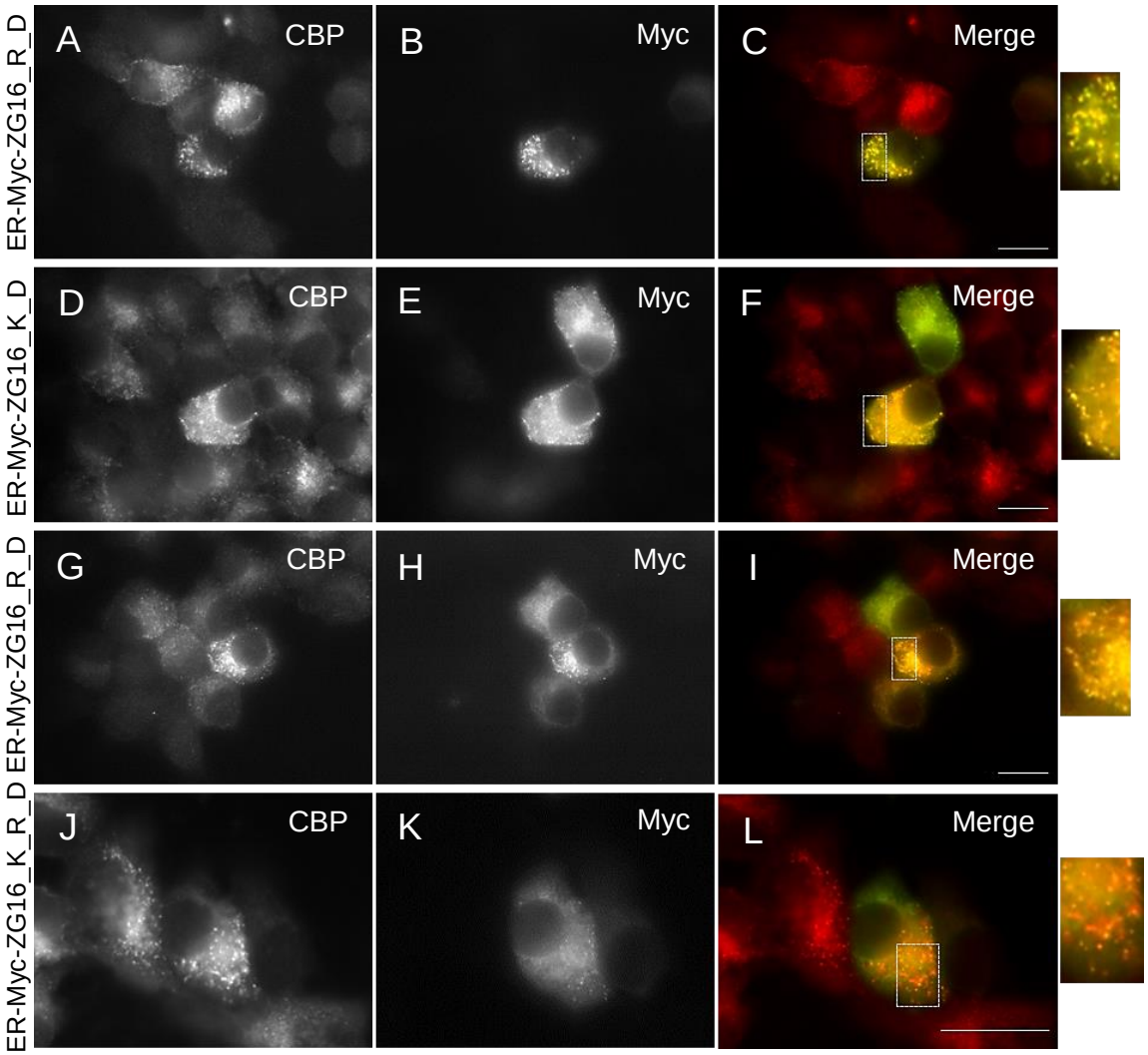

Figure 28. ER-Myc-ZG16p double and triple mutants are targeted to ZG in pancreatic acinar AR42J cells. AR42J cells were transfected with the mutants: ER-Myc-ZG16_K_R (A-C), ER-Myc-ZG16_K_D (D-F), ER-Myc-ZG16_R_D (G-I) or ER-Myc-ZG16_K_R_D (J-L); stimulated for granule formation and processed for indirect immunofluorescence 72 h after transfection using antibodies directed to carboxypeptidase A (CBP) (A, D, G and J) and the Myc tag (B, E, H and K). Overlays (Merge) of (A-B; D-E; G-H; J-K) are shown in (C, F, I, L). In the right column is shown the zoom of dashed areas on the merge panel (C,F, I, L). Yellow dots represent colocalization of the transfected protein (green) with the ZG marker, carboxypeptidase A (red). Bars, 20µm.

4.3.4. ZG16p binds to spherical and elongated tubular structures when expressed in the cytoplasm of mammalian cells

As described before (see Chapter 4.3.1) the cloning of ER-Myc-ZG16p followed two steps: first the removal of the signal peptide and insertion of a Myc tag at the N-terminus of ZG16p, and then the insertion of an ER-targeting signal in the N-terminus of the Myc tag. Once the first part was accomplished, the generated construct (Myc-ZG16dSP) was tested in COS-7 cells. Surprisingly, instead of an expected cytosolic localisation, ZG16p was found to label a membrane compartment composed of spherical and elongated tubular structures (Figure 29). In addition, we expressed Myc-ZG16dSP in cell lines originating from different tissues and species: COS-7 cells (Kidney, monkey), HepG2 cells (liver, human) and AR42J (pancreas, rat) and observed the same phenotype in all cell lines (Figure 29) indicating that the membrane binding partner of ZG16p is conserved across species and is not tissue specific.

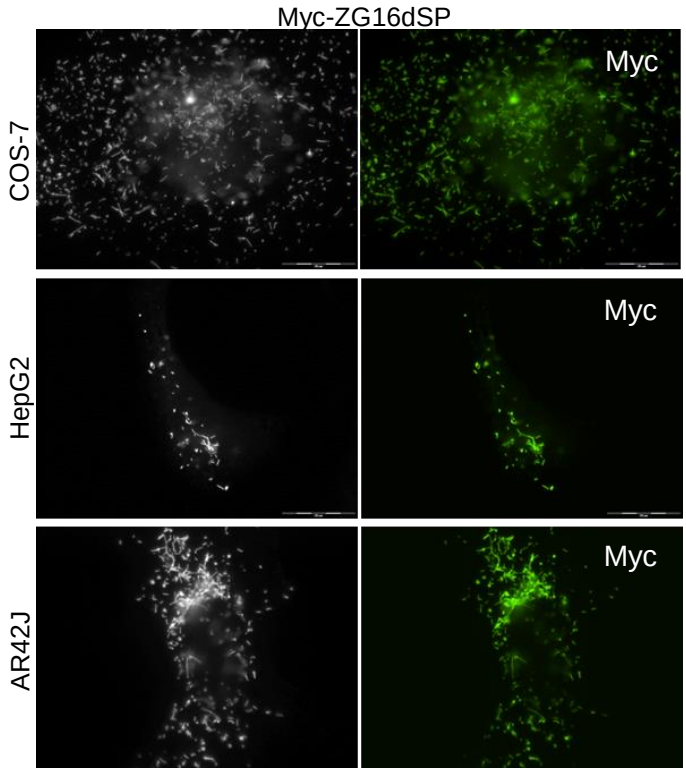

Figure 29. Expression of Myc-ZG16dSP in different cell lines shows a similar phenotype. COS-7 (monkey, kidney), HepG2 (human, liver) and AR42J (rat, pancreas) were transfected with Myc-ZG16dSP and processed for indirect immunofluorescence 24 h after transfection using antibodies directed to the Myc tag. In all cell lines the construct labels a membrane compartment composed of spherical and elongated tubular structures Bars, 20µm.

Next, a GFP-tagged construct was generated (GFP-ZG16dSP) in order to perform live cell microscopy and investigate if the observed structures are motile. Interestingly, transfection of COS-7 cells with GFP-ZG16dSP revealed a different phenotype from Myc-ZG16dSP (Figure 30). Instead of the spherical and elongated tubular structures observed after expression of Myc-ZG16dSP only spherical structures were observed along with

concentration of relatively large structures in the perinuclear region after expression of GFP-ZG16dSP (Figure 30). Thus, two distinct phenotypes were observed depending on the tag fused to ZG16p. We then generated an untagged version of ZG16p without the signal peptide (ZG16dSP) to investigate which one of the phenotypes is closest to a condition were ZG16p would escape from the ZG to the cytoplasm. Expression of ZG16dSP in COS-7 cell resulted in a phenotype similar to the one observed after expression of the Myc-ZG16dSP construct: the labelling of spherical and elongated structures (Figure 30).

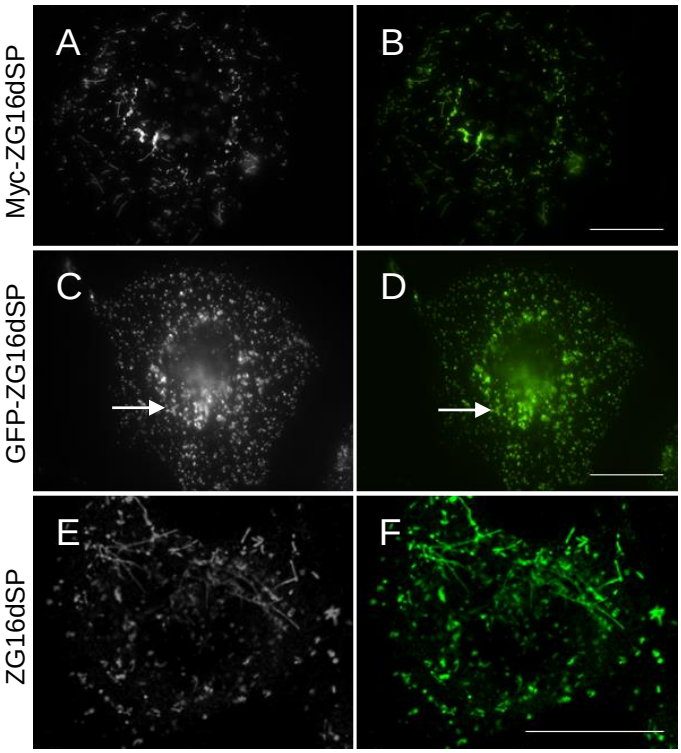

Figure 30. Expression of Myc-ZG16dSP, GFP-ZG16dSP and ZG16dSp in COS-7 cells reveals different phenotypes. COS-7 cells were transfected with Myc-ZG16dSP, GFP-ZG16dSP or ZG16dSp and processed for indirect immunofluorescence 24 h after transfection using antibodies directed to the Myc tag or to ZG16p. Myc-ZG16dSP and ZG16dSP show a similar phenotype with spherical and elongated tubular structures (A-B and E-F), while GFP-ZG16dSP shows a phenotype composed of spherical structures with concentration of relatively large structures in the perinuclear region (arrow) (C and D). Bars, 20µm.

These results show that it is clearly possible to distinguish two membrane phenotypes of ZG16p labelled structures after expression of the three plasmids: a similar phenotype after expression of Myc-ZG16dSP and ZG16dSP that is different from the phenotype obtained after expression of GFP-ZG16dSP. The GFP-tag is quite large (~28 kDa) when compared with the Myc-tag (~1 kDa) and it is almost double the size of ZG16p, what might limit the full extent of the interaction of ZG16p with the binding partner or with other components, resulting in a different membrane phenotype.

4.3.5. GFP-ZG16dSP and Myc-ZG16dSp bind to the same motile structures

As observed before (4.3.4), expression of GFP-ZG16dSP and Myc-ZG16dSP in mammalian cells results in the labelling of morphologically different membrane structures.

To verify if the labelling of both proteins corresponds to the same organelle/structure both constructs were co-transfected in COS-7 cells (Figure 31). Co-transfected cells showed a phenotype with labelled spherical and elongated structures, similar to expression of Myc-ZG16dSp or ZG16dSP alone. Furthermore, GFP-ZG16dSP and Myc-ZG16dSP colocalized showing that they were bound to the same organelle/structure (Figure 31 A-C). This finding shows that although expression of GFP-ZG16dSP or Myc-Zg16dSP alone results in different phenotypes, the labelling corresponds to the same structure/organelle. And, since co-expression of both plasmids results in a membrane compartment composed of spherical and elongated tubular structures that correspond to a phenotype similar to expression of Myc-ZG16dSP or ZG16dSP, we suggest that this is the "dominant" phenotype or the phenotype that would result from escape of ZG16p to the cytoplasm.

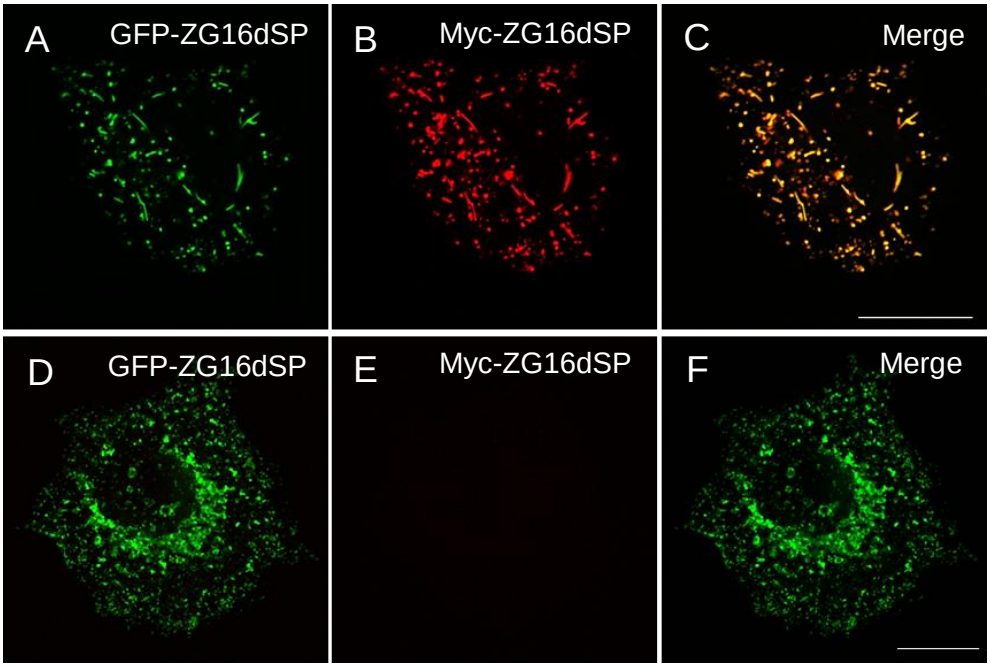

Figure 31. GFP-ZG16dSP and Myc-Zg16dSP bind to the same organelle. COS-7 cells were co-transfected with GFP-ZG16dSP and Myc-ZG16dSP and processed for indirect immunofluorescence 24 h after transfection using antibodies directed to the Myc tag. Overlays (Merge) of the confocal images are shown on the right (C and F). Yellow dots show colocalization of both proteins (C). Co-transfected cells show a phenotype similar to expression of Myc-ZG16dSP alone (A-C). This phenotype is clearly different from the one observed in cells transfected only with GFP-ZG6dSP (D-F). Bars, 20 µm

Additionally, we performed live cell experiments after co-expression of Myc-ZG16dSP and GFP-ZG16dSp in order to investigate the mobility of the labelled structures/organelles. Co-expression of both constructs allowed the visualization of the "dominant" phenotype as shown before. Figure 32 shows single planes taken every 13 second using a laser scanning confocal microscope. The yellow arrow highlights a mobile

membrane structure in co-transfected COS-7 cells. The fact that the observed structures are mobile and dynamic indicates that ZG16p is bound to a membranous organelle.

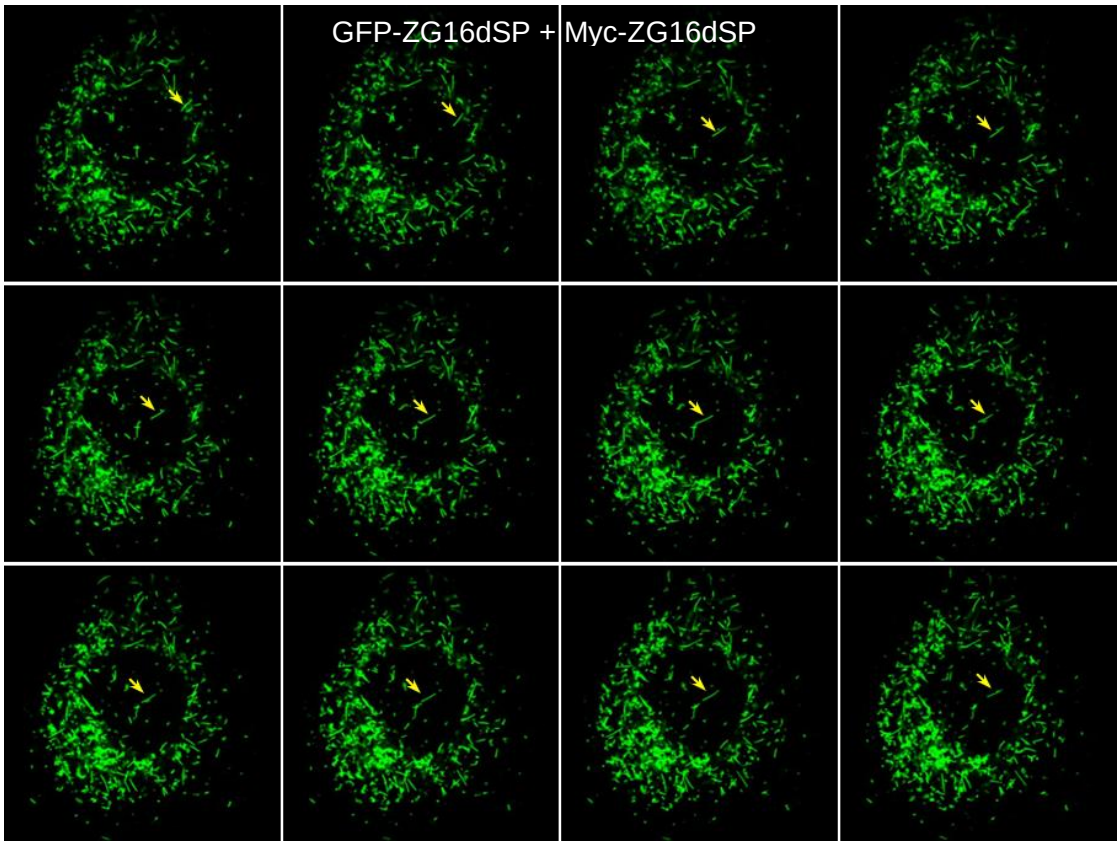

Figure 32. Cytoplasmic ZG16p binds to mobile organelles. COS-7 cells were co-transfected with GFP-ZG16dSP and Myc-ZG16dSP and prepared for live cell microscopy in the following day. Single planes were taken using a laser scanning confocal microscope. ZG16p positive organelles were tracked over an 11 minutes period taking pictures every 13 second. Co-transfection is indicated by the phenotype of the organelles (similar to Myc-ZG16dSP) and the green fluorescence (from GFP-ZG16dSP). Yellow arrow indicates an organelle with clear movement.

4.3.6. Cytoplasmic ZG16p binds to the endo-lysosomal compartment

Aiming at the identification of the organelles that are labelled by cytoplasmic ZG16p we performed colocalization experiments with endosomal and lysosomal markers. The protein EEA1 (early endosome antigen 1) is a known endosomal marker. COS-7 cells transfected with Myc-ZG16dSP or GFP-ZG16dSP were prepared for immunofluorescence with anti-Myc and anti-EEA1 antibodies (Figure 33). Myc-ZG16dSP colocalized partially with EEA1 (Figure 33 A-C), while GFP-ZG16dSP has a higher degree of colocalization (Figure 33 D-F). Both fusion proteins colocalized partially with the endosomal marker EEA1 but their localization is not restricted to endosomes containing EEA1 protein. Since

expression of Myc-ZG16p or GFP-ZG16p showed a different phenotype and a different degree of colocalization with the EEA1 marker it indicates that the fusion proteins might interfere with the normal dynamics of the endosome compartment. We have shown that when co-expressed both constructs bind to the same structures. Thus, if both ZG16p constructs bind to the same structure but show a different degree of colocalization with the same marker it indicates that those structures are being affected differently by the expressed proteins. In support of this we can observe that the phenotype of normal endosomes (cells not transfected) shown by staining of the EEA1 marker (Figure 33 G-H) is different from the phenotype observed after expression of GFP-ZG16p (Figure 33 D-F) or Myc-ZG16p (Figure 33 A-C).

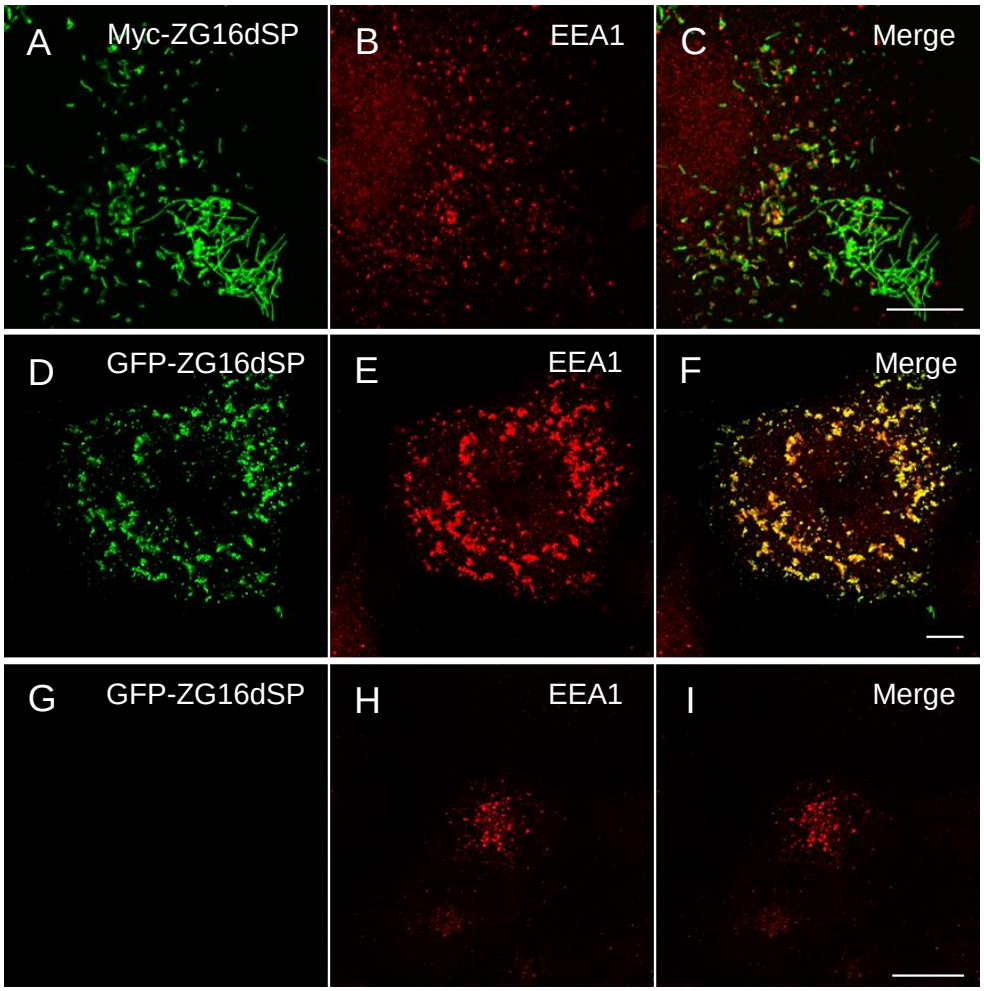

Figure 33. Expression of ZG16p in the cytoplasm partially colocalizes with the early endosomal marker (EEA1). COS-7 cells were transfected with GFP-ZG16dSP or Myc-ZG16dSP and processed for indirect immunofluorescence 24 h after transfection using antibodies directed to the Myc tag and EEA1. Overlays (Merge) of the confocal images are shown on the right (C, F and I). Yellow dots show colocalization of the transfected protein (green) with EEA1 marker (red). Myc-ZG16dSP show a partial colocalization with EEA1(C) and a higher degree of colocalization is observed between GFP-ZG16dSP and EEA1 (F). (H and I) show the typical phenotype for EEA1 in non transfected cells. Bars, 20µm.

In addition we have used the endosomal probe transferrin conjugated with the fluorophore Texas Red (TexasRed-Tf) to investigate the colocalization of endosomes with GFP-ZG16dSP. The serum protein transferrin is of major importance for the cellular iron uptake mechanism (Baravalle et al., 2005; Chung and Wessling-Resnick, 2003). Iron-loaded transferrin binds to the transferrin receptor (TfnR) and both are efficiently internalized into acidic early endosomes, in which both Fe^{3+} ions are released, with apotransferrin remaining bound to the receptor. The apotransferrin-TfnR complex is then recycled to the plasma membrane where the neutral pH of the extracellular environment causes its dissociation (Baravalle et al., 2005). Figure 34 shows partial colocalization between GFP-ZG16dSP and TexasRed-Tf (arrows) supporting the finding that cytoplasmic ZG16p interacts with the endosomal compartment.

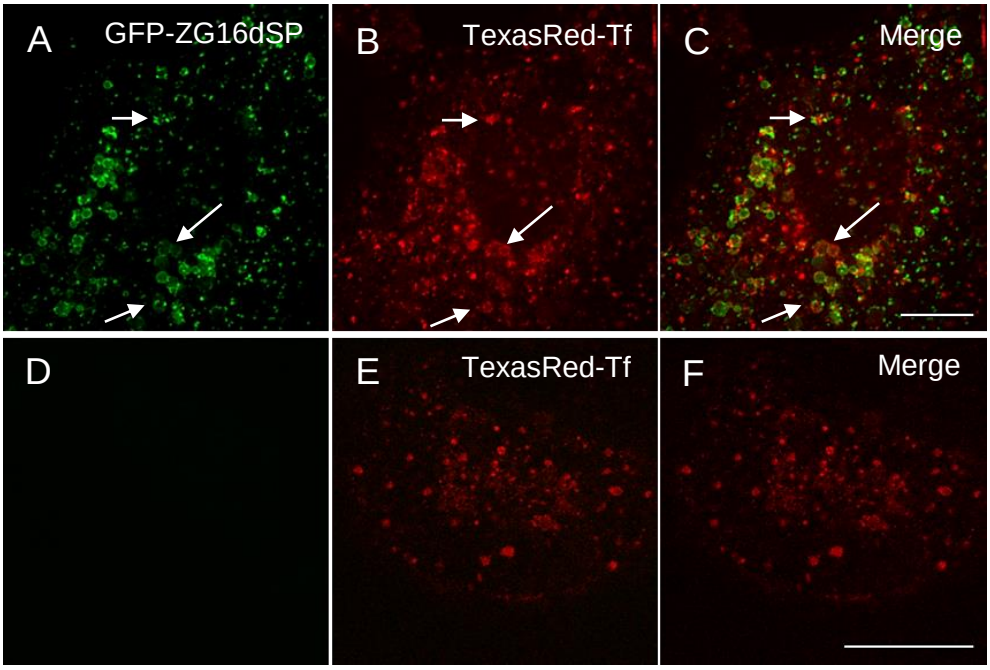

Figure 34. Expression of ZG16p in the cytoplasm partially colocalizes with the endosomal marker transferrin (TexasRed-Tf). COS-7 cells were transfected with GFP-ZG16dSP and incubated with TexasRed-transferrin (TexasRed-Tf) for 1 h and fixed with 4% paraformaldehyde. Overlays (Merge) of the confocal images are shown on the right column (C and F). Arrows indicate colocalization of the transfected protein (green) with TexasRed-Tf (red). (D-F) Images of non transfected cells. Bars, 20µm.

Next, we tested colocalization of Myc-ZG16dSP and ZG16dSP with the lysosomal compartment. The most abundant transmembrane proteins of the lysosomal membrane are the lysosomal associated membrane proteins LAMP-1 and LAMP-2 (Schwake et al., 2013). To investigate the interaction of ZG16dSP with lysosomes we used the construct GFP-Lamp1 either co-expressed with the ZG16dSP or Myc-ZG16dSP constructs in COS-7 cells.

Partial colocalization was observed by confocal microscopy between ZG16dSP and GFP-Lamp1 (Figure 35 A-C) and between Myc-ZG16dSP and GFP-Lamp1 (Figure 35 D-F). This indicates that cytoplasmic ZG16p also binds to lysosomes. Images of cells expressing GFP-Lamp1, ZG16dSp and Myc-ZG16dSP alone were taken during the same experiment (Figure 35 G-O), showing the characteristic phenotype that results from expression of each construct.

Taken together, these results indicate that expression of the lectin ZG16p in the cytoplasm leads to its interaction with the endo-lysosomal compartment.

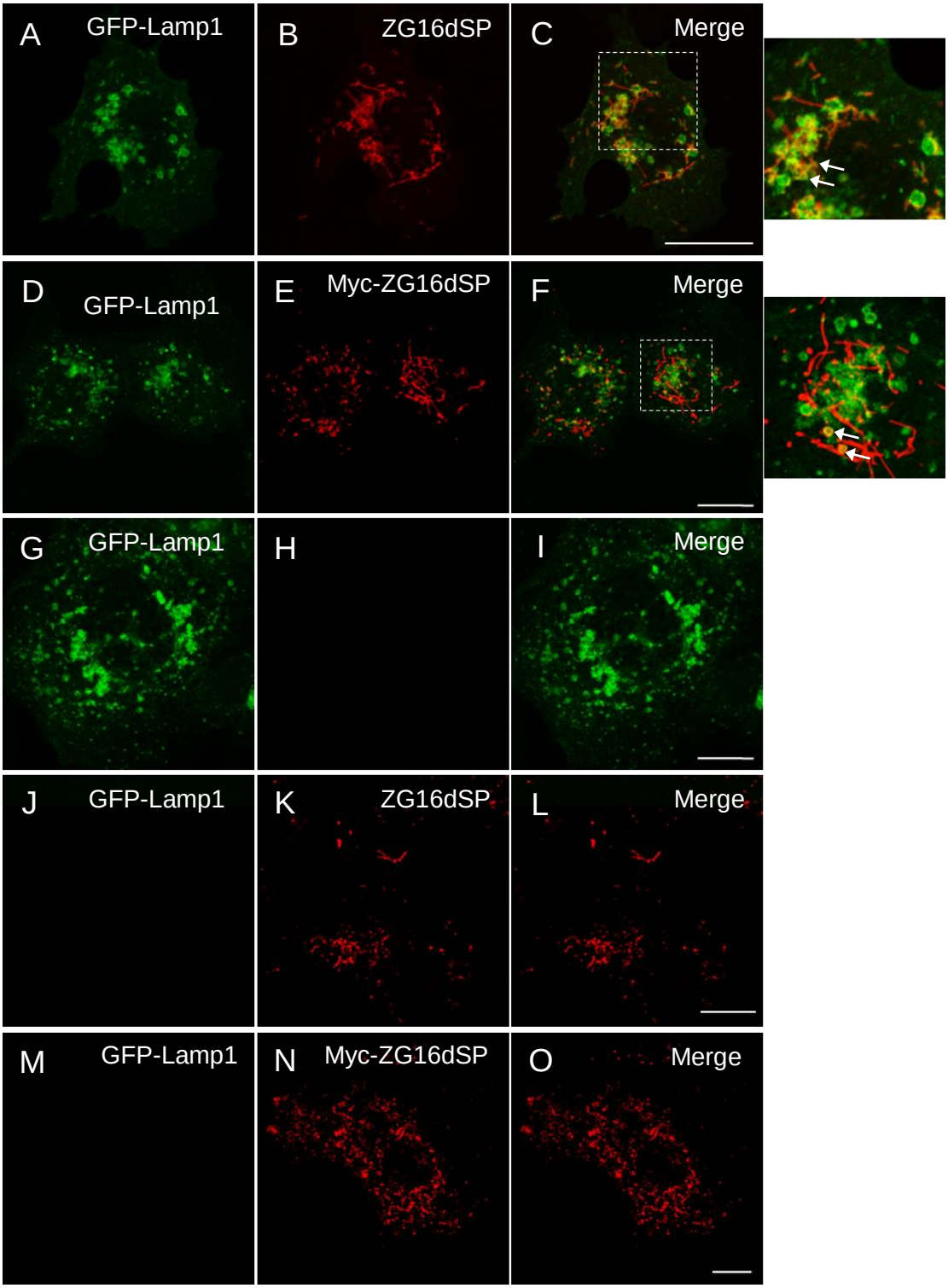

Figure 35. Expression of cytoplasmic ZG16p partially colocalizes with the lysosomal marker Lamp1. COS-7 cells were co-transfected either with GFP-Lamp1 and ZG16dSP or GFP-Lamp1 and Myc-Zg16dSP and processed for indirect immunofluorescence 24 h after transfection using antibodies directed to the Myc tag and ZG16p. Overlays (Merge) of the confocal images are shown on the right (C, F, I, L and O). Yellow dots represent colocalization of the lysosomal marker Lamp1 (green) with the cytoplasmatic ZG16p (red) (C and F). Both ZG16p constructs partially colocalize with GFP-Lamp1, as indicated by arrows on the right column (zoom of dashed areas on the corresponding merge panel – C and F). (G-O) Images of single transfected cells showing the phenotype corresponding to each construct taken in the same experiment. Bars, 20µm.

4.3.7. Cytoplasmic ZG16p binds to endo-lysosomal compartment through the proteoglycan binding site K33A.K36A.R37A.

We discovered that cytoplasmic ZG16p is able to bind to the endo-lysosomal compartment but the details of the interaction and the binding partner(s) were still unknown. To perceive if the proteoglycan and/or the glycan binding motifs, present in the ZG16p, were responsible for the cytoplasmic ZG16p interaction with the endo-lysosomal compartment, we generated several point mutations in a similar way to the ER-Myc-ZG16p construct (see Chapter 4.3.3). New constructs were generated based on Myc-ZG16dSP and GFP-ZG16dSP: Myc-ZG16dSP_K, Myc-ZG16dSP_R, Myc-ZG16dSP_D and GFP-ZG16dSP_K, GFP-ZG16dSP_R, GFP-ZG16dSP_D (K and R represent the mutation of proteoglycan binding sites, while D represents the mutation of the glycan binding site).

Expression of the Myc-tagged mutants in COS-7 cells revealed that only the Myc-ZG16dSP_K mutant inhibited the binding of cytoplasmic ZG16p to the endo-lysosomal compartment and was now observed spread through the cytoplasm (Figure 36). The same result was obtained in the case of the GFP-tagged mutants, where only GFP-ZG16dSP_K did not bind to the endo-lysosomal compartment (Figure 36). This indicates that the interaction of cytoplasmic ZG16p with the endo-lysosomal compartment is mostly electrostatic, being mediated by positive amino acids (K33A.K36A.R37A) present on the surface of ZG16p (see Figure 5).

Surprisingly, during the generation of a construct for expression of ZG16p in mammalian cells we discovered that ZG16p binds to the endo-lysosomal compartment when expressed in the cytoplasm. Although ZG16p is not present in the cytoplasm under normal conditions its release from the ZG might happen under disease conditions. Furthermore we showed that the binding of ZG16p to the endo-lysosomal compartment is mediated by a positive patch constituted by positive amino acids (K33 K36, R37) present on the surface of ZG16p. This further supports a potential (patho)physiological role of ZG16p in mammalian cells. We should not forget that the expression of ZG16p is not limited to the pancreas but is observed throughout the gastro-intestinal tract and other tissues as well (see Chapter 1.5.3.4).

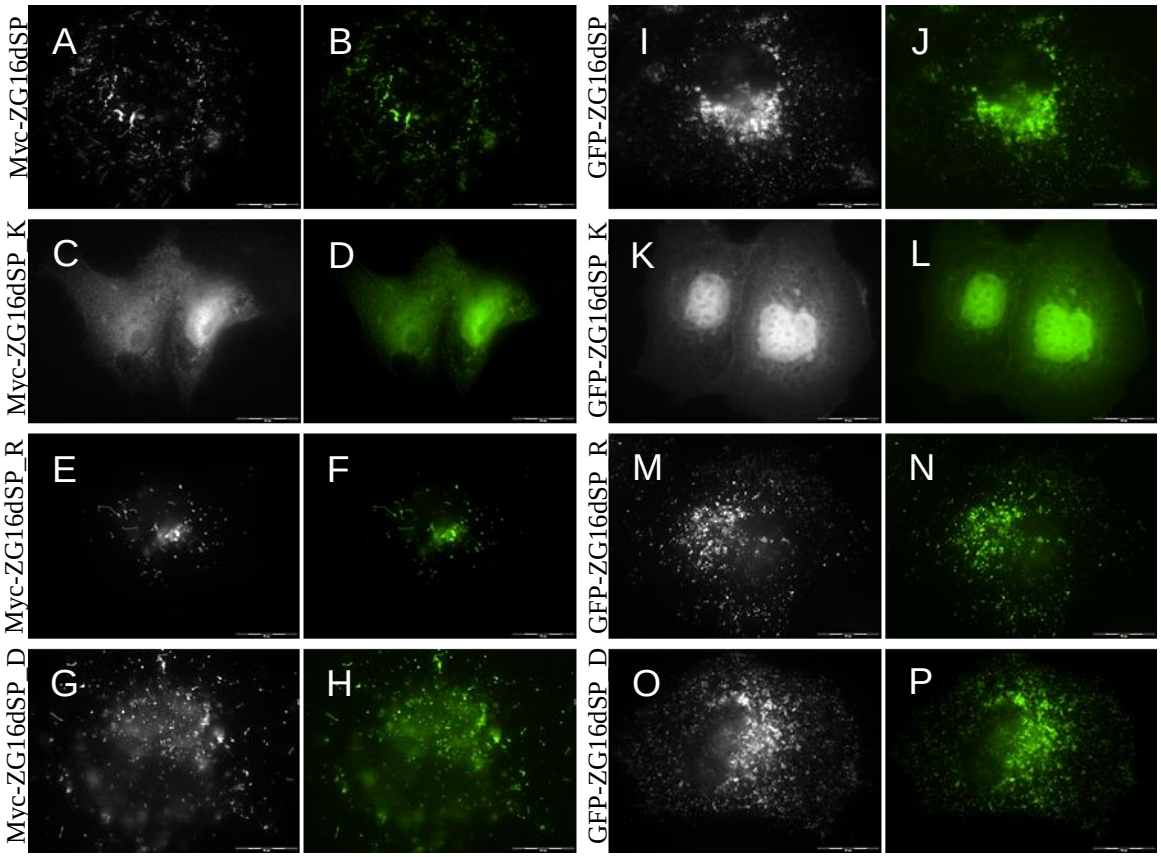

Figure 36. Mutation of the proteoglycan binding site K33A.K36A.R37A inhibits the binding of cytoplasmic ZG16p. COS-7 cells were transfected with Myc-ZG16dSP or GFP-ZG16dSP or with the mutants Myc-ZG16pdSP_K, Myc-ZG16dSP_R, Myc-ZG16dSP_D and GFP-ZG16dSP_K, GFP-ZG16dSP_R, GFP-ZG16dSP_D and processed for indirect immunofluorescence 24 h after transfection using antibodies directed to the Myc tag. Only the "K" mutant (Myc-ZG16dSP_K and GFP-ZG16dSP_K) shows a uniform cytoplasmatic and nuclear staining with no binding of the endo-lysosomal compartment (C-D and K-L). Bars, 20µm.

DISCUSSION

5. Discussion

The acinar cells of the exocrine pancreas are "specialists" in the synthesis, mass packaging/sorting, storage and regulated secretion of a complex mixture of digestive (iso)enzymes and associated proteins. This protein mixture is packaged in a condensed, predominantly inactive form into large (1 µm) zymogen granules (Arvan and Castle, 1992; Schrader, 2004). The digestive enzymes are released via the pancreatic duct system into the small intestine, where conversion of trypsinogen to trypsin is mediated by proteolytic cleavage via enterokinase, an enzyme of the duodenal mucosa. Activated trypsin then proteolytically cleaves and activates the other zymogens. Once in the intestinal tract, granule proteins are also supposed to fulfil important regulatory and protective functions, e.g. in host defence (e.g., ZG16p, Syncollin, GP2) (Bach et al., 2006; Hase et al., 2009; Parikh et al., 2012; Szmola and Sahin-Tóth, 2007; Tateno et al., 2012).

A first and crucial step in ZG biogenesis is the sorting of proteins to be packaged in the ZG. The zymogens progressively aggregate at the mildly acidic pH and high Ca^{2+} levels within the TGN and form dense core aggregates which are supposed to interact with the TGN membrane (Leblond et al., 1993). Whereas the selective aggregation of ZG proteins has been well documented, their interaction with the TGN/ZG membrane is poorly understood at the molecular level, and neither a common sorting signal nor a sorting receptor have been identified so far (Dikeakos and Reudelhuber, 2007; Fujita-Yoshigaki et al., 2013). Sorting during ZG biogenesis is supposed to take place also after the TGN, at the level of the ZG itself (Arvan and Castle, 1992).

The application of proteomics has largely contributed to the identification of novel ZG proteins (Borta et al., 2010; Chen et al., 2006; Gómez-Lázaro et al., 2010; Rindler et al., 2007), but was not yet accompanied by a better characterization of their functions. The analysis of ZG components has also led to the identification of unique mammalian proteins with unusual structural and biochemical properties (Cronshagen et al., 1994; Hase et al., 2009; Hodel et al., 2001; Kanagawa et al., 2011). Whereas most of the cargo zymogens are well characterized on the molecular and biochemical level, there is still very little information available on the non-enzymatic ZG proteins (e.g. at the ZGM), their biochemical properties, interplay and functions. The current lack of knowledge has greatly hampered the development of therapeutic and pharmacological approaches to diagnose, prevent and treat acinar cell injury and pancreatic disease. The identification of ZG content and membrane

components, their molecular characterization and the unravelling of their biochemical properties and functions are therefore highly relevant for the understanding of granule biogenesis and regulated secretion and will help point the way to treatments for diseases of the pancreas and the gastrointestinal tract.

5.1. Chymase and PpiB are two novel ZG proteins with proteoglycan-binding properties

As there is great need in the identification and molecular characterization of ZG and ZGM components, we have performed a suborganellar proteomics approach, based on carbonate-treatment of ZGM and analysis by 2D-PAGE of the corresponding supernatant (Wash) fraction, which has so far led to the identification of novel peripheral ZGM proteins with proteoglycan-binding properties (chymase, PpiB). In this part of the dissertation, we focused on the identification and characterization of a "basic" group of membrane-associated proteins (pI range 6.2-11). As a verification of our approach, two previously reported peripheral (basic) ZG proteins, the secretory lectin ZG16p (pI 9.2) and syncollin (pI 8.6), were identified in this study. ZG16p is supposed to interact with the ZGM via its lectin domain, whereas syncollin has been shown to interact with cholesterol and the GPI-anchored membrane glycoprotein GP2 (Kalus et al., 2002; Kleene et al., 1999b). Furthermore, no transmembrane proteins or classical membrane-anchored proteins were detected. On the basis of bioinformatic information and published results, almost all of the identified proteins are able to enter the secretory pathway, thus confirming their interaction with the luminal side of the ZGM. The two identified cytosolic proteins vinculin (fragment), an actin-binding protein, and ubiquitin carrier protein involved in ubiquitination/quality control may be associated with the cytosolic side of the ZG. Two novel proteins, rat mast cell chymase and PpiB, an ER-resident protein, were selected for further validation of our approach. By applying immunoblotting for the detection of ER and mast cell marker proteins, we were able to rule out that the presence of chymase and PpiB in our granule subfractions was the result of a contamination with ER or mast cell granules/proteins. The distribution of chymase and PpiB in the granule subfractions resembled that of ZG16p, a typical peripheral ZGM marker, further confirming that chymase and PpiB are genuine peripheral ZGM proteins. Chymase has been identified as a major, highly basic chymotrypsin-like serine protease of

mast cells, where it is stored in regulated secretory granules. Thus, its presence in ZGs of the exocrine pancreas is not that unusual at all. With respect to function, chymase is likely to act as a serine protease after ZG secretion. Chymase of mast cells is involved in inflammatory processes and tissue-remodelling (Leskinen et al., 2003). PpiB (Cyclophilin B) is a highly basic cyclosporin A-binding protein with peptidyl-prolyl cis-trans isomerase activity. It belongs to a group of enzymes (cyclophilins) that bind to the immunosuppressor cyclosporine A (Galat, 1993) and catalyse protein folding of prolin-containing polypeptide chains (Fischer et al., 1989; Takahashi et al., 1989; Wang and Heitman, 2005). PpiB is sorted to the secretory pathway via an ER targeting signal (Bose et al., 1994; Price et al., 1994) and has been reported to be retained in specialized regions of the ER (Arber et al., 1992), but also as a secretory protein without ER-retention signal (Mariller et al., 1996; Price et al., 1994). PpiB was also identified in other exocrine secretions such as human saliva in a recent proteomic approach (Walz et al., 2006). Thus, besides its intracellular localization, PpiB can also be found in the extracellular space, where it might contribute to intercellular communication (Bukrinsky, 2002; Daum et al., 2009). PpiB in ZG might act as a chaperone in protein folding, and can assist in protein sorting and/or regulation of an active/inactive conformation of digestive enzymes. However, a function in the regulation of membrane channels, Ca^{2+}-dependent processes or in immune defence after secretion are alternative or additional modes of action (Arber et al., 1992; Bram and Crabtree, 1994; Galat, 2003; Montague et al., 1997).

5.1.1. Several ZG enzymes are also membrane-associated

Interestingly, several known digestive enzymes, among them many lipid-interacting enzymes, were also identified in the Wash subfraction. The presence of these classical content (ZGC) proteins in a ZGM fraction is usually interpreted as a contamination. However, it should be noted that these enzymes remain partially attached to the ZGM even under more stringent purification conditions (e.g., KBr wash before carbonate treatment) or after further purification of crude ZGM by gradient centrifugation (Chen et al., 2006; Rindler et al., 2007). Interestingly, many of the membrane-associated enzymes identified in this study in a membrane Wash subfraction have been predicted to be potential luminal ZGM proteins in a recent topology analysis of purified ZGM (Chen et al., 2008). Thus, it is very

likely that the identified subset of peripheral digestive enzymes exhibits a more specific interaction with the ZGM than previously expected. Enzymes with lipid-binding properties might interact with membrane lipids to specifically associate with the ZGM. The presence of CEL at the ZGM might be mediated by its capability to bind to lipid surfaces. In support of this notion, sphingolipid-binding domains of CEL are supposed to mediate its interaction with lipid rafts (Aubert-Jousset et al., 2004). Furthermore, CEL has been found to be associated with lipid microdomains, which have been identified in ZGM (Berkane et al., 2007; Schmidt et al., 2001). Their importance for granule biogenesis has been demonstrated in recent studies (Gondré-Lewis et al., 2006; Schmidt et al., 2001). We also detected a prominent amount of RNase A at the ZGM. Interestingly, this interaction might be mediated by the interaction of RNase A with proteoglycans, for example, of a predicted submembranous granule matrix (Scheele et al., 1994; Schmidt et al., 2000). RNase A has been shown to interact with heparin and chondroitin sulfate (Dvorak and Morgan, 1998a, 1998b), and on the basis of these properties, a protein A-gold-RNase A technique has been developed to detect proteoglycans in cellular compartments and tissues (Dvorak and Morgan, 1999a). Protein A-gold-RNase A also labelled putative proteoglycans in ZG at the membrane and in the content (Dvorak and Morgan, 1999b). Furthermore, an interaction with proteoglycans has been described for chymase, PpiB, and CEL (Allain et al., 2002; Pejler and Maccarana, 1994; Rebaï et al., 2005; Vanpouille et al., 2004). This interaction is supposed to influence enzyme function (Dvorak and Morgan, 1998b; Pejler and Berg, 1995). The negatively charged proteoglycans in secretory granules of hematopoietic cells and mast cells are engaged in the binding of small positively charged molecules, such as histamine and proteases, and have therefore been considered to promote the efficient packaging and concentration of secretory products (Rönnberg et al., 2012). Similarly, proteoglycans within ZGs are supposed to interact electrostatically and through specific protein-protein and carbohydrate-protein binding domains with the secretory proteins of the granule content (Borta et al., 2010; Gómez-Lázaro et al., 2010; Scheele et al., 1994; Schmidt et al., 2000; Schrader, 2004).

5.2. Discovery of new properties of the unusual lectin ZG16p

5.2.1. Digestion of ZG under native conditions reveals several protease resistant proteins

We started the identification of peripheral, membrane-associated proteins of the ZGM by a suborganellar proteomics approach based on carbonate-treatment of ZGM and 2D-PAGE of the corresponding Wash subfraction and revealed a "basic" group of membrane associated proteins (see above). However, the identification of the complementary "acidic" group of proteins from the Wash subfraction was not as successful, mostly due to a difficulty in identification of the acidic proteins by MS. One approach to increase sequence coverage is to use proteases other than trypsin for digestion (Guo et al., 2014). Pancreatic enzymes are secreted in an inactive form (pro-enzymes) and are activated in the duodenum by EK. Thus, in an attempt to improve the coverage of the ZG proteome we designed an experiment to take advantage of the easy activation of zymogens by EK followed by separation of the resulting peptides by LC and identification by MS.

However, our goals were not accomplished since only the major zymogens were identified by this method. Two major drawbacks hampered the identification of the ZG proteome by the described method: a) the high amount of zymogens resulted in a high number of peptides that were hiding the lowest abundant peptides, and b) the high digestion rate observed, leading to the generation of very small peptides, not suited for analysis by MS. Nevertheless, this approach resulted in the discovery of a set of proteins that are highly resistant to proteolysis (e.g., CBP, CTRC, ELA and ZG16p). From these proteins only one is not an enzyme, the lectin ZG16p. It is generally accepted that the pancreatic enzymes have a certain degree of proteolytic resistance to each other. For example, it is known that chymotrypsin C is a regulator of trypsin activity. In the high Ca^{2+} environment of the duodenum it facilitates trypsinogen activation, while in the lower gastrointestinal tract (GIT), CTRC promotes trypsin degradation as a result of a reduction in Ca^{2+} concentration (Szmola and Sahin-Tóth, 2007). It was also shown that elastase is not significantly degraded during intestinal transit (Dominici and Franzini, 2002). Actually, bacterial enzymes are responsible for most of the degradation of endogenous pancreatic proteases in the intestine (Tooth et al., 2014). However, the discovery that a small secretory lectin is highly protease resistant, caught our attention. ZG16p (16 kDa) is the first mammalian lectin that was shown to possess a Jacalin-related β-prism fold. It localizes at the luminal side of the ZGM where it associates

with cholesterol-glycosphingolipid-enriched microdomains together with GP2, syncollin and sulfated proteoglycans (Kalus et al., 2002; Schmidt et al., 2001; Schrader, 2004). Furthermore, it was shown recently to bind to mannose via its carbohydrate recognition domain and to sulphated proteoglycans through a proteoglycan binding motif (see Chapter 1.5.3.1and 1.5.3.2). Furthermore, a function as a linker/helper protein in the binding of aggregated zymogens to the granule membrane has been proposed and it might as well have a role in host protection in the GIT (see Chapter 1.5.3.5). Other pancreatic lectins (e.g., the Reg family) were already shown to have some degree of protease resistance (Parikh et al., 2012). This family belongs to the C-type lectins and is structurally different from ZG16p (e.g., different 3D structure and glycan binding motifs). Nevertheless the Reg family lectins belong to a new set of multifunctional pancreatic lectins that besides the recognition of glycans might possess other functions either in the pancreas before secretion or in the extracellular environment after secretion. Moreover, expression of ZG16p and the Reg family lectins is not limited to the pancreas but extends to the GIT and other organs (see Chapter 1.5.3.4), pointing to a general (patho)physiological role of those pancreatic lectins. Although the Reg family lectins have been consistently studied in the last 20 years (Parikh et al., 2012), the lectin ZG16p has received much less attention. After the initial discovery in 1994 and its implication in the sorting of zymogens to ZG a few years later (Kleene 1999a), a thorough characterization of ZG16p structure and function only began recently (Kanagawa et al., 2011, 2014; Kumazawa-Inoue et al., 2012; Tateno et al., 2012).

We have discovered new biochemical properties of ZG16p that might be of major importance to its multiple (patho)physiological roles and focused our studies on the further characterization of ZG16p.

5.2.2. ZG16p protease resistance is an intrinsic property

The finding that ZG16p is protease resistant raised the question if the resistance was a result of the binding of ZG16p to proteoglycans in ZG or if it was an intrinsic characteristic of ZG16p. To answer this questions we generated and purified recombinant ZG16p with the purpose of testing the resistance of the purified protein against commercial trypsin. ZG16p was cloned in a bacterial expression vector without the signal peptide since in the mature form of the lectin the SP is not present. Two constructs with two different tags at the N-

terminus of ZG16p were generated: one with a histidine tag (His-ZG16p) and another with a histidine and a Myc tag (HMyc-ZG16p). This allowed us to purify both constructs with aid of the His tag and distinguish them by the molecular weight and by immunostaining with specific antibodies due to the presence of the Myc tag. Finally, digestion of both recombinant proteins with trypsin proved that core protein of ZG16p is protease resistant. Although partial digestion was observed, it was shown by immunoblotting that only the N-terminal tags were cleaved. After digestion the size of the recombinant proteins was equal to the endogenous protein and the N-terminal tags were no longer detected by the antibodies. Furthermore, cleavage of the C-terminus is unlikely because the last ≈20 aa are buried in the ZG16p molecule (Figure 37) and thus not accessible for enzymatic cleavage.

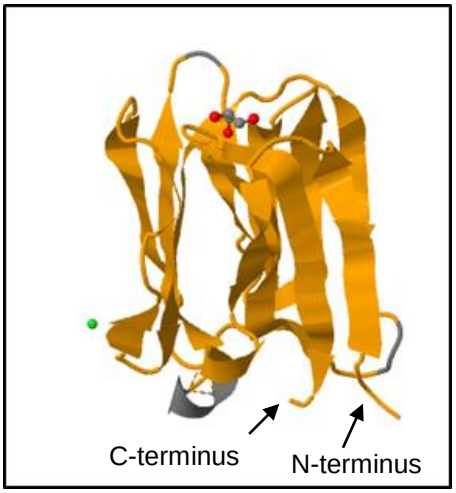

Figure 37. Tertiary structure of ZG16p (PDB entry 3APA) with indication of C- and N- terminus.

Remarkably, ZG16p has 16 potential cleavage sites for trypsin (see Supplementary Figure 2) but it was shown to be highly protease resistance. The molecular determinants for the protease resistance remain to be discovered but we suggest that the tertiary structure of ZG16p must have a crucial role. ZG16p has a β-prism I fold consisting of 3 β-sheets that confer high stability to the protein (see Chapter 5.2.4). β-Sheet proteins have a higher percentage of residues that form contacts with residues distant in the primary sequence than α-helical proteins (Junker and Clark, 2010) what accounts for the increased stability. Proteolytic stability generally correlates with thermal stability of proteins (Akasako et al., 1995; Daniel et al., 1982; McLendon and Radany, 1978; Parsell and Sauer, 1989) and most proteins in their native conformation offer some resistance to proteases, whereas they are rapidly degraded after unfolding (Markert et al., 2001). Futhermore, it is known that β-sheets are involved in the protease resistance of other proteins. For example, the protease resistant prion protein (PrP^{Sc}), an infectious agent responsible for a group of different rare animal and

human diseases known as transmissible spongiform encephalopathies (TSEs). The conversion of PrP^{C} (normal cellular prion protein) into PrP^{Sc} involves a conformational change of the protein in which the total amount of β-sheets increases and that of α-helical secondary structures decreases. These conformational differences are the only demonstrated structural differences between PrP^{Sc} and PrP^{C} (Sajnani et al., 2012). Furthermore, it has been described that the breakdown of β-sheets in PrP^{Sc} by denaturation results in loss of infectivity and proteinase K-sensitivity, suggesting a relationship between the structure and proteinase K-resistance (Sajnani and Requena, 2012).

5.2.3. ZG16p interacts with a high molecular weight complex

ZG16p is thought to mediate sorting of ZG proteins by interacting with aggregated zymogens and the predicted submembranous granule matrix composed by high molecular weight components (see Chapter 1.5.3.5). Here we show that ZG16p interacts with a protease resistant high molecular weight complex that prevents the migration of ZG16p in SDS-PAGE. Preparation of digested ZG (ZG_EK) at 95˚C in SDS loading buffer and separation by SDS-PAGE resulted in the migration of ZG16p to its expected (monomeric) size (16 kDa). In contrast, when the sample was prepared at room temperature, ZG16p was found at the top (stacking) gel indicating that it did not enter the gel. Furthermore, we have tested the ZGC, ZGM and Wash fractions in order to rule out the presence of aggregates (ZGC) or binding of ZG16p to membranes (ZGM) as the cause for retention of ZG16p on the top of the gel. The Wash subfraction is obtained after treatment of the ZGM with sodium carbonate at pH 11.5 followed by centrifugation to separate the "washed" membranes containing integral membrane proteins from a solution rich in membrane-associated proteins and proteoglycans (Figure 3). By comparing both fractions we were able to rule out the presence of lipids as part of the high molecular weight complex since it was observed that ZG16p is retained on top of the gel when digested ZGM or Wash samples are prepared at RT. Both fractions only share the membrane associated proteins (e.g., ZG16p) and sulfated proteoglycans (see Chapter 1.3.1), suggesting that the interaction of ZG16p with sulphated proteoglycans is responsible for the impairment of ZG16p migration in SDS-PAGE when the sample is prepared in SDS loading buffer at RT. Furthermore, the recombinant ZG16p was used as a control to confirm that ZG16p migrates to the correct molecular mass even

when prepared at RT in SDS loading buffer. Recently, it was shown by immunoblotting with an anti-heparan sulfate antibody (HepSS-1) that the proteoglycans of rat pancreatic ZG have an apparent molecular weight of 120,000-500,000 Da (Kumazawa-Inoue et al., 2012). This further indicates that the ZG proteoglycans are large molecules and may form a high molecular weight complex within ZG.

The comparison of treatment with heparin lyases demonstrated that the heparan sulfate proteoglycans of ZG are preferentially digested with heparin lyase II (heparitinase II) (Kumazawa-Inoue et al., 2012). For that reason, we have used the enzyme heparitinase II to digest the GAGs of the proteoglycans of ZG_EK and ZGM_EK in order to break down the high molecular weight complexes and to allow ZG16p to enter the SDS-PAGE. This would further support our hypothesis that ZG proteoglycans are part of a HMW complex and responsible for retaining ZG16p at the top of the PA gel. However, this issue could not be addressed successfully. Most probably denaturation of the digested samples is required to provide access of the enzyme HPRT to the GAGs, but this would also interfere with our assay by promoting the release of ZG16p. In addition, we cannot rule out that the binding of ZG16p to the proteoglycans protects the GAGs from being digested. Further experiments may benefit from different digestion conditions and by using other enzymes (e.g., chondroitinase ABC). So far, the identification of the proteoglycan core proteins within ZG by MS analysis was not successful (Kumazawa-Inoue et al., 2012). It will be a great challenge for future studies to identify and characterize the high molecular weight components such as proteoglycans in ZG fractions to unveil the complex architecture and putative interactions at the granule membrane (Borta et al., 2010).

5.2.4. ZG16p is a dimeric protein

Although a potential ZG16p dimer was reported in earlier studies by immunoblotting (Kalus et al., 2002; Kleene et al., 1999b) it was recently suggested that ZG16p is a monomeric protein based on analysis by size exclusion chromatography of recombinant ZG16p (Kanagawa et al., 2011). However, this observation was based on analysis of a recombinant protein that lacks 8 aa at the C-terminus (160-167). This region might be important for formation or stabilization of ZG16p dimers.

We have investigated the formation of ZG16p dimers by denaturation of endogenous and recombinant proteins at different temperature and incubation times. Since endogenous and recombinant proteins have different molecular weights, the dimerization of each protein should result in the formation of dimers with different molecular weights. This was confirmed by immunoblotting with the appearance of a band double in size of the monomeric form for all proteins. In addition, the band that corresponds to the dimeric form decreased with rise of temperature and time of incubation but resisted at least for 10 min. at 95˚C, indicating that denaturation of ZG16p is only achieved after a long exposure to high temperatures. These results indicate that ZG16p forms highly stable dimers. Oligomeric proteins are abundant in nature. It was suggested that 35% or more of the cellular proteins are oligomeric (Goodsell and Olson, 2000), although the proportion of oligomeric protein structures deposited in the Protein Data Bank is significantly lower (Ali and Imperiali, 2005).

ZG16p was the first Jacalin related lectin found in mammals and the structural alignment reveals that ZG16p is strikingly similar to the banana lectin Banlec (Figure 38). The percentage of sequence identity between both proteins is only 25.3% while the structure similarity is of 95%. Banlec is a dimer and displays substantial conformational stability in the presence of chaotropic agents (Gupta et al., 2008) and during high-temperature (400–500 K) simulations (Gupta et al., 2009). The stability of the dimer results from strong hydrogen bonds and water bridges at the interface (Gupta et al., 2008).

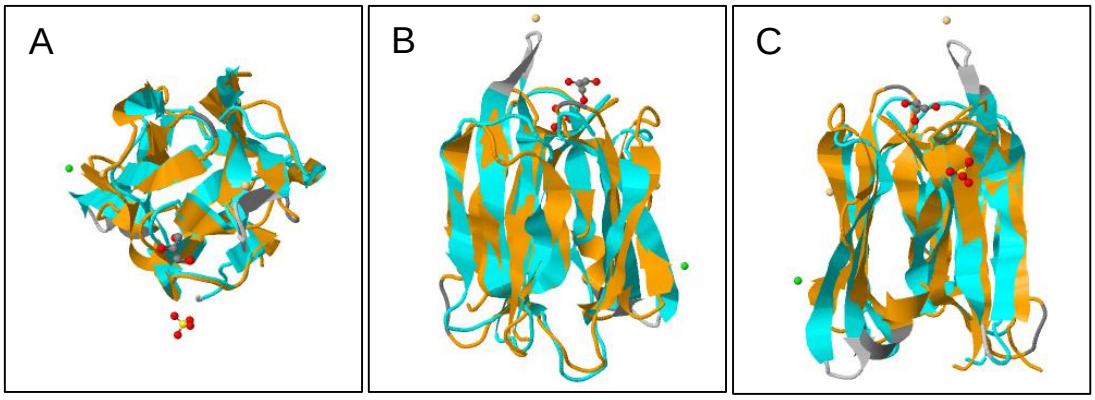

Figure 38. Structural alignment of ZG16p (PDB entry 3APA) and Banlec (PDB entry 2BMY.A). Different views are shown to demonstrate the high similarity between both structures: (A) top view, (B, C) lateral view. The blue structure corresponds to Banlec and the yellow to ZG16p.

Based on our results and the similarity of the tertiary structure of ZG16p and Banlec we suggest that ZG16p is also a highly stable homodimeric protein. The slow denaturation

of the endogenous and recombinant ZG16p observed (Figure 15) may reflect the stability mediated by the presence of inter- and intramolecular hydrogen bonds (Figure 39).

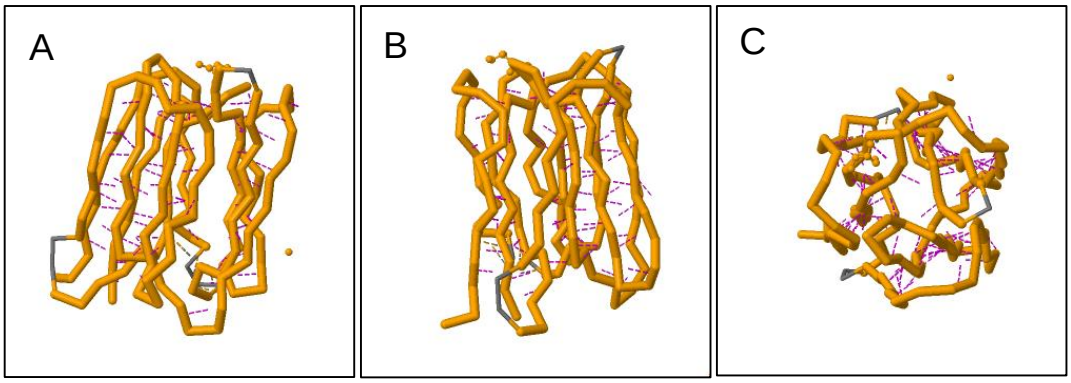

Figure 39. Tertiary structure of ZG16p (PDB entry 3APA) showing the hydrogen bounds formed between the 3 β-sheets. (A, B) lateral view; (C) top view.

Although both proteins are structurally very similar, they show some functional differences: BanLec possesses two carbohydrate-binding sites including the signature motifs GG and GXXXD (Meagher et al., 2005; Singh et al., 2005), which are partly conserved in ZG16p; ZG16p has only one carbohydrate recognition domain and a proteoglycan binding motif in the place of the second CRD of Banlec. Another major difference is that the surface of Banlec is mainly negative in contrast with the presence of positive patches on the surface of ZG16p (Kumazawa-Inoue et al., 2012). These differences account for the different binding activity.

5.3. Targeting of ZG16p to ZG in AR42J cells is not dependent on its CRD and PGM domains

Whereas most of the cargo zymogens are well characterized on the molecular level, there is still very little information available on the molecular components of the granule membrane (ZGM), their biochemical properties, interplay and functions (Borta et al., 2010; Chen et al., 2006; Rindler et al., 2007; Wagner and Williams, 1994). Furthermore, the specific interaction of regulated secretory proteins with the TGN/ZGM and their ultimate sorting into immature granules is poorly understood, especially in exocrine systems, where specific sorting signals and receptor proteins have so far not been identified (Dikeakos and Reudelhuber, 2007). It was suggested that ZG16p mediates the binding of aggregated secretory proteins to the predicted submembranous matrix (see Chapter 1.5.3.5). This protein scaffold underneath the ZGM is supposed to serve as the backbone of a complex membrane matrix, and a bridge between the ZGM and the zymogens. ZG16p may act as a linker molecule between the ZGM/submembranous matrix and aggregated secretory proteins and thus, in protein sorting. We examined if the glycan binding motifs are required for proper targeting of ZG16p to ZG, first by deletion of the CRD and later by point mutation of CRD and PGM and expression in AR42J cells, a pancreatic cell model.

5.3.1. Deletion of CRD inhibits targeting of ZG16p to ZG

AR42J cells have been used as a model system for granule formation and pancreatic exocrine secretion. Treatment with the glucocorticoid dexamethasone induces both the differentiation of AR42J cells into acinar-like cells and the *de novo* formation of electron-opaque secretory granules, which contain the major pancreatic zymogens (Logsdon et al., 1985). To investigate the targeting of ZG16p in AR42J cells we have first generated a construct with ZG16p tagged at the N-terminus (ER-Myc-ZG16p) (Figure 18). We confirmed that this construct is targeted to ZG by colocalization with CBP (ZG marker) in AR42J cells. Then, we deleted the CRD (GXXXD) (ER-Myc-ZG16dCRD) to verify if the absence of this domain would influence the targeting of ZG16p in AR42J cells. Colocalization of ER-Myc-ZG16dCRD and CBP was not observed, indicating that the mutant is not targeted to ZG in AR42J cells. Furthermore, by absence of colocalization with

two Golgi markers (TGN38 and p115) we showed that the ER-Myc-ZG16dCRD construct is not transported to the Golgi either. However, the control (ER-Myc-ZG16p) colocalized with both Golgi markers.

The ZG proteins are synthesized by ribosomes and inserted into the lumen of the ER. The Golgi complex receives the proteins from the ER and processes them further. Then, the sorting of proteins to be packaged in ZG takes place at the TGN. Our results indicate that the deletion of the CRD inhibits the transport of ZG16p from the ER to the Golgi complex, thus disrupting the targeting to ZG. However the deletion of the CRD (total of 5 aa) might interfere with the correct folding of the protein. Polypeptides that fail to fold properly or never become part of a multisubunit complex are retained within the ER and later transported back across the ER membrane into the cytosol and degraded by the proteasome (Meusser et al., 2005).

5.3.2. Point mutations of CRD and PGM do not inhibit the targeting of ZG16p

To confirm that inhibition of ZG16p targeting was due to the impairment of the CRD and not to instability of the protein caused by the deletion of the domain, we inhibited the CRD by point mutation. Only one amino acid was changed, keeping the protein as similar to the wild type as possible. The aspartic acid residue of the CRD (GXXXD) was previously demonstrated by point mutation (D151A) to be essential for binding of ZG16p to mannose (Tateno et al., 2012). To confirm that the CRD is responsible for the targeting of ZG16p, we performed a point mutation of D151A (ER-Myc-ZG16_D) followed by expression in AR42J cells. Colocalization between ER-Myc-ZG16_D and CBP indicated that this mutant was properly targeted to ZG in AR42J cells. ZG16p also possesses a PGM that mediates the binding to sulphated proteoglycans, and it was shown that point mutation of the PGM residues (K33A, K36A, and R37A) and (R55A and R58A) abolishes the binding (Kumazawa-Inoue et al., 2012). Thus, we also generated point mutations in those PGM residues (resulting in ER-Myc-ZG16_K (K33A, K36A, and R37A) and ER-Myc-ZG16_R (R55A and R58A)) to verify if they interfere with the targeting of ZG16p. Finally, double and triple mutants were generated (ER-Myc-ZG16_K_R, ER-Myc-ZG16_R_D and ER-Myc-ZG16_K_R_D). All mutants colocalized with the ZG marker CBP showing that they

are properly targeted to ZG in AR42J cells. This indicates that both domains (CRD and PGM) might not be directly involved in the targeting of ZG16p. However, once ZG16p is able to form stable homodimers, it is possible that the endogenous ZG16p present in AR42J cells dimerizes with the expressed mutants and targets them to ZG. Furthermore, it was suggested that the addition of the signal peptide, which is necessary for the translocation into the ER, is sufficient for the transportation and storage of cargo proteins in secretory granules of exocrine cells (Fujita-Yoshigaki et al., 2013). This is in line with a model known as "sorting by retention" (see Chapter 1.2) that proposes that proteins that are not destined for regulated secretion are loaded to immature granules at the TGN, and then are progressively removed from immature secretory granules via clathrin-coated vesicles (Klumperman et al., 1998). Through the selective removal of nongranular proteins, immature granules are converted into mature granules (Fujita-Yoshigaki et al., 2013).

We favour a model (Figure 40), in which a predicted submembranous matrix attached to the luminal side of the granule membrane fulfils important functions during the sorting and packaging of secretory proteins (Scheele et al., 1994; Schrader, 2004). We have identified novel ZG membrane/matrix proteins with proteoglycan-binding properties and presented evidence that a subset of peripheral digestive enzymes exhibits a more specific interaction with the ZGM than previously expected (Chapter 4.1.1). In light of the recent findings, the submembranous matrix might help in the retention of the proteins destined for regulated secretion by acting as a bridge between the ZGM and the aggregated zymogens. We showed here that ZG16p would be able to act as crosslinker as it can form stable dimers, thus potentially supporting the binding of aggregated zymogens to the submembranous granule matrix.

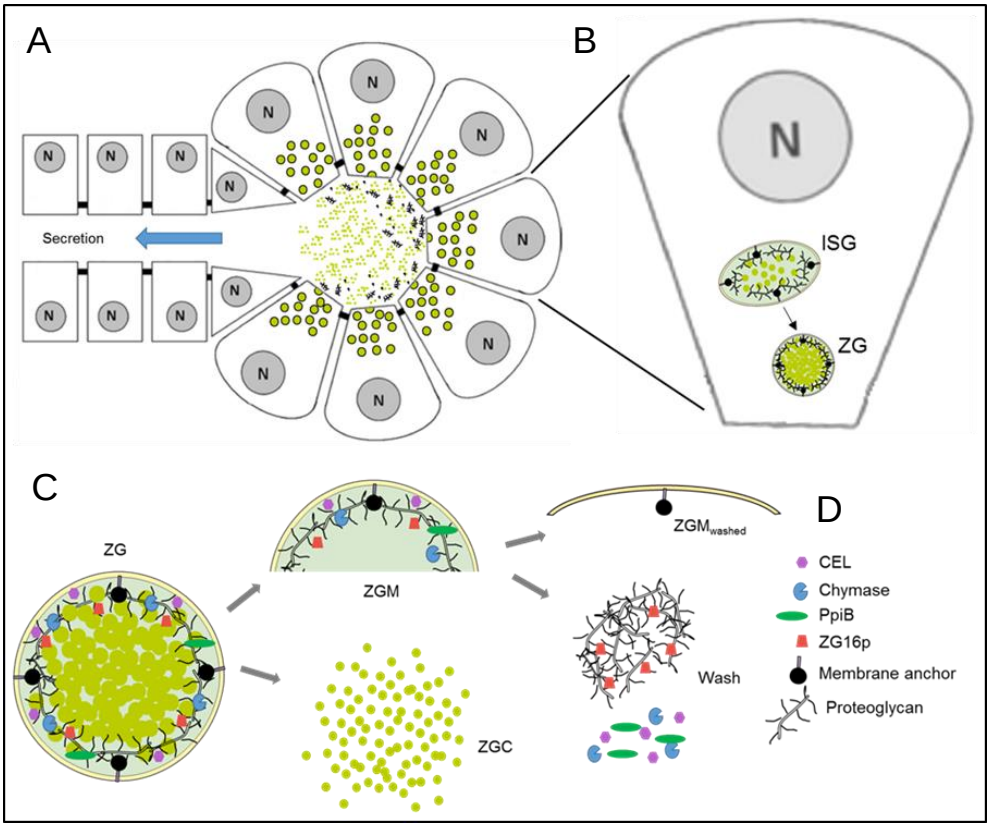

Figure 40. Proteoglycan matrix model. (A) Acinar unit. Zymogens are secreted into the pancreatic duct and further transported to the duodenum. (B) Acinar cell. Immature secretory granules (ISG) undergo maturation to form ZG. Their maturation involves further concentration of the cargo proteins with selective removal of components not destined for regulated secretion, and a reduction in granule size. A glycoconjugate scaffold underneath the ZGM is suggested to serve as the backbone of a complex membrane matrix, and a bridge between the ZGM and the zymogens. A membrane anchor is constituted by lipid microdomains and associated proteins (e.g., GP2) that are involved in the attachment of the matrix proteoglycans to the granule membrane. (C) Close view of ZG. The proteoglycan matrix is represented by a glycoconjugate scaffold underneath the ZGM, composed of proteoglycans, glycoproteins, ZG16p and other proteins (see Chapter 1.4). Separation of ZG into a ZGM fraction and a content fraction (ZGC) is obtained by gentle lysis of ZG followed by centrifugation. Carbonate treatment of the ZGM results into two subfractions: the treated membranes with integral membrane proteins (ZGM$_{washed}$) and a subfraction with membrane-associated proteins and a high molecular weight complex of proteoglycans and ZG16p (Wash). (D) Components of the proteoglycan matrix. Sulfated proteoglycans within ZG are supposed to interact electrostatically and through specific protein-protein and carbohydrate-protein binding domains with the secretory products of the granule content and promote the efficient packaging and concentration of secretory products. ZG16p interacts with sulfated proteoglycans and may act as a linker between the matrix and aggregated zymogens due to dimer formation. Chymase and PpiB were identified in ZG for the first time in this study and both were described previously to interact with sulfated proteoglycans; CEL was shown to be enriched in the wash subfraction and has been previously found to be associated with lipid microdomains and to interact with proteoglycans.

5.4. ZG16p as a new tool for the study of the endo-lysosomal compartment

5.4.1. Cytosolic ZG16p labels the endo-lysosomal compartment

ZG16p has an ER-targeting signal (SP) that directs the nascent protein to the ER. From there it is transported to the Golgi complex where it enters the secretory pathway and thereafter remains confined in membrane-bound organelles. However, we discovered that when ZG16p is expressed in the cytoplasm it binds to the endo-lysosomal compartment, as indicated by partial colocalization with endosomal and lysosomal markers. Remarkably, this interaction was observed after expression of ZG16p in various mammalian cell lines, pointing to a conserved ZG16p interaction partner across species. Additionally, we observed that expression of ZG16p tagged with Myc or GFP at the N-terminus results in two different endo-lysosomal phenotypes. The Myc-ZG16p is bound to a compartment composed of spherical and elongated tubular membrane structures, while GFP-ZG16p is bound to a membrane compartment composed by spherical structures only, with concentration of relatively large structures in the perinuclear region (Figure 41). These structures are likely lysosomes. It is important to note that the organelle morphology observed with the Myc-tagged ZG16p is similar to the phenotype obtained after expression of an untagged version of ZG16p. For that reason, we suggest that this corresponds to the "physiological" phenotype or the phenotype that would result from an "escape" of native ZG16p to the cytoplasm. Furthermore, by co-expressing both tagged proteins it was demonstrated by confocal microscopy that both proteins colocalize with the same structures. This indicates that the tags do not interfere with the binding of ZG16p but might restrict the interaction with other components or even with itself (e.g., dimerization) resulting in different organelle morphologies. The Myc tag in contrary to the GFP tag is a small peptide and is less likely to disrupt the properties or localization of the tagged protein (Palmer and Freeman, 2004). The morphological differences observed after expression of Myc-ZC16p and GFP-ZG16p also indicate that the binding of ZG16p to endo-lysosomes might alter this compartment. This is supported by the different organelle morphologies observed after expression of the tagged proteins and also by comparison of organelle morphology in non-transfected cells.

In order to characterize the binding of ZG16p to the endo-lysosomal compartment we manipulated the binding domains of ZG16p by point mutation. Several Myc-ZG16p and GFP-ZG16p constructs were generated with mutation of the CRD (Myc-ZG16p_D and GFP-

ZG16p_D) and the PGM (Myc-ZG16_K, Myc-ZG16_R, GFP-ZG16_K and GFP-ZG16_R). Interestingly, only the mutants Myc-ZG16_K and GFP-ZG16_K abolished the binding to the endo-lysosomal compartment (Figure 41). This demonstrates that the binding of ZG16p to endo-lysosomes is mediated by a positive patch on the surface of ZG16p (aa K33, K36 and R37) and is most probably due to electrostatic interaction with membrane components of the endo-lysosomal compartment. We have already started an approach to identify the lysosomal binding partner of ZG16p by expression of GFP-ZG16p in COS-7 cells and co-immunoprecipitation with anti-GFP antibodies and crosslinking (data not shown).

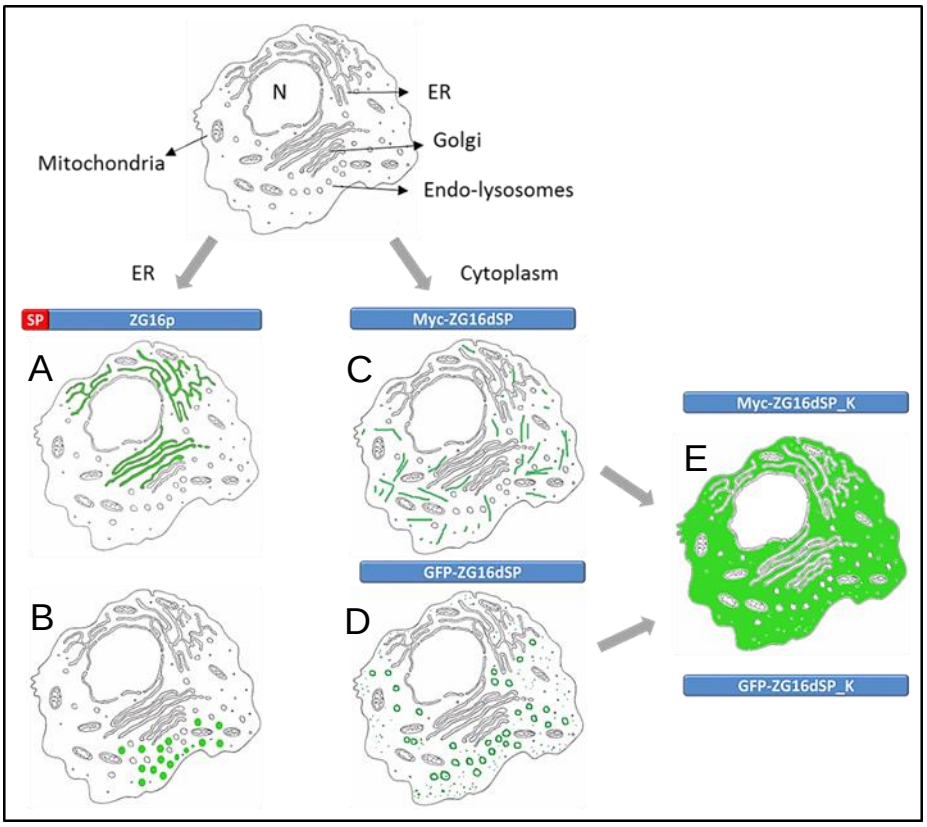

Figure 41. ZG16p is able to interact with different cell compartments. ZG16p has a signal peptide (SP) that targets the lectin to the ER (A), from where is able to enter the regulated secretory pathway (B). Expression of ZG16p without the SP leads to its interaction with the endo-lysosomal compartment (C and D). ZG16p tagged with Myc or GFP at the N-terminus results in two different endo-lysosomal phenotypes: Myc-ZG16p is bound to a compartment composed of spherical and elongated tubular membrane structures (C), while GFP-ZG16p is bound to a membrane compartment composed by spherical structures (D). However, mutation of the proteoglycan binding motif (K33A, K36A, and R37A) abolishes the binding of ZG16p to the endo-lysosomal compartment (E) for both tagged proteins (Myc-ZG16_K and GFP-ZG16_K).

Altogether, these results reveal an interesting feature of ZG16p as a new endo-lysosomal interacting protein. Furthermore, ZG16p has the capacity to modulate the endo-lysosomal compartment. These observations indicate that ZG16p may be used as a novel

and specific tool to label (and manipulate) parts of the endosomal/lysosomal trafficking pathway. Lectins have the ability to act as recognition molecules inside cells, on cell surfaces and in physiological fluids (Reuter and Gabius, 1999) and have already been successfully used in the detection and assay of glycoconjugates in tissues, on cells or subcellular organelles and on gels, blots and many other techniques (Sharon and Lis, 2004) showing that lectins are very versatile biomolecules with great applicability in bioanalytical techniques and in biomedical diagnosis (Gemeiner et al., 2009).

5.4.2. Does ZG16p have a role in the course of pancreatitis?

As discussed above, ZG16p can interact with the endo-lysosomal compartment when expressed in the cytoplasm. Although this might be of debatable physiological importance as under normal conditions ZG16p is not present in the cytoplasm, it might be relevant under pathophysiological conditions. Interestingly, a treatment of mice with supraphysiological doses of cerulein inducing acute pancreatitis led to a rapid down regulation (12 h) of ZG16p mRNA in mouse pancreas with recovery of mRNA levels within 3 days (Neuschwander-Tetri et al., 2004). During the course of pancreatitis the activated zymogens are capable of damaging vital cellular components (Logsdon and Ji, 2013) as a result of early activation and escape from the ZG. We can speculate that ZG16p might be able to escape from ZG under conditions of a pancreatitis and would be able to interact and interfere with the endo-lysosomal compartment. It has been recently suggested that disordering of the endo-lysosomal traffic is associated with pancreatitis via impairment of autophagy (see Chapter 1.6.1). Recent studies have begun to elucidate the role of autophagy both in the normal function of the exocrine pancreas (Vaccaro, 2012) and in pancreatitis, the most common disease of this organ (Gukovskaya and Gukovsky, 2012). The predominant view is that efficient, physiologic autophagy is prosurvival, whereas defective autophagy can lead not only to the accumulation of vacuoles and active trypsin in acinar cells but also to inflammation and cell death, all key responses of pancreatitis (Gukovskaya and Gukovsky, 2012). Autophagic dysfunction might occur at various steps, including decreased or defective formation of autophagosomes, their impaired fusion with lysosomes, or inefficient lysosomal proteolytic activity. Importantly, genetic alterations which specifically target the

lysosomal or autophagic function induce pancreatitis-like injury (Gukovskaya and Gukovsky, 2012).

The high number and size of endo-lysosomes observed in transfected cells when compared with non-transfected cells suggests that the binding of ZG16p to the endo-lysosomal compartment might interfere with the normal function of this compartment. Thus, understanding the effect of the binding of ZG16p to endo-lysosomes is of major biological importance. Additionally, the expression of ZG16p is not restricted to the pancreas (see Chapter 1.5.3.4) pointing to a potential (patho)physiological role in other locations.

CONCLUSIONS

6. Conclusions

We favour a model, in which a predicted submembranous matrix attached to the luminal side of the granule membrane fulfils important functions during the sorting and packaging of secretory proteins (Scheele et al., 1994; Schrader, 2004). We have identified novel ZG membrane/matrix proteins with proteoglycan-binding properties and presented evidence that a subset of peripheral digestive enzymes exhibits a more specific interaction with the ZGM than previously expected (Chapter 4.1.1). Proteoglycans within ZGs are supposed to interact electrostatically and through specific protein-protein and carbohydrate-protein binding domains with the secretory proteins of the granule content (Borta et al., 2010; Gómez-Lázaro et al., 2010; Scheele et al., 1994; Schmidt et al., 2000; Schrader, 2004). Furthermore, we have discovered new characteristics of ZG16p that might be of major importance to understand its (patho)physiological role. ZG16p is highly resistant to proteases, binds to a high molecular weight complex (also protease resistant) and forms homodimers. By point mutation we have shown that ZG16p domains (CRD and PGM) are not directly involved in the targeting of ZG16p to ZG in AR41J cells. In the light of the recent findings we suggest that the submembranous matrix might help in the retention of the proteins destined for regulated secretion by acting as a bridge between the ZGM and the aggregated zymogens. We have shown that ZG16p would be able to act as a crosslinker as it can form stable dimers, thus supporting the binding of aggregated zymogens to the submembranous granule matrix. In addition, we discovered that cytosolic ZG16p can interact with and modulate the endo-lysosomal compartment. These observations indicate that ZG16p may be used as a novel and specific tool to label (and manipulate) parts of the endosomal/lysosomal trafficking pathway. As disturbed autophagic processes have been linked to pancreatitis, an understanding of the binding and impact of ZG16p on endo-lysosomes is of biological and clinical importance.

BIBLIOGRAPHY

Bibliography

Adler, G., Gerhards, G., Schick, J., Rohr, G., and Kern, H.F. (1983). Effects of in vivo cholinergic stimulation of rat exocrine pancreas. Am. J. Physiol. *244*, G623–G629.

Aebersold, R., and Mann, M. (2003). Mass spectrometry-based proteomics. Nature *422*, 198–207.

Akasako, A., Haruki, M., Oobatake, M., and Kanaya, S. (1995). High resistance of Escherichia coli ribonuclease HI variant with quintuple thermostabilizing mutations to thermal denaturation, acid denaturation, and proteolytic degradation. Biochemistry *34*, 8115–8122.

Ali, M.H., and Imperiali, B. (2005). Protein oligomerization: how and why. Bioorg. Med. Chem. *13*, 5013–5020.

Allain, F., Vanpouille, C., Carpentier, M., Slomianny, M.-C., Durieux, S., and Spik, G. (2002). Interaction with glycosaminoglycans is required for cyclophilin B to trigger integrin-mediated adhesion of peripheral blood T lymphocytes to extracellular matrix. PNAS *99*, 2714–2719.

Arber, S., Krause, K.H., and Caroni, P. (1992). s-Cyclophilin is retained intracellularly via a unique COOH-terminal sequence and colocalizes with the calcium storage protein calreticulin. J. Cell Biol. *116*, 113–125.

Arendorf, T.M., and Walker, D.M. (1980). The prevalence and intra-oral distribution of Candida albicans in man. Arch. Oral Biol. *25*, 1–10.

Arvan, P., and Castle, D. (1992). Protein sorting and secretion granule formation in regulated secretory cells. Trends Cell Biol. *2*, 327–331.

Arvan, P., and Castle, D. (1998). Sorting and storage during secretory granule biogenesis: looking backward and looking forward. Biochem. J *332*, 593–610.

Aubert-Jousset, E., Garmy, N., Sbarra, V., Fantini, J., Sadoulet, M.-O., and Lombardo, D. (2004). The combinatorial extension method reveals a sphingolipid binding domain on pancreatic bile salt-dependent lipase: role in secretion. Structure *12*, 1437–1447.

Bach, J.-P., Borta, H., Ackermann, W., Faust, F., Borchers, O., and Schrader, M. (2006). The secretory granule protein syncollin localizes to HL-60 cells and neutrophils. J. Histochem. Cytochem. *54*, 877–888.

Baravalle, G., Schober, D., Huber, M., Bayer, N., Murphy, R.F., and Fuchs, R. (2005). Transferrin recycling and dextran transport to lysosomes is differentially affected by bafilomycin, nocodazole, and low temperature. Cell Tissue Res. *320*, 99–113.

Bartoli, C., Baeza, N., Figarella, C., Pellegrini, I., and Figarella-Branger, D. (1998). Expression of peptide-23/pancreatitis-associated protein and Reg genes in human pituitary and

adenomas: comparison with other fetal and adult human tissues. J. Clin. Endocrinol. Metab. *83*, 4041–4046.

Beaudoin, A.R., St-Jean, P., and Grondin, G. (1991). Ultrastructural localization of GP2 in acinar cells of pancreas: presence of GP2 in endocytic and exocytic compartments. J. Histochem. Cytochem. *39*, 575–588.

Berg, N.B., and Young, R.W. (1971). Sulfate metabolism in pancreatic acinar cells. J. Cell Biol. *50*, 469–483.

Berkane, A.A., Nguyen, H.T.T., Tranchida, F., Waheed, A. a, Deyris, V., Tchiakpe, L., Fasano, C., Nicoletti, C., Desseaux, V., Ajandouz, E.H., et al. (2007). Proteomic of lipid rafts in the exocrine pancreas from diet-induced obese rats. Biochem. Biophys. Res. Commun. *355*, 813–819.

Bieger, W., and Scheele, G. (1980). Two-dimensional isoelectric focusing/sodium dodecyl sulfate gel electrophoresis of protein mixtures containing active or potentially active proteases: analysis of human exocrine pancreatic proteins. Anal. Biochem. *109*, 222–230.

Bockman, D.E. (2008). Anatomy and Fine Structure. In The Pancreas: An Integrated Textbook of Basic Science, Medicine, and Surgery, H.G. Beger, A.L. Warshaw, M.W. Büchler, R.A. Kozarek, M.M. Lerch, J.P. Neoptolemos, K. Shiratori, D.C. Whitcomb, and B.M. Rau, eds. (Oxford, UK.: Blackwell Publishing Ltd), pp. 50–57.

Borgonovo, B., Ouwendijk, J., and Solimena, M. (2006). Biogenesis of secretory granules. Curr. Opin. Cell Biol. *18*, 365–370.

Borta, H., Aroso, M., Rinn, C., Gomez-Lazaro, M., Vitorino, R., Zeuschner, D., Grabenbauer, M., Amado, F., and Schrader, M. (2010). Analysis of low abundance membrane-associated proteins from rat pancreatic zymogen granules. J. Proteome Res. *9*, 4927–4939.

Bose, S., Mücke, M., and Freedman, R.B. (1994). The characterization of a cyclophilin-type peptidyl prolyl cis-trans-isomerase from the endoplasmic-reticulum lumen. Biochem. J. *300 (Pt 3*, 871–875.

Braganza, J.M., Lee, S.H., McCloy, R.F., and McMahon, M.J. (2011). Chronic pancreatitis. Lancet *377*, 1184–1197.

Bram, R.J., and Crabtree, G.R. (1994). Calcium signalling in T cells stimulated by a cyclophilin B-binding protein. Nature *371*, 355–358.

Braun, M., and Thévenod, F. (2000). Photoaffinity labeling and purification of ZG-16p, a high-affinity dihydropyridine binding protein of rat pancreatic zymogen granule membranes that regulates a K+-selective conductance. Mol. Pharmacol. *57*, 308–316.

Bruneau, N., and Lombardo, D. (1995). Chaperone function of a Grp 94-related protein for folding and transport of the pancreatic bile salt-dependent lipase. J. Biol. Chem. *270*, 13524–13533.

Bruneau, N., Lombardo, D., and Bendayan, M. (2000). The affinity binding sites of pancreatic bile salt-dependent lipase in pancreatic and intestinal tissues. J. Histochem. Cytochem. *48*, 267–276.

Bukrinsky, M.I. (2002). Cyclophilins: Unexpected messengers in intercellular communications. Trends Immunol. *23*, 323–325.

Bunn-Moreno, M.M., and Campos-Neto, A. (1981). Lectin(s) extracted from seeds of Artocarpus integrifolia (jackfruit): potent and selective stimulator(s) of distinct human T and B cell functions. J. Immunol. *127*, 427–429.

Cabana, C., Hugon, J.S., and Lamy, F. (1981). Freeze-fracture and deep-etching studies on zymogen-granule membranes of the rat pancreas. Cell Tissue Res. *214*, 355–367.

De Caro, A., Lohse, J., and Sarles, H. (1979). Characterization of a protein isolated from pancreatic calculi of men suffering from chronic calcifying pancreatitis. Biochem. Biophys. Res. Commun. *87*, 1176–1182.

Cash, H.L., Whitham, C. V, Behrendt, C.L., and Hooper, L. V (2006). Symbiotic bacteria direct expression of an intestinal bactericidal lectin. Science (80-.). *313*, 1126–1130.

Chen, X., and Andrews, P.C. (2008). Purification and proteomics analysis of pancreatic zymogen granule membranes. Methods Mol. Biol. *432*, 275–287.

Chen, X., Walker, A.K., Strahler, J.R., Simon, E.S., Tomanicek-Volk, S.L., Nelson, B.B., Hurley, M.C., Ernst, S.A., Williams, J.A., and Andrews, P.C. (2006). Organellar proteomics: analysis of pancreatic zymogen granule membranes. Mol. Cell. Proteomics *5*, 306–312.

Chen, X., Ulintz, P.J., Simon, E.S., Williams, J. a, and Andrews, P.C. (2008). Global topology analysis of pancreatic zymogen granule membrane proteins. Mol. Cell. Proteomics *7*, 2323–2336.

Chung, J., and Wessling-Resnick, M. (2003). Molecular mechanisms and regulation of iron transport. Crit. Rev. Clin. Lab. Sci. *40*, 151–182.

Colomer, V., Kicska, G.A., and Rindler, M.J. (1996). Secretory granule content proteins and the luminal domains of granule membrane proteins aggregate in vitro at mildly acidic pH. J. Biol. Chem. *271*, 48–55.

Cronshagen, U., Voland, P., and Kern, H.F. (1994). cDNA cloning and characterization of a novel 16 kDa protein located in zymogen granules of rat pancreas and goblet cells of the gut. Eur. J. Cell Biol. *65*, 366–377.

Dahan, S., Anderson, K.L., Weller, S., Krueger, E., and Mcniven, M.A. (2005). Agonist-induced vesiculation of the Golgi apparatus in pancreatic acinar cells. Gastroenterology *129*, 2032–2046.

Van Damme, E.J., Barre, a, Verhaert, P., Rougé, P., and Peumans, W.J. (1996). Molecular cloning of the mitogenic mannose/maltose-specific rhizome lectin from Calystegia sepium. FEBS Lett. *397*, 352–356.

Daniel, R.M., Cowan, D.A., Morgan, H.W., and Curran, M.P. (1982). A correlation between protein thermostability and resistance to proteolysis. Biochem. J. *207*, 641–644.

Dartsch, H., Kleene, R., and Kern, H.E. (1998). In vitro condensation-sorting of enzyme proteins isolated from rat pancreatic acinar cells. Eur. J. Cell Biol. *75*, 211–222.

Daum, S., Schumann, M., Mathea, S., Aumüller, T., Balsley, M.A., Constant, S.L., De Lacroix, B.F., Kruska, F., Braun, M., and Schiene-Fischer, C. (2009). Isoform-specific inhibition of cyclophilins. Biochemistry *48*, 6268–6277.

Delacour, D., Koch, A., and Jacob, R. (2009). The role of galectins in protein trafficking. Traffic *10*, 1405–1413.

Dikeakos, J.D., and Reudelhuber, T.L. (2007). Sending proteins to dense core secretory granules: still a lot to sort out. J. Cell Biol. *177*, 191–196.

Dominici, R., and Franzini, C. (2002). Fecal elastase-1 as a test for pancreatic function: a review. Clin. Chem. Lab. Med. *40*, 325–332.

Drissi, R., Dubois, M.-L., and Boisvert, F.-M. (2013). Proteomics methods for subcellular proteome analysis. FEBS J. *280*, 5626–5634.

Duplan, L., Michel, B., Boucraut, J., Barthellémy, S., Desplat-Jegoc, S., Marin, V., Gambarelli, D., Bernard, D., Berthézène, P., Alescio-Lautier, B., et al. (2001). Lithostathine and pancreatitis-associated protein are involved in the very early stages of Alzheimer's disease. Neurobiol. Aging *22*, 79–88.

Dvorak, A.M., and Morgan, E.S. (1998a). Ribonuclease-gold labels chondroitin sulphate in guinea pig basophil granules. Histochem. J. *30*, 603–608.

Dvorak, A.M., and Morgan, E.S. (1998b). Ribonuclease-gold labels heparin in human mast cell granules. New use for an ultrastructural enzyme affinity technique. J. Histochem. Cytochem. *46*, 695–706.

Dvorak, A.M., and Morgan, E.S. (1999a). Ribonuclease-gold ultrastructural localization of heparin in isolated human lung mast cells stimulated to undergo anaphylactic degranulation and recovery in vitro. Clin. Exp. Allergy *29*, 1118–1128.

Dvorak, A.M., and Morgan, E.S. (1999b). Ribonuclease-gold labels proteoglycan-containing cytoplasmic granules and ribonucleic acid-containing organelles - A survey. Histol. Histopathol. *14*, 597–626.

Ermund, A., Schütte, A., Johansson, M.E. V, Gustafsson, J.K., and Hansson, G.C. (2013). Studies of mucus in mouse stomach, small intestine, and colon. I. Gastrointestinal mucus layers have

different properties depending on location as well as over the Peyer's patches. Am. J. Physiol. Gastrointest. Liver Physiol. *305*, G341–7.

Faust, F., Gomez-Lazaro, M., Borta, H., Agricola, B., and Schrader, M. (2008). Rab8 is involved in zymogen granule formation in pancreatic acinar AR42J cells. Traffic *9*, 964–979.

Feng, D., Park, O., Radaeva, S., Wang, H., Yin, S., Kong, X., Zheng, M., Zakhari, S., Kolls, J.K., and Gao, B. (2012). Interleukin-22 ameliorates cerulein-induced pancreatitis in mice by inhibiting the autophagic pathway. Int. J. Biol. Sci. *8*, 249–257.

Fenn, J.B., Mann, M., Meng, C.K., Wong, S.F., and Whitehouse, C.M. (1989). Electrospray ionization for mass spectrometry of large biomolecules. Science (80-.). *246*, 64–71.

Fischer, G., Berger, E., and Bang, H. (1989). Kinetic β-deuterium isotope effects suggest a covalent mechanism for the protein folding enzyme peptidylprolyl cis/trans-isomerase. FEBS Lett. *250*, 267–270.

Fortunato, F., and Kroemer, G. (2009). Impaired autophagosome-lysosome fusion in the pathogenesis of pancreatitis. Autophagy *5*, 850–853.

Freedman, S.D., and Scheele, G.A. (1993). Reversible pH-induced homophilic binding of GP2, a glycosyl-phosphatidylinositol-anchored protein in pancreatic zymogen granule membranes. Eur. J. Cell Biol. *61*, 229–238.

Freedman, S.D., Kern, H.F., and Scheele, G.A. (1994). Apical membrane trafficking during regulated pancreatic exocrine secretion-role of alkaline pH in the acinar lumen and enzymatic cleavage of GP2, a GPI-linked protein. Eur. J. Cell Biol. *65*, 354–365.

Freedman, S.D., Kern, H.F., and Scheele, G.A. (1998a). Cleavage of GPI-anchored proteins from the plasma membrane activates apical endocytosis in pancreatic acinar cells. Eur. J. Cell Biol. *75*, 163–173.

Freedman, S.D., Kern, H.F., and Scheele, G.A. (1998b). Acinar lumen pH regulates endocytosis, but not exocytosis, at the apical plasma membrane of pancreatic acinar cells. Eur. J. Cell Biol. *75*, 153–162.

Fröhlich, T., and Arnold, G.J. (2006). Proteome research based on modern liquid chromatography--tandem mass spectrometry: separation, identification and quantification. J. Neural Transm. *113*, 973–994.

Fujita-Yoshigaki, J., Matsuki-Fukushima, M., Yokoyama, M., and Katsumata-Kato, O. (2013). Sorting of a HaloTag protein that has only a signal peptide sequence into exocrine secretory granules without protein aggregation. Am. J. Physiol. Gastrointest. Liver Physiol. *305*, G685–96.

Fukumoto, Y., Okita, K., Kodama, T., Noda, K., Harada, T., Mizuta, M., and Takemoto, T. (1980). Studies of alpha-napthylisothiocyanate-induced hepatic disturbance. Hepatogastroenterology. *27*, 457–464.

Gabius, H.-J., André, S., Kaltner, H., and Siebert, H.-C. (2002). The sugar code: functional lectinomics. Biochim. Biophys. Acta *1572*, 165–177.

Gaisano, H.Y., and Gorelick, F.S. (2009). New insights into the mechanisms of pancreatitis. Gastroenterology *136*, 2040–2044.

Galat, A. (1993). Peptidylproline cis-trans-isomerases: immunophilins. Eur. J. Biochem. *216*, 689–707.

Galat, A. (2003). Peptidylprolyl cis/trans isomerases (immunophilins): biological diversity-targets-functions. Curr. Top. Med. Chem. *3*, 1315–1347.

Gallagher, J.T. (1989). The extended family of proteoglycans: social residents of the pericellular zone. Curr. Opin. Cell Biol. *1*, 1201–1218.

Gallagher, J.T., Lyon, M., and Steward, W.P. (1986). Structure and function of heparan sulphate proteoglycans. Biochem. J. *236*, 313–325.

Gemeiner, P., Mislovicová, D., Tkác, J., Svitel, J., Pätoprstý, V., Hrabárová, E., Kogan, G., and Kozár, T. (2009). Lectinomics II. A highway to biomedical/clinical diagnostics. Biotechnol. Adv. *27*, 1–15.

Geron, E., Schejter, E.D., and Shilo, B.-Z. (2013). Targeting secretion to the apical surface by mDia1-built actin tracks. Commun. Integr. Biol. *6*, e25660.

Ghazarian, H., Idoni, B., and Oppenheimer, S.B. (2011). A glycobiology review: carbohydrates, lectins and implications in cancer therapeutics. Acta Histochem. *113*, 236–247.

Gómez-Lázaro, M., Rinn, C., Aroso, M., Amado, F., and Schrader, M. (2010). Proteomic analysis of zymogen granules. Expert Rev. Proteomics *7*, 735–747.

Gondré-Lewis, M.C., Petrache, H.I., Wassif, C. a, Harries, D., Parsegian, A., Porter, F.D., and Loh, Y.P. (2006). Abnormal sterols in cholesterol-deficiency diseases cause secretory granule malformation and decreased membrane curvature. J. Cell Sci. *119*, 1876–1885.

Goodsell, D.S., and Olson, A.J. (2000). Structural symmetry and protein function. Annu. Rev. Biophys. Biomol. Struct. *29*, 105–153.

Gorelick, F., and Thrower, E. (2009). The acinar cell and early pancreatitis responses. Clin. Gastroenterol. Hepatol. *7*, S10–14.

Gorelik, E., Galili, U., and Raz, A. (2001). On the role of cell surface carbohydrates and their binding proteins (lectins) in tumor metastasis. Cancer Metastasis Rev. *20*, 245–277.

Greene, L.J., Hirs, C.H., and Palade, G.E. (1963). On the protein composition of bovine pancreatic zymogen granules. J. Biol. Chem. *238*, 2054–2070.

Grondin, G., St-Jean, P., and Beaudoin, A.R. (1992). Cytochemical and immunocytochemical characterization of a fibrillar network (GP2) in pancreatic juice: possible role as a sieve in the pancreatic ductal system. Eur. J. Cell Biol. *57*, 155–164.

Gukovskaya, A.S., and Gukovsky, I. (2012). Autophagy and pancreatitis. Am. J. Physiol. Gastrointest. Liver Physiol. *303*, G993–G1003.

Gukovsky, I., and Gukovskaya, A. (2010). Impaired autophagy underlies key pathological responses of acute pancreatitis. Autophagy *6*, 428–429.

Gukovsky, I., Pandol, S.J., and Gukovskaya, A.S. (2011). Organellar dysfunction in the pathogenesis of pancreatitis. Antioxid. Redox Signal. *15*, 2699–2710.

Guo, X., Trudgian, D., Lemoff, A., Yadavalli, S., and Mirzaei, H. (2014). Confetti: a multiprotease map of the HeLa proteome for comprehensive proteomics. Mol. Cell. Proteomics *13*, 1573–1584.

Guo, X.W., Merlin, D., Laboisse, C., and Hopfer, U. (1997). Purinergic agonists, but not cAMP, stimulate coupled granule fusion and Cl- conductance in HT29-Cl.16E. Am. J. Physiol. *273*, C804–9.

Gupta, G., Sinha, S., and Surolia, A. (2008). Unfolding energetics and stability of banana lectin. Proteins *72*, 754–760.

Gupta, G., Vishveshwara, S., and Surolia, A. (2009). Stability of dimeric interface in banana lectin: Insight from molecular dynamics simulations. IUBMB Life *61*, 252–260.

Han, X., Aslanian, A., and Yates, J.R. (2008). Mass spectrometry for proteomics. Curr. Opin. Chem. Biol. *12*, 483–490.

Hanoulle, X., Melchior, A., Sibille, N., Parent, B., Denys, A., Wieruszeski, J.M., Horvath, D., Allain, F., Lippens, G., and Landrieu, I. (2007). Structural and functional characterization of the interaction between cyclophilin B and a heparin-derived oligosaccharide. J. Biol. Chem. *282*, 34148–34158.

Hartupee, J.C., Zhang, H., Bonaldo, M.F., Soares, M.B., and Dieckgraefe, B.K. (2001). Isolation and characterization of a cDNA encoding a novel member of the human regenerating protein family: Reg IV. Biochim. Biophys. Acta *1518*, 287–293.

Hase, K., Kawano, K., Nochi, T., Pontes, G.S., Fukuda, S., Ebisawa, M., Kadokura, K., Tobe, T., Fujimura, Y., Kawano, S., et al. (2009). Uptake through glycoprotein 2 of FimH(+) bacteria by M cells initiates mucosal immune response. Nature *462*, 226–230.

Hashimoto, D., Ohmuraya, M., Hirota, M., Yamamoto, A., Suyama, K., Ida, S., Okumura, Y., Takahashi, E., Kido, H., Araki, K., et al. (2008). Involvement of autophagy in trypsinogen activation within the pancreatic acinar cells. J. Cell Biol. *181*, 1065–1072.

Hayashi, T., Matsubara, A., Ohara, S., Mita, K., Hasegawa, Y., Usui, T., Arihiro, K., Norimura, S., Sentani, K., Oue, N., et al. (2009). Immunohistochemical analysis of Reg IV in urogenital organs: Frequent expression of Reg IV in prostate cancer and potential utility as serum tumor marker. Oncol. Rep. *21*, 95–100.

Hegyi, P., Maléth, J., Venglovecz, V., and Rakonczay, Z. (2011). Pancreatic ductal bicarbonate secretion: challenge of the acinar acid load. Front. Physiol. *2*, 1–3.

Ho, M.-R., Lou, Y.-C., Wei, S.-Y., Luo, S.-C., Lin, W.-C., Lyu, P.-C., and Chen, C. (2010). Human RegIV protein adopts a typical C-type lectin fold but binds mannan with two calcium-independent sites. J. Mol. Biol. *402*, 682–695.

Hodel, A., An, S.J., Hansen, N.J., Lawrence, J., Wasle, B., Schrader, M., and Edwardson, J.M. (2001). Cholesterol-dependent interaction of syncollin with the membrane of the pancreatic zymogen granule. Biochem. J. *356*, 843–850.

Hokin, L.E. (1955). Isolation of the zymogen granules of dog pancreas and a study of their properties. Biochim. Biophys. Acta *18*, 379–388.

Hoops, T.C., and Rindler, M.J. (1991). Isolation of the cDNA encoding glycoprotein-2 (GP-2), the major zymogen granule membrane protein. Homology to uromodulin/Tamm-Horsfall protein. J. Biol. Chem. *266*, 4257–4263.

Iovanna, J.L., and Dagorn, J.-C. (2005). The multifunctional family of secreted proteins containing a C-type lectin-like domain linked to a short N-terminal peptide. Biochim. Biophys. Acta *1723*, 8–18.

Iovanna, J., Frigerio, J., Dusetti, N., Ramare, F., Raibaud, P., and Dragorn, J. (1993). Lithostathine, an inhibitor of CaCO3, crystal growth in pancreatic juice, induces bacterial aggregation. Pancreas *8*, 597–601.

Iwai, N., and Inagami, T. (1990). Molecular cloning of a complementary DNA to rat cyclophilin-like protein mRNA. Kidney Int. *37*, 1460–1465.

Jessen, B.A., Mullins, J.S., De Peyster, A., and Stevens, G.J. (2003). Assessment of hepatocytes and liver slices as in vitro test systems to predict in vivo gene expression. Toxicol. Sci. *75*, 208–222.

Johansson, M., Sjövall, H., and Hansson, G. (2013). The gastrointestinal mucus system in health and disease. Nat. Rev. Gastroenterol. Hepatol. *10*, 352–361.

Johansson, M.E. V, Phillipson, M., Petersson, J., Velcich, A., Holm, L., and Hansson, G.C. (2008). The inner of the two Muc2 mucin-dependent mucus layers in colon is devoid of bacteria. PNAS *105*, 15064–15069.

Junker, M., and Clark, P.L. (2010). Slow formation of aggregation-resistant beta-sheet folding intermediates. Proteins *78*, 812–824.

Kalus, I., Hodel, A., Koch, A., Kleene, R., Edwardson, J.M., and Schrader, M. (2002). Interaction of syncollin with GP-2, the major membrane protein of pancreatic zymogen granules, and association with lipid microdomains. Biochem. J. *362*, 433–442.

Kanagawa, M., Satoh, T., Ikeda, A., Nakano, Y., Yagi, H., Kato, K., Kojima-Aikawa, K., and Yamaguchi, Y. (2011). Crystal structures of human secretory proteins ZG16p and ZG16b reveal a Jacalin-related β-prism fold. Biochem. Biophys. Res. Commun. *404*, 201–205.

Kanagawa, M., Liu, Y., Hanashima, S., Ikeda, A., Chai, W., Nakano, Y., Kojima-Aikawa, K., Feizi, T., and Yamaguchi, Y. (2014). Structural basis for multiple sugar recognition of Jacalin-related human ZG16p lectin. J. Biol. Chem. *289*, 16954–16965.

Karas, M., and Hillenkamp, F. (1988). Laser desorption ionization of proteins with molecular masses exceeding 10,000 daltons. Anal. Chem. *60*, 2299–2301.

Kasai, H., Li, Y.X., and Miyashita, Y. (1993). Subcellular distribution of Ca2+ release channels underlying Ca2+ waves and oscillations in exocrine pancreas. Cell *74*, 669–677.

Keim, V., Rohr, G., Stöckert, H.G., and Haberich, F.J. (1984). An additional secretory protein in the rat pancreas. Digestion *29*, 242–249.

Kern, H.F., Rausch, U., and Scheele, G.A. (1987). Regulation of gene expression in pancreatic adaptation to nutritional substrates or hormones. Gut *28 Suppl*, 89–94.

Kerrigan, A.M., and Brown, G.D. (2009). C-type lectins and phagocytosis. Immunobiology *214*, 562–575.

Kim, M.-S., Pinto, S.M., Getnet, D., Nirujogi, R.S., Manda, S.S., Chaerkady, R., Madugundu, A.K., Kelkar, D.S., Isserlin, R., Jain, S., et al. (2014). A draft map of the human proteome. Nature *509*, 575–581.

Kleene, R., Kastner, B., Rosser, R., and Kern, H.F. (1999a). Complex formation among rat pancreatic secretory proteins under mild alkaline pH conditions. Digestion *60*, 305–313.

Kleene, R., Dartsch, H., and Kern, H. (1999b). The secretory lectin ZG16p mediates sorting of enzyme proteins to the zymogen granule membrane in pancreatic acinar cells. Eur. J. Cell Biol. *78*, 79–90.

Klumperman, J., Kuliawat, R., Griffith, J.M., Geuze, H.J., and Arvan, P. (1998). Mannose 6-phosphate receptors are sorted from immature secretory granules via adaptor protein AP-1, clathrin, and syntaxin 6-positive vesicles. J. Cell Biol. *141*, 359–371.

Kolset, S.O., and Gallagher, J.T. (1990). Proteoglycans in haemopoietic cells. Biochim. Biophys. Acta *1032*, 191–211.

Kumazawa-Inoue, K., Mimura, T., Hosokawa-Tamiya, S., Nakano, Y., Dohmae, N., Kinoshita-Toyoda, A., Toyoda, H., and Kojima-Aikawa, K. (2012). ZG16p, an animal homolog of β-prism fold plant lectins, interacts with heparan sulfate proteoglycans in pancreatic zymogen granules. Glycobiology *22*, 258–266.

Küry, P., Abankwa, D., Kruse, F., Greiner-Petter, R., and Muller, H.W. (2004). Gene expression profiling reveals multiple novel intrinsic and extrinsic factors associated with axonal regeneration failure. Eur. J. Neurosci. *19*, 32–42.

Lane, C.S. (2005). Mass spectrometry-based proteomics in the life sciences. Cell. Mol. Life Sci. *62*, 848–869.

Larsson, J.M.H., Thomsson, K.A., Rodríguez-Piñeiro, A.M., Karlsson, H., and Hansson (2013). Studies of mucus in mouse stomach, small intestine, and colon. III. Gastrointestinal Muc5ac and Muc2 mucin O-glycan patterns reveal a regiospecific distribution. Am. J. Physiol. Gastrointest. Liver Physiol. *305*, G357–63.

Laurine, E., Grégoire, C., Fändrich, M., Engemann, S., Marchal, S., Thion, L., Mohr, M., Monsarrat, B., Michel, B., Dobson, C.M., et al. (2003). Lithostathine quadruple-helical filaments form proteinase K-resistant deposits in Creutzfeldt-Jakob disease. J. Biol. Chem. *278*, 51770–51778.

Lebel, D., Grondin, G., and Paquette, J. (1988). In vitro stability of pancreatic zymogen granules: roles of pH and calcium. Biol. Cell *63*, 343–353.

Leblond, F.A., Viau, G., Lainé, J., and Lebel, D. (1993). Reconstitution in vitro of the pH-dependent aggregation of pancreatic zymogens en route to the secretory granule: implication of GP-2. Biochem. J. *291*, 289–296.

Lee, M.G., and Muallem, S. (2008). Physiology of Duct Cell Secretion. In The Pancreas: An Integrated Textbook of Basic Science, Medicine, and Surgery, H.G. Beger, A.L. Warshaw, M.W. Büchler, R.A. Kozarek, M.M. Lerch, J.P. Neoptolemos, K. Shiratori, D.C. Whitcomb, and B.M. Rau, eds. (Oxford, UK: Blackwell Publishing Ltd), pp. 78–90.

Lee, M.G., Ohana, E., Park, H.W., Yang, D., and Muallem, S. (2012). Molecular mechanism of pancreatic and salivary gland fluid and HCO3 secretion. Physiol. Rev. *92*, 39–74.

Lehotzky, R.E., Partch, C.L., Mukherjee, S., Cash, H.L., Goldman, W.E., Gardner, K.H., and Hooper, L. V (2010). Molecular basis for peptidoglycan recognition by a bactericidal lectin. PNAS *107*, 7722–7727.

Leskinen, M.J., Kovanen, P.T., and Lindstedt, K.A. (2003). Regulation of smooth muscle cell growth, function and death in vitro by activated mast cells - A potential mechanism for the weakening and rupture of atherosclerotic plaques. In Biochemical Pharmacology, pp. 1493–1498.

Lewis, B. (2008). Development of the Pancreas and Related Structures. In The Pancreas: An Integrated Textbook of Basic Science, Medicine, and Surgery, H.G. Beger, A.L. Warshaw, M.W. Büchler, R.A. Kozarek, M.M. Lerch, J.P. Neoptolemos, K. Shiratori, D.C. Whitcomb, and B.M. Rau, eds. (Oxford, UK: Blackwell Publishing Ltd.), pp. 42–49.

De Lisle, R.C., and Hopfer, U. (1986). Electrolyte permeabilities of pancreatic zymogen granules: implications for pancreatic secretion. Am. J. Physiol. *250*, G489–96.

De Lisle, R.C., Schulz, I., Tyrakowski, T., Haase, W., and Hopfer, U. (1984). Isolation of stable pancreatic zymogen granules. Am. J. Physiol. *246*, G411–G418.

Löbler, M., Saß, M., Kunze, C., Schmitz, K.P.K., and Hopt, U.T.U. (2002). Biomaterial patches sutured onto the rat stomach induce a set of genes encoding pancreatic enzymes. Biomaterials *23*, 577–583.

Logsdon, C.D., and Ji, B. (2013). The role of protein synthesis and digestive enzymes in acinar cell injury. Nat. Rev. Gastroenterol. Hepatol. *10*, 362–370.

Logsdon, C.D., Moessner, J., Williams, J. a, and Goldfine, I.D. (1985). Glucocorticoids increase amylase mRNA levels, secretory organelles, and secretion in pancreatic acinar AR42J cells. J. Cell Biol. *100*, 1200–1208.

Lombardo, D. (2001). Bile salt-dependent lipase: its pathophysiological implications. Biochim. Biophys. Acta *1533*, 1–28.

Lombardo, D., and Guy, O. (1980). Studies on the substrate specificity of a carboxyl ester hydrolase from human pancreatic juice. II. Action on cholesterol esters and lipid-soluble vitamin esters. Biochim. Biophys. Acta *611*, 147–155.

Longnecker, D.S., Lilja, H.S., French, J., Kuhlmann, E., and Noll, W. (1979). Transplantation of azaserine-induced carcinomas of pancreas in rats. Cancer Lett. *7*, 197–202.

Lowenfels, A.B., Maisonneuve, P., Cavallini, G., Ammann, R.W., Lankisch, P.G., Andersen, J.R., Dimagno, E.P., Andrén-Sandberg, A., and Domellöf, L. (1993). Pancreatitis and the risk of pancreatic cancer. International Pancreatitis Study Group. N. Engl. J. Med. *328*, 1433–1437.

Lowenfels, A.B., Maisonneuve, P., DiMagno, E.P., Elitsur, Y., Gates, L.K., Perrault, J., and Whitcomb, D.C. (1997). Hereditary pancreatitis and the risk of pancreatic cancer. International Hereditary Pancreatitis Study Group. J. Natl. Cancer Inst. *89*, 442–446.

Mareninova, O.A., Hermann, K., French, S.W., O'Konski, M.S., Pandol, S.J., Webster, P., Erickson, A.H., Katunuma, N., Gorelick, F.S., Gukovsky, I., et al. (2009). Impaired autophagic flux mediates acinar cell vacuole formation and trypsinogen activation in rodent models of acute pancreatitis. J. Clin. Invest. *119*, 3340–3355.

Mariller, C., Haendler, B., Allain, F., Denys, A., and Spik, G. (1996). Involvement of the N-terminal part of cyclophilin B in the interaction with specific Jurkat T-cell binding sites. Biochem. J. *317*, 571–576.

Markert, Y., Köditz, J., Mansfeld, J., Arnold, U., and Ulbrich-Hofmann, R. (2001). Increased proteolytic resistance of ribonuclease A by protein engineering. Protein Eng. *14*, 791–796.

Masedunskas, A., Porat-Shliom, N., and Weigert, R. (2012). Regulated exocytosis: novel insights from intravital microscopy. Traffic *13*, 627–634.

Massarwa, R., Schejter, E.D., and Shilo, B.Z. (2009). Apical Secretion in Epithelial Tubes of the Drosophila Embryo Is Directed by the Formin-Family Protein Diaphanous. Dev. Cell *16*, 877–888.

McLendon, G., and Radany, E. (1978). Is protein turnover thermodynamically controlled? J. Biol. Chem. *253*, 6335–6337.

Meagher, J.L., Winter, H.C., Ezell, P., Goldstein, I.J., and Stuckey, J.A. (2005). Crystal structure of banana lectin reveals a novel second sugar binding site. Glycobiology *15*, 1033–1042.

Messenger, S.W., Falkowski, M. a, and Groblewski, G.E. (2014). Ca(2+)-regulated secretory granule exocytosis in pancreatic and parotid acinar cells. Cell Calcium *55*, 369–375.

Meusser, B., Hirsch, C., Jarosch, E., and Sommer, T. (2005). ERAD: the long road to destruction. Nat. Cell Biol. *7*, 766–772.

Mitchell, R.M.S., Byrne, M.F., and Baillie, J. (2003). Pancreatitis. Lancet *361*, 1447–1455.

Miyake, H., Hara, S., Eto, H., Kaminodo, S., and Hara, I. (2004). Global analysis of gene expression profiles in ileum in a rat bladder augmentation model using cDNA microarrays. Int. J. Urol. *11*, 1009–1012.

Moniaux, N., Song, H., Darnaud, M., Garbin, K., Gigou, M., Mitchell, C., Samuel, D., Jamot, L., Amouyal, P., Amouyal, G., et al. (2011). Human hepatocarcinoma-intestine-pancreas/pancreatitis-associated protein cures fas-induced acute liver failure in mice by attenuating free-radical damage in injured livers. Hepatology *53*, 618–627.

Montague, J.W., Hughes, F.M., and Cidlowski, J.A. (1997). Native recombinant cyclophilins A, B, and C degrade DNA independently of peptidylprolyl cis-trans-isomerase activity. Potential roles of cyclophilins in apoptosis. J. Biol. Chem. *272*, 6677–6684.

Nakamura-Tsuruta, S., Uchiyama, N., Peumans, W.J., Van Damme, E.J.M., Totani, K., Ito, Y., and Hirabayashi, J. (2008). Analysis of the sugar-binding specificity of mannose-binding-type Jacalin-related lectins by frontal affinity chromatography-an approach to functional classification. FEBS J. *275*, 1227–1239.

Nanakin, A., Fukui, H., Fujii, S., Sekikawa, A., Kanda, N., Hisatsune, H., Seno, H., Konda, Y., Fujimori, T., and Chiba, T. (2007). Expression of the REG IV gene in ulcerative colitis. Lab. Invest. *87*, 304–314.

Neuschwander-Tetri, B. a, Fimmel, C.J., Kladney, R.D., Wells, L.D., and Talkad, V. (2004). Differential expression of the trypsin inhibitor SPINK3 mRNA and the mouse ortholog of secretory granule protein ZG-16p mRNA in the mouse pancreas after repetitive injury. Pancreas *28*, e104–e111.

Oue, N., Mitani, Y., Aung, P.P., Sakakura, C., Takeshima, Y., Kaneko, M., Noguchi, T., Nakayama, H., and Yasui, W. (2005). Expression and localization of Reg IV in human neoplastic

and non-neoplastic tissues: Reg IV expression is associated with intestinal and neuroendocrine differentiation in gastric adenocarcinoma. J. Pathol. *207*, 185–198.

Palade, G. (1975). Intracellular aspects of the process of protein synthesis. Science *189*, 867.

Palmer, E., and Freeman, T. (2004). Investigation into the use of C- and N-terminal GFP fusion proteins for subcellular localization studies using reverse transfection microarrays. Comp. Funct. Genomics *5*, 342–353.

Pâquet, M.R., St-Jean, P., Roberge, M., and Beaudoin, A.R. (1982). Isolation of zymogen granules from rat pancreas and characterization of their membrane proteins. Eur. J. Cell Biol. *28*, 20–26.

Parikh, A., Stephan, A., and Tzanakakis, E. (2012). Regenerating proteins and their expression, regulation, and signaling. Biomol. Concepts *3*, 57–70.

Parsell, D.A., and Sauer, R.T. (1989). The structural stability of a protein is an important determinant of its proteolytic susceptibility in Escherichia coli. J. Biol. Chem. *264*, 7590–7595.

Pejler, G., and Berg, L. (1995). Regulation of rat mast cell protease 1 activity. Protease inhibition is prevented by heparin proteoglycan. Eur. J. Biochem. *233*, 192–199.

Pejler, G., and Maccarana, M. (1994). Interaction of heparin with rat mast cell protease 1. J. Biol. Chem. *269*, 14451–14456.

Pelaseyed, T., Bergström, J.H., Gustafsson, J.K., Ermund, A., Birchenough, G.M.H., Schütte, A., van der Post, S., Svensson, F., Rodríguez-Piñeiro, A.M., Nyström, E.E.L., et al. (2014). The mucus and mucins of the goblet cells and enterocytes provide the first defense line of the gastrointestinal tract and interact with the immune system. Immunol. Rev. *260*, 8–20.

Price, E.R., Jin, M., Lim, D., Pati, S., Walsh, C.T., and McKeon, F.D. (1994). Cyclophilin B trafficking through the secretory pathway is altered by binding of cyclosporin A. PNAS *91*, 3931–3935.

Prydz, K., and Dalen, K.T. (2000). Synthesis and sorting of proteoglycans. J. Cell Sci. *113*, 193–205.

Raval, S., Gowda, S.B., Singh, D.D., and Chandra, N.R. (2004). A database analysis of jacalin-like lectins: sequence-structure-function relationships. Glycobiology *14*, 1247–1263.

Rebaï, O., Le Petit-Thevenin, J., Bruneau, N., Lombardo, D., and Vérine, A. (2005). In vitro angiogenic effects of pancreatic bile salt-dependent lipase. Arterioscler. Thromb. Vasc. Biol. *25*, 359–364.

Reggio, H.A., and Palade, G.E. (1978). Sulfated compounds in the zymogen granules of the guinea pig pancreas. J. Cell Biol. *77*, 288–314.

Reuter, G., and Gabius, H.J. (1999). Eukaryotic glycosylation: Whim of nature or multipurpose tool? Cell. Mol. Life Sci. *55*, 368–422.

Rindler, M.J. (1992). Biogenesis of storage granules and vesicles. Curr. Opin. Cell Biol. *4*, 616–622.

Rindler, M.J. (2006). Isolation of zymogen granules from rat pancreas. In Current Protocols in Cell Biology, pp. 3.18.1–3.18.16.

Rindler, M.J., and Hoops, T.C. (1990). The pancreatic membrane protein GP-2 localizes specifically to secretory granules and is shed into the pancreatic juice as a protein aggregate. Eur. J. Cell Biol. *53*, 154–163.

Rindler, M.J., Xu, C.F., Gumper, I., Smith, N.N., and Neubert, T.A. (2007). Proteomic analysis of pancreatic zymogen granules: Identification of new granule proteins. J. Proteome Res. *6*, 2978–2992.

Rinn, C., Aroso, M., Prüssing, J., Islinger, M., and Schrader, M. (2012). Modulating zymogen granule formation in pancreatic AR42J cells. Exp. Cell Res. *318*, 1855–1866.

Rodríguez-Piñeiro, A.M., Bergström, J.H., Ermund, A., Gustafsson, J.K., Schütte, A., Johansson, M.E. V, and Hansson, G.C. (2013). Studies of mucus in mouse stomach, small intestine, and colon. II. Gastrointestinal mucus proteome reveals Muc2 and Muc5ac accompanied by a set of core proteins. Am. J. Physiol. Gastrointest. Liver Physiol. *305*, G348–56.

Rönnberg, E., Melo, F.R., and Pejler, G. (2012). Mast cell proteoglycans. J. Histochem. Cytochem. *60*, 950–962.

Rutten, W.J., De Pont, J.J., Bonting, S.L., and Daemen, F.J. (1975). Lysophospholipids in pig pancreatic zymogen granules in relation to exocytosis. Eur. J. Biochem. *54*, 259–265.

Sajnani, G., and Requena, J.R. (2012). Prions, proteinase K and infectivity. Prion *6*, 430–432.

Sajnani, G., Silva, C.J., Ramos, A., Pastrana, M.A., Onisko, B.C., Erickson, M.L., Antaki, E.M., Dynin, I., Vázquez-Fernández, E., Sigurdson, C.J., et al. (2012). PK-sensitive PrP is infectious and shares basic structural features with PK-resistant PrP. PLoS Pathog. *8*, e1002547.

Sarles, H. (1986). Etiopathogenesis and definition of chronic pancreatitis. Dig. Dis. Sci. *31*, 91S–107S.

Sastry, M. V, Banarjee, P., Patanjali, S.R., Swamy, M.J., Swarnalatha, G. V, and Surolia, A. (1986). Analysis of saccharide binding to Artocarpus integrifolia lectin reveals specific recognition of T-antigen (beta-D-Gal(1--3)D-GalNAc). J. Biol. Chem. *261*, 11726–11733.

Scheele, G.A. (1975). Two-dimensional gel analysis of soluble proteins. Charaterization of guinea pig exocrine pancreatic proteins. J. Biol. Chem. *250*, 5375–5385.

Scheele, G.A., and Palade, G.E. (1975). Studies on the guinea pig pancreas. Parallel discharge of exocrine enzyme activities. J. Biol. Chem. *250*, 2660–2670.

Scheele, G., Pash, J., and Bieger, W. (1981). Identification of proteins according to biological activity following separation by two-dimensional isoelectric focusing/sodium dodecyl sulfate gel electrophoresis: analysis of human exocrine pancreatic proteins. Anal. Biochem. *112*, 304–313.

Scheele, G.A., Palade, G.E., and Tartakoff, A.M. (1978). Cell fractionation studies on the guinea pig pancreas. Redistribution of exocrine proteins during tissue homogenization. J. Cell Biol. *78*, 110–130.

Scheele, G.A., Fukuoka, S., and Freedman, S.D. (1994). Role of the GP2/THP family of GPI-anchored proteins in membrane trafficking during regulated exocrine secretion. Pancreas *9*, 139–149.

Schick, J., Kern, H., and Scheele, G. (1984a). Hormonal stimulation in the exocrine pancreas results in coordinate and anticoordinate regulation of protein synthesis. J. Cell Biol. *99*, 1569–1574.

Schick, J., Verspohl, R., Kern, H., and Scheele, G. (1984b). Two distinct adaptive responses in the synthesis of exocrine pancreatic enzymes to inverse changes in protein and carbohydrate in the diet. Am. J. Physiol. *247*, G611–G616.

Schmidt, K., Dartsch, H., Linder, D., Kern, H.F., and Kleene, R. (2000). A submembranous matrix of proteoglycans on zymogen granule membranes is involved in granule formation in rat pancreatic acinar cells. J. Cell Sci. *113*, 2233–2242.

Schmidt, K., Schrader, M., Kern, H.F., and Kleene, R. (2001). Regulated apical secretion of zymogens in rat pancreas. Involvement of the glycosylphosphatidylinositol-anchored glycoprotein GP-2, the lectin ZG16p, and cholesterol-glycosphingolipid-enriched microdomains. J. Biol. Chem. *276*, 14315–14323.

Schrader, M. (2004). Membrane targeting in secretion. In Subcellular Biochemistry, Volume 37: Membrane Dynamics and Domains, P.J. Quinn, ed. (New York: Kluwer Academic / Plenum Publishers), pp. 391–421.

Schwake, M., Schröder, B., and Saftig, P. (2013). Lysosomal membrane proteins and their central role in physiology. Traffic *14*, 739–748.

Sharma, A., Chandran, D., Singh, D.D., and Vijayan, M. (2007). Multiplicity of carbohydrate-binding sites in beta-prism fold lectins: occurrence and possible evolutionary implications. J. Biosci. *32*, 1089–1110.

Sharon, N., and Lis, H. (2004). History of lectins: from hemagglutinins to biological recognition molecules. Glycobiology *14*, 53R–62R.

Silva, A.M.N., Vitorino, R., Domingues, M.R.M., Spickett, C.M., and Domingues, P. (2013). Post-translational modifications and mass spectrometry detection. Free Radic. Biol. Med. *65*, 925–941.

Singh, D.D., Saikrishnan, K., Kumar, P., Surolia, a, Sekar, K., and Vijayan, M. (2005). Unusual sugar specificity of banana lectin from Musa paradisiaca and its probable evolutionary origin. Crystallographic and modelling studies. Glycobiology *15*, 1025–1032.

Steinhilber, W., Poensgen, J., Rausch, U., Kern, H.F., and Scheele, G.A. (1988). Translational control of anionic trypsinogen and amylase synthesis in rat pancreas in response to caerulein stimulation. PNAS *85*, 6597–6601.

Sun, X., and Jiang, X. (2013). Combination of FASP and fully automated 2D-LC-MS/MS allows in-depth proteomic characterization of mouse zymogen granules. Biomed. Chromatogr. *27*, 407–408.

Swaney, D.L., Wenger, C.D., and Coon, J.J. (2010). Value of using multiple proteases for large-scale mass spectrometry-based proteomics. J. Proteome Res. *9*, 1323–1329.

Swanson, M.D., Winter, H.C., Goldstein, I.J., and Markovitz, D.M. (2010). A lectin isolated from bananas is a potent inhibitor of HIV replication. J. Biol. Chem. *285*, 8646–8655.

Switzar, L., Giera, M., and Niessen, W.M.A. (2013). Protein digestion: an overview of the available techniques and recent developments. J. Proteome Res. *12*, 1067–1077.

Szmola, R., and Sahin-Tóth, M. (2007). Chymotrypsin C (caldecrin) promotes degradation of human cationic trypsin: identity with Rinderknecht's enzyme Y. PNAS *104*, 11227–11232.

Takahashi, N., Hayano, T., and Suzuki, M. (1989). Peptidyl-prolyl cis-trans isomerase is the cyclosporin A-binding protein cyclophilin. Nature *337*, 473–475.

Tamura, H., Ohtsuka, M., Washiro, M., Kimura, F., Shimizu, H., Yoshidome, H., Kato, A., Seki, N., and Miyazaki, M. (2009). Reg IV expression and clinicopathologic features of gallbladder carcinoma. Hum. Pathol. *40*, 1686–1692.

Tanaka, K., Waki, H., and Ido, Y. (1988). Protein and Polymer Analyses up to m/z 100 000 by Laser Ionization Time-of-Flight Mass Spectrometry. Rapid Commun. Mass Spectrom. *2*, 151–153.

Tanaka, Y., Guhde, G., Suter, A., Eskelinen, E.L., Hartmann, D., Lüllmann-Rauch, R., Janssen, P.M., Blanz, J., von Figura, K., and Saftig, P. (2000). Accumulation of autophagic vacuoles and cardiomyopathy in LAMP-2-deficient mice. Nature *406*, 902–906.

Tartakoff, A., Greene, L.J., and Palade, G.E. (1974). Studies on the Guinea Pig Pancreas. J. Biol. Chem. *249*, 7420–7431.

Tartakoff, A.M., Jamieson, J.D., Scheele, G.A., and Palade, G.E. (1975). Studies on the pancreas of the guinea pig. Parallel processing and discharge of exocrine proteins. J. Biol. Chem. *250*, 2671–2677.

Tateno, H. (2010). SUEL-related lectins, a lectin family widely distributed throughout organisms. Biosci. Biotechnol. Biochem. *74*, 1141–1144.

Tateno, H., Yabe, R., Sato, T., Shibazaki, A., Shikanai, T., Gonoi, T., Narimatsu, H., and Hirabayashi, J. (2012). Human ZG16p recognizes pathogenic fungi through non-self polyvalent mannose in the digestive system. Glycobiology *22*, 210–220.

Thévenod, F. (2002). Ion channels in secretory granules of the pancreas and their role in exocytosis and release of secretory proteins. Am. J. Physiol. Cell Physiol. *283*, C651–C672.

Thévenod, F., Anderie, I., and Schulz, I. (1994). Monoclonal antibodies against MDR1 P-glycoprotein inhibit chloride conductance and label a 65-kDa protein in pancreatic zymogen granule membranes. J. Biol. Chem. *269*, 24410–24417.

Thorn, P., Lawrie, A.M., Smith, P.M., Gallacher, D. V, and Petersen, O.H. (1993). Local and global cytosolic Ca2+ oscillations in exocrine cells evoked by agonists and inositol trisphosphate. Cell *74*, 661–668.

Thrower, E.C., Gorelick, F.S., and Husain, S.Z. (2010). Molecular and cellular mechanisms of pancreatic injury. Curr. Opin. Gastroenterol. *26*, 484–489.

Tooth, D., Garsed, K., Singh, G., Marciani, L., Lam, C., Fordham, I., Fields, A., Banwait, R., Lingaya, M., Layfield, R., et al. (2014). Characterisation of faecal protease activity in irritable bowel syndrome with diarrhoea: origin and effect of gut transit. Gut *63*, 753–760.

Tooze, J., Kern, H.F., Fuller, S.D., and Howell, K.E. (1989). Condensation-sorting events in the rough endoplasmic reticulum of exocrine pancreatic cells. J. Cell Biol. *109*, 35–50.

Tooze, S.A., Martens, G.J.M., and Huttner, W.B. (2001). Secretory granule biogenesis: Rafting to the SNARE. Trends Cell Biol. *11*, 116–122.

Vaccaro, M.I. (2012). Zymophagy: Selective autophagy of secretory granules. Int. J. Cell Biol. *2012*, 1–7.

Valentijn, K.M., Gumkowski, F.D., and Jamieson, J.D. (1999). The subapical actin cytoskeleton regulates secretion and membrane retrieval in pancreatic acinar cells. J. Cell Sci. *112*, 81–96.

Vanpouille, C., Denys, A., Carpentier, M., Pakula, R., Mazurier, J., and Allain, F. (2004). Octasaccharide is the minimal length unit required for efficient binding of cyclophilin B to heparin and cell surface heparan sulphate. Biochem. J. *382*, 733–740.

Vasiloudes, P., Paul, N., Tooze, J., and Kern, H.F. (1991). Acceleration of asynchronous enzyme transport in the rat exocrine pancreas following hormonal stimulation in vivo. Eur. J. Cell Biol. *54*, 27–37.

Violette, S., Festor, E., Pandrea-Vasile, I., Mitchell, V., Adida, C., Dussaulx, E., Lacorte, J.-M., Chambaz, J., Lacasa, M., and Lesuffleur, T. (2003). Reg IV, a new member of the regenerating gene family, is overexpressed in colorectal carcinomas. Int. J. Cancer. *103*, 185–193.

Wagner, A.C., and Williams, J.A. (1994). Pancreatic zymogen granule membrane proteins: molecular details begin to emerge. Digestion *55*, 191–199.

Walz, A., Stühler, K., Wattenberg, A., Hawranke, E., Meyer, H.E., Schmalz, G., Blüggel, M., and Ruhl, S. (2006). Proteome analysis of glandular parotid and submandibular-sublingual saliva in comparison to whole human saliva by two-dimensional gel electrophoresis. Proteomics *6*, 1631–1639.

Wang, B.J., and Cui, Z.J. (2007). How does cholecystokinin stimulate exocrine pancreatic secretion? From birds, rodents, to humans. Am. J. Physiol. Regul. Integr. Comp. Physiol. *292*, R666–R678.

Wang, P., and Heitman, J. (2005). The cyclophilins. Genome Biol. *6*, 226.1–226.6.

Wasle, B., and Edwardson, J.M. (2002). The regulation of exocytosis in the pancreatic acinar cell. Cell. Signal. *14*, 191–197.

Weiss, F.U., Halangk, W., and Lerch, M.M. (2008). New advances in pancreatic cell physiology and pathophysiology. Best Pract. Res. Clin. Gastroenterol. *22*, 3–15.

Whitcomb, D.C. (2004). Mechanisms of disease: Advances in understanding the mechanisms leading to chronic pancreatitis. Nat. Clin. Pract. Gastroenterol. Hepatol. *1*, 46–52.

Whitcomb, D.C., and Beger, H.G. (2008). Definitions of Pancreatic Diseases and their Complications. In The Pancreas: An Integrated Textbook of Basic Science, Medicine, and Surgery, H.G. Beger, A.L. Warshaw, M.W. Büchler, R.A. Kozarek, M.M. Lerch, J.P. Neoptolemos, K. Shiratori, D.C. Whitcomb, and B.M. Rau, eds. (Oxford, UK: Blackwell Publishing Ltd), pp. 1–6.

Wilhelm, M., Schlegl, J., Hahne, H., Moghaddas Gholami, A., Lieberenz, M., Savitski, M.M., Ziegler, E., Butzmann, L., Gessulat, S., Marx, H., et al. (2014). Mass-spectrometry-based draft of the human proteome. Nature *509*, 582–587.

Williams, J.A. (2006). Regulation of pancreatic acinar cell function. Curr. Opin. Gastroenterol. *22*, 498–504.

Williams, J.A. (2013). Proteomics as a systems approach to pancreatitis. Pancreas *42*, 905–911.

Xiao, R., Badger, T.M., and Simmen, F.A. (2005). Dietary exposure to soy or whey proteins alters colonic global gene expression profiles during rat colon tumorigenesis. Mol. Cancer *4*, 1.

Yoshimori, T., Semba, T., Takemoto, H., Akagi, S., Yamamoto, A., and Tashiro, Y. (1990). Protein disulfide-isomerase in rat exocrine pancreatic cells is exported from the endoplasmic reticulum despite possessing the retention signal. J. Biol. Chem. *265*, 15984–15990.

Yu, S., Michie, S. a, and Lowe, A.W. (2004). Absence of the major zymogen granule membrane protein, GP2, does not affect pancreatic morphology or secretion. J. Biol. Chem. *279*, 50274–50279.

Zhang, Y., Fonslow, B.R., Shan, B., Baek, M.-C., and Yates III, J.R. (2013). Protein analysis by shotgun/bottom-up proteomics. Chem. Rev. *113*, 2343–2394.

Zheng, X., Lu, D., and Sadler, J.E. (1999). Apical sorting of bovine enteropeptidase does not involve detergent-resistant association with sphingolipid-cholesterol rafts. J. Biol. Chem. *274*, 1596–1605.

Zheng, X.L., Kitamoto, Y., and Sadler, J.E. (2009). Enteropeptidase, a type II transmembrane serine protease. Front. Biosci. *1*, 242–249.

Zhou, Y.-B., Cao, J.-B., Yang, H.-M., Zhu, H., Xu, Z.-G., Wang, K.-S., Zhang, X., Wang, Z.-Q., and Han, Z.-G. (2007). hZG16, a novel human secreted protein expressed in liver, was down-regulated in hepatocellular carcinoma. Biochem. Biophys. Res. Commun. *355*, 679–686.

APPENDIX

Appendix

Supplementary Table 1. Identification by mass spectrometry of basic spots from the Wash subfraction after analysis by 2D-PAGE.

Spot	UniProtKB	Protein name	Theoretical MW (kDa)	MW (kDa) in gel	Theoretical *p*I	Score	Sequence coverage	Matching Peptides	Localization	Function and References
B1	LIPR1_RAT	Pancreatic lipase related protein 1	52.3	31.7	5.79	317	31%	12	Zymogen granules of the exocrine pancreas.	AB hydrolase superfamily. Lipase family.[1]
B2			52.3	34.2	5.79	95.9	20%	8		
B3			52.3	34.0	5.79	290	31%	13		
B7			52.3	34.0	5.79	337	24%	11		
B18			52.3	25.2	5.79	268	34%	10		
B20			52.3	25.6	5.79	184	26%	8		
B21			52.3	25.2	5.79	193	31%	11		
B22			52.3	20.8	5.79	208	36%	10		
B24			52.3	20.8	5.79	171	26%	8		
B32			52.3	16.3	5.79	193	28%	8		
B11	LIPP_RAT	Pancreatic triacylglycerol lipase	51.4	31.1	6.31	143	30%	11	Zymogen granules of the exocrine pancreas.	Plays an important role in fat metabolism.[2]
B12			51.4	31.2	6.31	184	28%	11		
B19			51.4	22.6	6.31	300	43%	15		
B25			51.4	21.6	6.31	295	35%	12		
B34			51.4	16.1	6.31	178	26%	9		
B4	AMYP_RAT	[#]Pancreatic alpha-amylase	57.1	35.8	8.34	235	38%	13	Zymogen granules of the exocrine pancreas.	Endohydrolysis of 1,4-alpha-D-glucosidic linkages in oligosaccharides and polysaccharides.[3]
B5			57.1	35.8	8.34	185	41%	14		
B6			57.1	35.8	8.34	314	35%	12		
B30			57.1	19.3	8.34	328	40%	14		

Spot	UniProtKB	Protein name	Theoretical MW (kDa)	MW (kDa) in gel	Theoretical *p*I	Score	Sequence coverage	Matching Peptides	Localization	Function and References
B33			57.1	14.3	8.34	291	40%	14		
B8	CEL_RAT	#Bile salt-activated lipase	66.9	33.6	5.31	191	15%	7	Zymogen granules of the exocrine pancreas. Content protein, but also strongly membrane associated.	Catalyzes fat and vitamin absorption. Acts in concert with pancreatic lipase and colipase for the complete digestion of dietary triglycerides.[4]
B9			66.9	33.6	5.31	219	24%	14		
B10			66.9	33.6	5.31	225	19%	11		
B15			66.9	32.7	5.31	88.2	14%	7		
B23			66.9	20.2	5.31	182	25%	12		
B37			66.9	16.9	5.31	134	15%	7		
B29			66.9	17.5	5.31	126	24%	10		
B28			66.9	18.7	5.31	174	21%	11		
B40			66.9	12.9	5.31	135	18%	7		
B42			66.9	10.9	5.31	55.8	7%	3		
B16	MCPT1_RAT	#Mast cell protease I (RMCP1) (Chymase)	28.5	27.5	9.54	130	50%	9	Cytoplasmic granules of mast cells	Major secreted protease of mast cells with suspected roles in vasoactive peptide generation, extracellular matrix degradation, and regulation of gland secretion.[5]
B17	CELA1_RAT	Chymotrypsin-like elastase family member 1	28.9	28	8.79	60.8	15%	3	Zymogen granules of the exocrine pancreas.	Hydrolysis of proteins, including elastin.[6]
B14	VINC_RAT	Vinculin	116.5	31	5.77	55.6	28%	17	Cytoplasm, cytoskeleton. Cell junction, adherens junction. Cell membrane;	Involved in cell adhesion. May be involved in the attachment of the actin-based microfilaments to the plasma membrane. May also play important roles in cell morphology and locomotion.[7]

Spot	UniProtKB	Protein name	Theoretical MW (kDa)	MW (kDa) in gel	Theoretical *p*I	Score	Sequence coverage	Matching Peptides	Localization	Function and References
									Peripheral membrane protein.	
B13	TRY3_RAT	Cationic trypsin-3	26.2	25.7	7.45	186	44%	7	Zymogen granules of the exocrine pancreas. Content protein.	S1-peptidase, serine protease.[8]
B27	RNS1B_RAT	#Ribonuclease pancreatic beta-type	16.8	16	8.63	136	51%	6	Zymogen granules of the exocrine pancreas. Content protein.	Endonuclease that catalyzes the cleavage of RNA. Acts on single stranded and double stranded RNA.[9]
B26	PPIB_RAT	#Peptidyl-prolyl cis-trans isomerase B (PPIase)	22.7	22	9.42	55.8	49%	3	Endoplasmic reticulum lumen	PPIases accelerate the folding of proteins. Catalyzes the cis-trans isomerization of proline imidic peptide bonds in oligopeptides.[10]
B31	ZG16_RAT	#Zymogen granule membrane protein 16 (Secretory lectin ZG16)	18.2	17.5	9.17	210	72%	9	Zymogen granules, peripheral membrane protein	May act as a linker molecule between the submembranous matrix on the luminal side of zymogen granule membrane (ZGM) and aggregated secretory proteins during granule formation at the TGN.[11]

Spot	UniProtKB	Protein name	Theoretical MW (kDa)	MW (kDa) in gel	Theoretical *p*I	Score	Sequence coverage	Matching Peptides	Localization	Function and References
B38	SYCN_RAT	#Syncollin	15.9	15.4	8.61	120	29%	7	Cytoplasmic vesicle, secretory vesicle membrane; Peripheral membrane protein.	Compound exocytosis. Associated with lipid rafts in a cholesterol-dependent manner. Interacts with GP2.[12]
B36	B2RZA9_RAT	Ubiquitin carrier protein	17.8	16.7	8.68	56.8	45%	7		Ubl conjugation pathway
B35	LIPR2_RAT	Pancreatic lipase-related protein 2	52.5	14.1	5.92	88.8	22%	9	Zymogen granules of the exocrine pancreas.	Lipid degradation.[13]
B41		Not identified								
B45		Not identified								
B39	COL_RAT	Colipase	12.2	11.8	8.04	57	36%	4	Zymogen granules of the exocrine pancreas. Content protein.	Cofactor of pancreatic lipase. Allows the lipase to anchor itself to the lipid-water interface.[14]
B44			12.2	9.6	8.04	125	43%	5		
B43			12.2	9.2	8.04	85.3	64%	7		
B46	Q9EQZ8_RAT	Chymopasin	28.1	27.3	8.56	51	40%	7	Zymogen granules of the exocrine pancreas.	S1-peptidase, serine protease.[15]

References

(1) Lowe, M. E., The triglyceride lipases of the pancreas. *J Lipid Res* **2002,** *43* (12), 2007-16.

(2) Payne, R. M.; Sims, H. F.; Jennens, M. L.; Lowe, M. E., Rat pancreatic lipase and two related proteins: enzymatic properties and mRNA expression during development. *Am J Physiol* **1994,** *266* (5 Pt 1), G914-21.

(3) MacDonald, R. J.; Crerar, M. M.; Swain, W. F.; Pictet, R. L.; Thomas, G.; Rutter, W. J., Structure of a family of rat amylase genes. *Nature* **1980,** *287* (5778), 117-22.

(4) Kissel, J. A.; Fontaine, R. N.; Turck, C. W.; Brockman, H. L.; Hui, D. Y., Molecular cloning and expression of cDNA for rat pancreatic cholesterol esterase. *Biochim Biophys Acta* **1989,** *1006* (2), 227-36.

(5) Lutzelschwab, C.; Pejler, G.; Aveskogh, M.; Hellman, L., Secretory granule proteases in rat mast cells. Cloning of 10 different serine proteases and a carboxypeptidase A from various rat mast cell populations. *J Exp Med* **1997,** *185* (1), 13-29.

(6) MacDonald, R. J.; Swift, G. H.; Quinto, C.; Swain, W.; Pictet, R. L.; Nikovits, W.; Rutter, W. J., Primary structure of two distinct rat pancreatic preproelastases determined by sequence analysis of the complete cloned messenger ribonucleic acid sequences. *Biochemistry* **1982,** *21* (6), 1453-63.

(7) Coll, J. L.; Ben-Ze'ev, A.; Ezzell, R. M.; Rodriguez Fernandez, J. L.; Baribault, H.; Oshima, R. G.; Adamson, E. D., Targeted disruption of vinculin genes in F9 and embryonic stem cells changes cell morphology, adhesion, and locomotion. *Proc Natl Acad Sci U S A* **1995,** *92* (20), 9161-5.

(8) Fletcher, T. S.; Alhadeff, M.; Craik, C. S.; Largman, C., Isolation and characterization of a cDNA encoding rat cationic trypsinogen. *Biochemistry* **1987,** *26* (11), 3081-6.

(9) Beintema, J. J., Rat pancreatic ribonuclease: agreement between the corrected amino acid sequence and the sequence derived from its messenger RNA. *FEBS Lett* **1983,** *159* (1-2), 191-5.

(10) Iwai, N.; Inagami, T., Molecular cloning of a complementary DNA to rat cyclophilin-like protein mRNA. *Kidney Int* **1990,** *37* (6), 1460-5.

(11) Cronshagen, U.; Voland, P.; Kern, H. F., cDNA cloning and characterization of a novel 16 kDa protein located in zymogen granules of rat pancreas and goblet cells of the gut. *Eur. J. Cell Biol.* **1994,** *65* (2), 366-77.

(12) Edwardson, J. M.; An, S.; Jahn, R., The secretory granule protein syncollin binds to syntaxin in a Ca2(+)- sensitive manner. *Cell* **1997,** *90* (2), 325-33.

(13) Wishart, M. J.; Andrews, P. C.; Nichols, R.; Blevins, G. T., Jr.; Logsdon, C. D.; Williams, J. A., Identification and cloning of GP-3 from rat pancreatic acinar zymogen granules as a glycosylated membrane-associated lipase. *J Biol Chem* **1993,** *268* (14), 10303-11.

(14) Wicker, C.; Puigserver, A., Rat pancreatic colipase mRNA: nucleotide sequence of a cDNA clone and nutritional regulation by a lipidic diet. *Biochem Biophys Res Commun* **1990,** *167* (1), 130-6.

(15) Sogame, Y.; Kataoka, K.; Kato, M.; Sakagami, J.; Osawa, S.; Takatera, A.; Mitsuyoshi, M.; Usui, N.; Mitsui, S.; Yamaguchi, N., Molecular cloning and characterization of chymopasin, a novel serine protease from rat pancreas. *Pancreas* **2002,** *25* (4), 378-86.

Supplementary Table 2. Proteins identified by mass spectrometry from the enterokinase samples

Rank	Accession Number (Expasy)	Protein Name	Species	Total Ion Score	Accession Number	Protein MW	Protein PI	Peptide Count	Total Ion Score C.I. %	Best Ion Score C.I. %
1	P00689	Pancreatic alpha-amylase	Rattus norvegicus	495,51	AMYP_RAT	57141	8,34	21	100	98,972
2	P07338	Chymotrypsinogen B	Rattus norvegicus	251,56	CTRB1_RAT	27831	4,9	9	100	99,98
3	P19223	Carboxypeptidase B	Rattus norvegicus	172,43	CBPB1_RAT	47485	5,44	5	100	97,529
4	P54316	Pancreatic lipase related protein 1	Rattus norvegicus	154,4	LIP1_RAT	52345	5,79	4	100	99,869

Rank	Accession Number (Expasy)	Protein Name	Species	Total Ion Score	Accession Number	Protein MW	Protein PI	Peptide Count	Total Ion Score C.I. %	Best Ion Score C.I. %
5	P00731	Carboxypeptidase A1	Rattus norvegicus	113,85	CBPA1_RAT	47168	5,45	4	100	96,831
6	P19222	Carboxypeptidase A2	Rattus norvegicus	99,076	CBPA2_RAT	46883	5,17	4	100	94,656
7	P27657	Pancreatic triacylglycerol lipase	Rattus norvegicus	91,454	LIPP_RAT	51407	6,31	2	100	99,352
8	P08426	Cationic trypsin III	Rattus norvegicus	72,57	TRY3_RAT	26252	7,45	1	99,982	99,99

Supplementary Table 3. Distribution (%) of ZG proteins to different ZG subfractions

Protein	ZGC	ZGM	ZGM_{carb}	Wash
Amylase	86.5 ± 3.8	13.5 ± 3.8	24.3 ± 4.0	75.7 ± 4.0
GP2	2.2 ± 1.3	97.8 ± 1.3	86.0 ± 5.3	14.0 ± 5.3
ZG16p	1.8 ± 2.4	98.3 ± 2.4	21.8 ± 3.3	78.3 ± 3.3
Chymase	2.8 ± 1.0	97.2 ± 1.0	11.0 ± 3.6	89.0 ± 3.6
PpiB	1.2 ± 1.3	98.8 ± 1.3	15.0 ± 4.4	85.0 ± 4.4
CEL	21.0 ± 4.0	79.0 ± 3.6	71.0 ± 3.6	29.0 ± 3.6
RNase	61.3 ± 6.5	38.7 ± 6.5	17.3 ± 2.5	82.7 ± 2.5

Distribution to ZGC and ZGM (% of total ZGC + ZGM) and distribution to ZGM_{carb} and Wash (% of total ZGM). Data are from at least three independent experiments and are expressed as means ± standard deviation.

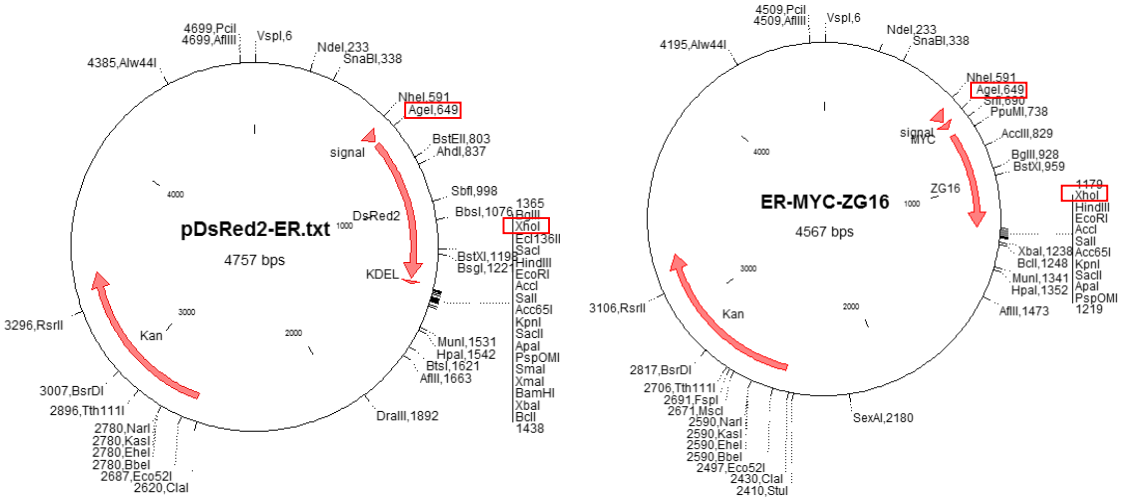

Supplementary Figure 1. Restriction map of the vector pDsRed2-ER (A) and ER-Myc-ZG16p (B). The DsRed2 and KDEL (ER retention signal) sequences were replaced by Myc-ZG16p. The red boxes indicate the restriction enzymes used for cloning.

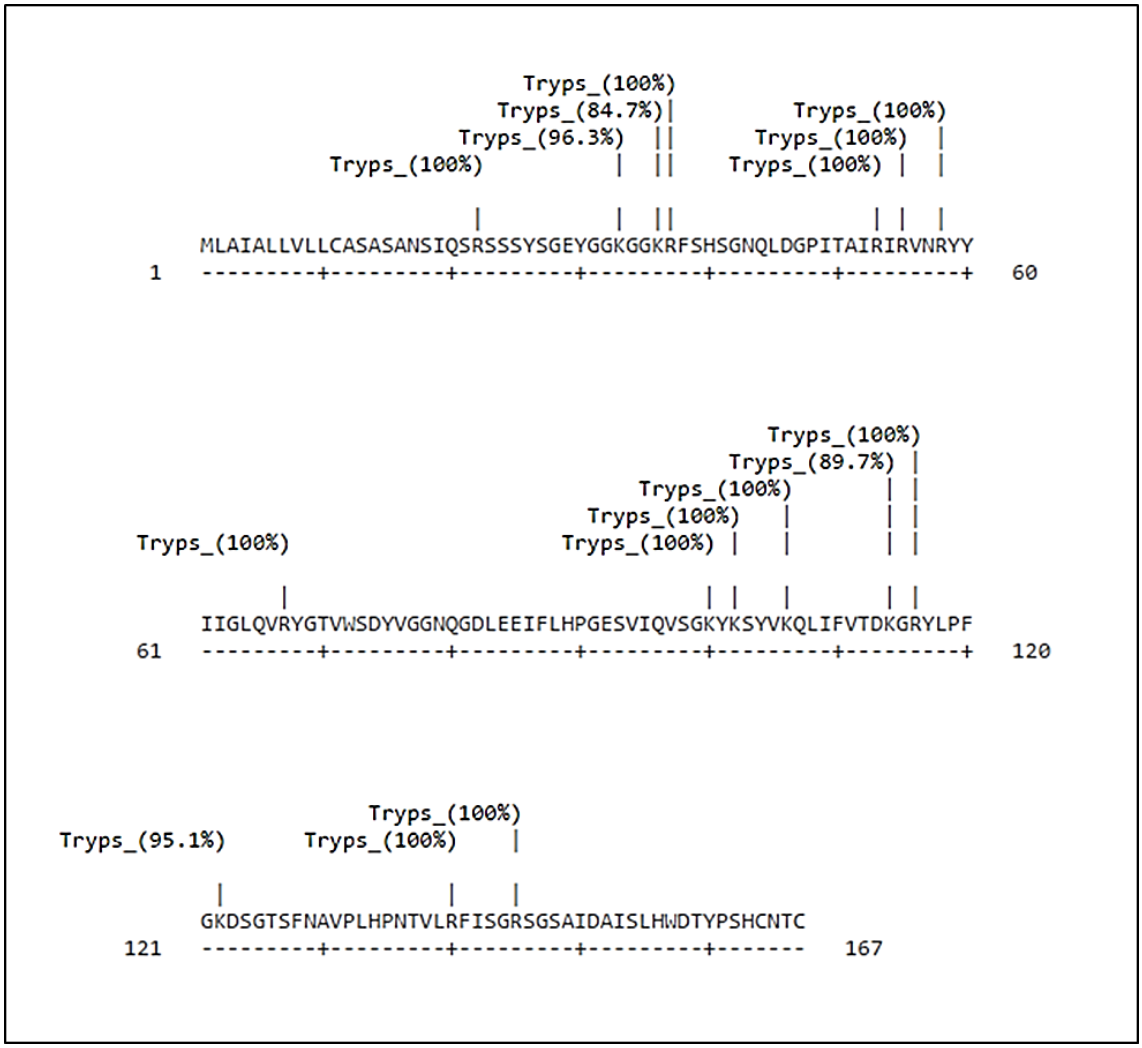

Supplementary Figure 2. Prediction of the potential cleavage sites for trypsin in ZG16p given by the ExPASy PeptideCutter tool.

Publications obtained during this project

Borta H*, Aroso M*, Rinn C, Gomez-Lazaro M, Vitorino R, Zeuschner D, Grabenbauer M, Amado F, Schrader M. Analysis of low abundance membrane-associated proteins from rat pancreatic zymogen granules. J Proteome Res. 2010, 9:4927-39 (* contributed equally to this work)

Gómez-Lázaro M, Rinn C, Aroso M, Amado F, Schrader M. Proteomic analysis of zymogen granules. Expert Rev Proteomics. 2010 Oct;7(5):735-47.

Gomez-Lazaro M, Aroso M, Schrader M. (2011). Rab8. The Pancreapedia: Exocrine Pancreas Knowledge Base, DOI: http://dx.doi.org/10.3998/panc.2011.2

Rinn C, Aroso M, Schrader M. (2011). The secretory lectin ZG16p. The Pancreapedia: Exocrine Pancreas Knowledge Base, DOI: http://dx.doi.org/10.3998/panc.2011.17

Rinn C, Aroso M, Prüssing J, Islinger M, Schrader M. Modulating zymogen granule formation in pancreatic AR42J cells. Exp Cell Res. 2012, 318:1855-66.

Bonekamp NA, Grille S, Cardoso MJ, Almeida M, Aroso M, Gomes S, Magalhaes AC, Ribeiro D, Islinger M, Schrader M. Self-interaction of human Pex11pß during peroxisomal growth and division. PLoS One. 2013, 8:e53424.

Aroso M, Agricola B, Schrader M. Submembranous proteoglycans are required for granule formation and regulated secretion of zymogens in the acinar cells of the exocrine pancreas. 2014/15 (about to be submitted).

Aroso M, Schrader M. Novel insights into the biochemical properties of the unique mammalian lectin ZG16p. 2014/15 (in preparation).

Aroso M, Gomez-Lazaro M, Schrader M. ZG16p – a novel tool to label and modulate the endo-lysosomal compartment in mammalian cells. 2014/15 (in preparation).

Other Scientific Presentations

Poster presentations at scientific congresses

"Accessing the Proteome of Zymogen Granules". M. Aroso, R. Vitorino, F. Amado, and M. Schrader. 1st Hands-on course on Proteins and Proteomics. July 12-25, 2008. Faculdade de Ciencias e Tecnologia, Universidade Nova de Lisboa. Portugal.

"Endogeneous peptides from rat salivary glands". R. Vitorino, M. Aroso, A. Caseiro, M. Schrader, and F. Amado. 5th Portuguese ProCura Meeting on Proteomics and Mass Spectrometry; in conjunction with the 1st International Congress on Analytical Proteomics (1ST ICAP), September 30-October 3, 2009. Caparica (Lisbon), Portugal.

"Suborganellar proteomics: Getting a grip on pancreatic zymogen granule membrane proteins". M. Aroso, M. G. Lázaro, C. Rinn, R. Vitorino, F. Amado, and M. Schrader. 5th Portuguese ProCura Meeting on Proteomics and Mass Spectrometry; in conjunction with the 1st International Congress on Analytical Proteomics (1ST ICAP), September 30-October 3, 2009. Caparica (Lisbon), Portugal.

"Proteomic analysis of protein complexes in zymogen granules of the exocrine pancreas by BN-PAGE". M. Aroso, R. Vitorino, R. Ferreira, F. Amado, and M. Schrader. 4th EuPA Congress and 6th Portuguese ProCura Meeting on Proteomics and Mass Spectrometry, October 23-27, 2010. Estoril, Portugal.

"Separation and analysis of protein complexes in zymogen granule membranes by 2D-BN/SDS-PAGE" M. Aroso, R. Vitorino, M. Islinger, R. Ferreira, F. Amado, and M. Schrader. 2nd International Congress on Analytical Proteomics (2nd ICAP), July 18-20, 2011. Ourense, Spain.